AN INTEGRATED FRAMEWORK FOR MODELING AND MITIGATING WATER TEMPERTURE IMPACTS IN THE SACRAMENTO RIVER

by

RAYMOND JASON CALDWELL

B.S., University of Louisiana at Monroe, 1997

M.S., North Carolina State University, 2005

A thesis submitted to the

Faculty of the Graduate School of the

University of Colorado in partial fulfillment

of the requirement for the degree of

Doctor of Philosophy

Department of Civil, Environmental, and Architectural Engineering

2013

This thesis entitled:
An Integrated Framework for Modeling and Mitigating Water Temperature Impacts in the Sacramento River
written by Raymond Jason Caldwell
has been approved for the Department of Civil, Environmental, and Architectural Engineering

_____
Dr. Balaji Rajagopalan

_____
Dr. Barry Eakins

_____
Dr. Harihar Rajaram

_____
Dr. Edith Zagona

_____
Dr. Subhrendu Gangopadhyay

Date _____

The final copy of this thesis has been examined by the signatories, and we find that both the content and the form meet acceptable presentation standards of scholarly work in the above mentioned discipline

Caldwell, Raymond Jason (Ph.D., Civil, Environmental, and Architectural Engineering)
An Integrated Framework for Modeling and Mitigating Water Temperature Impacts in the Sacramento River

Thesis directed by Professor Balaji Rajagopalan

Increasing demands on the limited and variable water supply across the West can result in insufficient streamflow to sustain healthy fish habitat. In addition, construction of dams and diversions along rivers for the purpose of storing and distributing the limited supply of water can further deteriorate natural flow regimes and, often, obstruct important migratory pathways for cold water fish reproduction and development. The thermal impacts on the ecology of river ecosystems have been well documented, yet there is no comprehensive modeling framework in place for skillfully modeling climate-related impacts. In regulated systems, such as the Sacramento River system, these impacts are an interaction of volume and temperature of water release from the reservoir and the subsequent exchange with the environment downstream.

We develop an integrated framework for modeling and mitigating water temperature impacts and demonstrate it on the Sacramento River system. The approach has four broad components that can be coupled to produce decision tools towards efficient management of water resources for stream temperature mitigation: (i) a suite of statistical models for modeling stream temperature attributes using hydrology and climate variables of critical importance to fish habitat; (ii) a reservoir thermal model for modeling the thermal structure and, consequently, the water release temperature, (iii) a stochastic weather generator to simulate weather sequences consistent with long-range (e.g., seasonal) outlooks; and, (iv) a set of decision rules (i.e., rubric) for reservoir water releases in response to outputs from the above components.

The statistical stream temperature models and stochastic weather generators are coupled to the reservoir thermal model and validated for their ability to reproduce observed stream

temperature variability along with characterizing the uncertainty at a compliance point downstream. We develop and validate a Decision Support Tool (DST) developed by coupling the stream temperature forecast model with the stochastic weather generator to the decision rubric. The DST incorporates forecast uncertainties and reservoir operating options to help mitigate stream temperature impacts for fish habitat, while efficiently using the reservoir water supply and cold pool storage. The use of these coupled tools in simulating impacts of future climate on stream temperature variability is also demonstrated.

Keywords: Water temperature; generalized linear model; stochastic weather generation; water management; seasonal forecasting; climate impacts

DEDICATION

I dedicate this work to the love of my life, Chip Guidroz.

May the days ahead continue to bless us with endless opportunities to grow and learn.

"Knowledge is love and light and vision." – Helen Keller

"All the knowledge I possess everyone else can acquire, but my heart is all my own." - Goethe

ACKNOWLEDGMENTS

I would like to express my deepest appreciation to all those who provided me the possibility to complete this dissertation. A special gratitude I give to my advisor, Dr. Balaji Rajagopalan, for his infinite wisdom, stimulating guidance, remarkable patience, and unwavering support. To my other committee members, Drs. Edith Zagona, Harihar Rajaram, Subhrendu Gangopadhyay, and Barry Eakins, the combined wealth of expertise you have shared in the completion of multiple journal articles and through invaluable one-on-one conversions will always be remembered as a generous gift of your time. I have also had the great pleasure of publishing individual articles from the dissertation with a spirited group of scientists: Dr. Laurel Saito, Dr. Blair Hanna, Dr. Marketa Elsner, Yong Lai, and Jennifer Bountry; I am grateful for their wisdom.

I would also like to acknowledge the National Aeronautics and Science Administration's Earth-Sun Science Applied Sciences Program, Grant # NNX08AK72G, and the associated authors [Danner et al., 2007] of that grant for providing funding to complete this work and for encouraging the continual advance of scientific endeavors through remarkable contributions to the research community. Specifically, I extend my thanks to Drs. Eric Danner and Andrew Pike of the Southwest Fisheries Science Center for their critical guidance during peer-review, extensive knowledge of California fisheries, and assistance on data collection, processing, and evaluation.

Over the last four years, the staff at the National Geophysical Data Center (NGDC) and the Bureau of Reclamation’s Technical Services Center (TSC) provided steadfast encouragement to complete this work and often ensured the integrity of my sanity. In particular, I would like to recognize Sue McClean, Lisa Taylor, and the Waffle Room team from NGDC and Victoria

Sankovich, Nicole Novembre, Dr. John England, Karen Weghorst, and the remaining members of the Flood Hydrology and Consequences Group at the TSC. The Research and Development Office at the Bureau of Reclamation also provided the opportunity to apply research from this dissertation in their Science and Technology Program. Additionally, Russ Yaworsky and Stacey Smith in the Sacramento office of the Bureau of Reclamation provided helpful guidance on reservoir operations and datasets essential to the completion of this work.

It is without question that I owe a great debt to my family and friends. To my mom and dad, Sandy and Carl Caulder, you have always blessed my life with unconditional love, honest advice, and the wisdom of parents. To my brother and his family, you have taught me that perseverance, endurance, and faith are the key to attaining our dreams. Ten years ago, I discovered that the path to success begins within; today, I have reached the pinnacle of my education with a clean mind and body. For that, I thank God.

CONTENTS

TABLES

FIGURES

1 INTRODUCTION

Water allocations in the western United States require consideration of the competing short- and long-term needs of many socioeconomic factors, including, but not limited to: agriculture, urban use (municipal and industrial), flood mitigation, hydropower generation, and environmental regulation. Increasing demands on the limited and variable water supply across the West can result in insufficient streamflow to sustain healthy fish habitat and populations. In the late summer and early fall, high air temperature and low flow conditions can cause rapid increases in water temperature, creating critical conditions, particularly for cold water fish such as salmon. In addition, construction of dams and diversions along rivers for the purpose of storing and distributing the limited supply of water can further deteriorate natural flow regimes and, often, obstruct important migratory pathways for fish reproduction and development.

In the Sacramento River Basin (SRB) of California, the long-term decline in salmon populations has made management of the remaining freshwater habitat critical. This is magnified by the increasing demands on water resources and an extended drought that has enveloped the western United States in recent years. The construction of Shasta (SHD) and Keswick Dams (KWD) in the SRB headwaters during the mid-20th century provided additional storage facilities to meet regional water needs; however, hundreds of kilometers of spawning habitat above the dams were lost. The declines of the winter run and the late fall runs of Chinook salmon in the SRB have been listed on the endangered and threatened species lists, respectively, by the Environmental Protection Agency (EPA). In 2008 and 2009, the Pacific Fishery Management Council (PFMC) closed the river to commercial and recreational fishing, resulting in economic losses in excess of $500M and over 2000 jobs.

The management of freshwater resources is one of the greatest challenges currently facing society. With increasing demand, alteration of water systems, and a changing climate, the thermal regimes of freshwater habitats are being substantially impacted. The thermal impacts on the ecology of river ecosystems have been well documented Poole and Berman, 2001; Caissie, 2006; McCullough et al., 2009], yet there is no comprehensive modeling framework in place for accurately modeling climate-related impacts. In regulated systems, these impacts are a complex function of the interaction of release volume and temperature and the subsequent exchange with the environment downstream. Danner et al. [2012] proposed a coupled modeling framework that links mesoscale weather and ecological models to generate inputs for a physically-based water temperature model for monitoring and forecasting water temperature at fine spatiotemporal scales. The integrated framework also provides the capability to develop long-range (e.g., seasonal) outlooks of risk through coupling with statistical methods. These long-range projections are an important and complementary decision support tool (DST) for reservoir managers interested in meeting the multiple criteria of many competing demands for water supply. By integrating state-of-the-art modeling systems with statistical analysis and prediction methods, a comprehensive set of DSTs can be developed that will best guide water resource management decisions in the SRB.

In this research, we develop an integrated framework for modeling and mitigating water temperature impacts and demonstrate it on the Sacramento River system. The approach has four broad components that can be coupled to produce decision tools towards efficient management of water resources for stream temperature mitigation. These are: (i) a suite of statistical models for modeling stream temperature attributes using hydrology and climate variables that are of critical importance for fish habitat – such as, average daily stream temperature, number of hours

of temperature threshold exceedance, etc.; (ii) a reservoir thermal model for modeling the thermal structure and consequently, the water release temperature, (iii) a stochastic weather generator to simulate weather sequences that are consistent with long-range (e.g., seasonal) outlooks and, (iv) a set of decision rules (i.e., rubric) for water releases from the reservoir in response to weather sequences and the reservoir thermal structure obtained from the above components. These components are coupled to develop tools that will help water managers plan for efficient mitigation of stream temperature impacts on fish habitat.

The statistical stream temperature models and stochastic weather generators are coupled to the reservoir thermal model and validated for their ability to reproduce observed stream temperature variability along with characterizing the uncertainty at a compliance point downstream from the reservoir. We develop and validate a Decision Support Tool (DST) developed by coupling the stream temperature forecast model along with the stochastic weather generator to the decision rubric. The DST incorporates forecast uncertainties and reservoir operating options to help mitigate stream temperature impacts for fish habitat, while efficiently using the water and cold pool storage in the reservoir. The use of these coupled tools in simulating impacts of future climate on stream temperature variability is also demonstrated. The integrated framework and remainder of the dissertation organization is detailed in the following sections, along with a description of the study region and datasets applied.

1.1 Study Region and Data

As discussed, the current research focuses in the upper SRB (Figure 1.1). Shasta Reservoir was retrofitted with temperature control devices in the mid-1990s, which allows selective withdrawals from different depths (and, therefore, different temperatures) in the reservoir based on water temperature requirements downstream. Keswick Reservoir serves as a

"pass-through" structure with minimal attenuation in temperature and flow released from Shasta. Downstream are three important temperature compliance points at Balls Ferry (BSF), Jellys Ferry, and Bend Bridge. As BSF is the most influenced by any mitigation efforts from the dams, this point is selected as the focus of the current research. It is highly likely that if temperature objectives are not met at this location that the points downstream will have even poorer compliance statistics. We will use the flow and water temperature data available at several key sites along the river, including: SHD and BSF. The flow at BSF is not included as the releases upstream drive this variable.

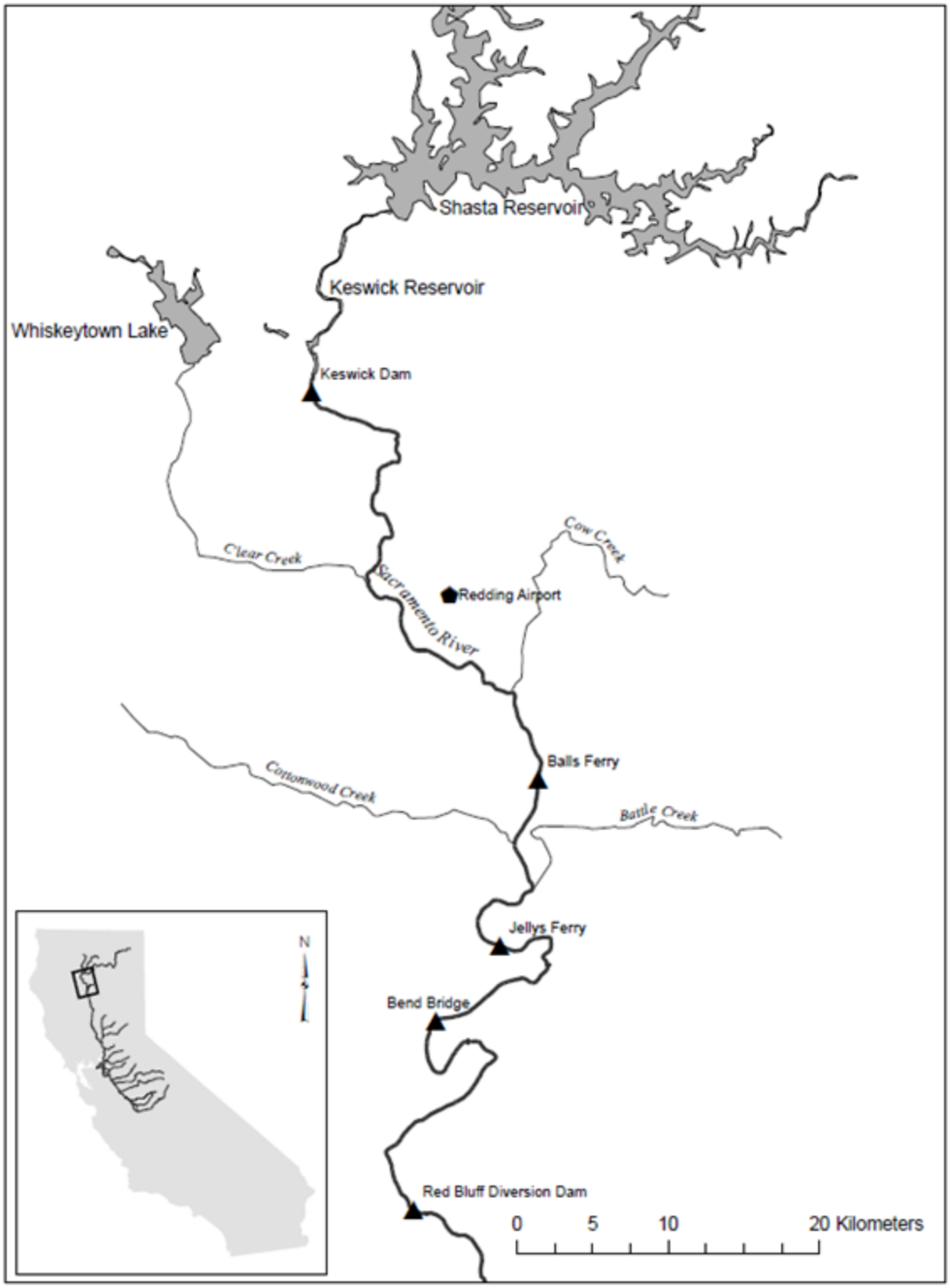

Figure 1.1: Map of the study area on the Sacramento River for the application of the modeling framework with compliance points, meteorological site, and primary infrastructure (adapted from Danner et al., 2012).

The upper SRB generally lies in a wide, flat valley with a gentle slope below Keswick Dam with the headwaters in steep terrain above Shasta Reservoir. Since we focus in the stretch of river below Shasta, the climate is generally cool and wet during the winter and hot and dry during the summer months (Figure 1.2). A single meteorological site with hourly observations is available in the valley at Redding, CA, which is approximately half-way between Keswick Dam and Balls Ferry. The site provides a variety of meteorological variables (except solar radiation); and, we use both daily (e.g., maximum and minimum air temperature and precipitation) and hourly (e.g., air temperature, dew point temperature, cloud cover, wind direction/speed, among others) data from the site.

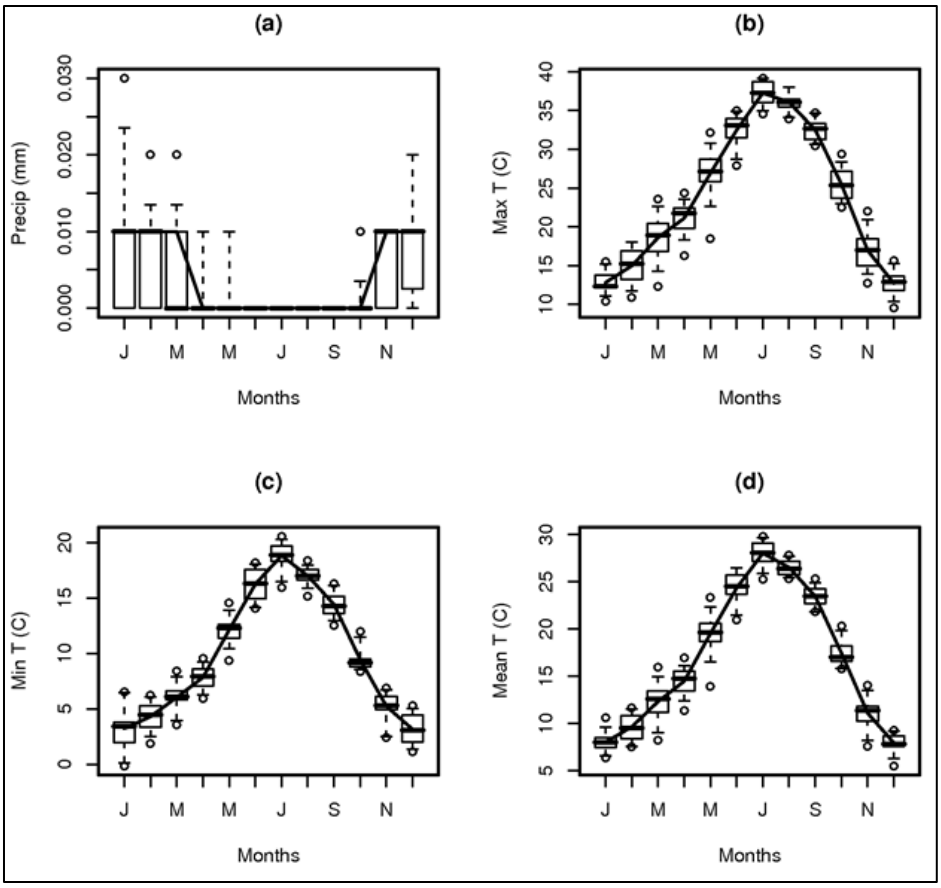

Figure 1.2: Monthly box plots of the observed daily (a) precipitation, (b) maximum air temperature, (c) minimum air temperature, and (d) mean air temperature at Redding, California, for the period 1994-2007. The height of the box plot represents the interquartile range, the horizontal line inside the box is the median, whiskers extend to the 5th and 95th percentiles, and the solid black line across boxes indicates the mean.

The flow, water temperature, and meteorological variables serve as input to the various components of the decision support tool. The historical hydrologic information is primarily available for the period 1994 to present, but was limited to the period through 2007 to use more recent years as verification of the various tools.

1.2 Integrated Framework

The remainder of the dissertation presents a description of dynamic and statistical water temperature models in Chapter 2 and five articles (submitted or soon-to-be-submitted) in Chapters 3 through 7 that rely on an over-arching framework leading to the development of a decision support tool for water managers in the Sacramento River Basin. Figure 1.3 shows a flow chart of the integrated framework.

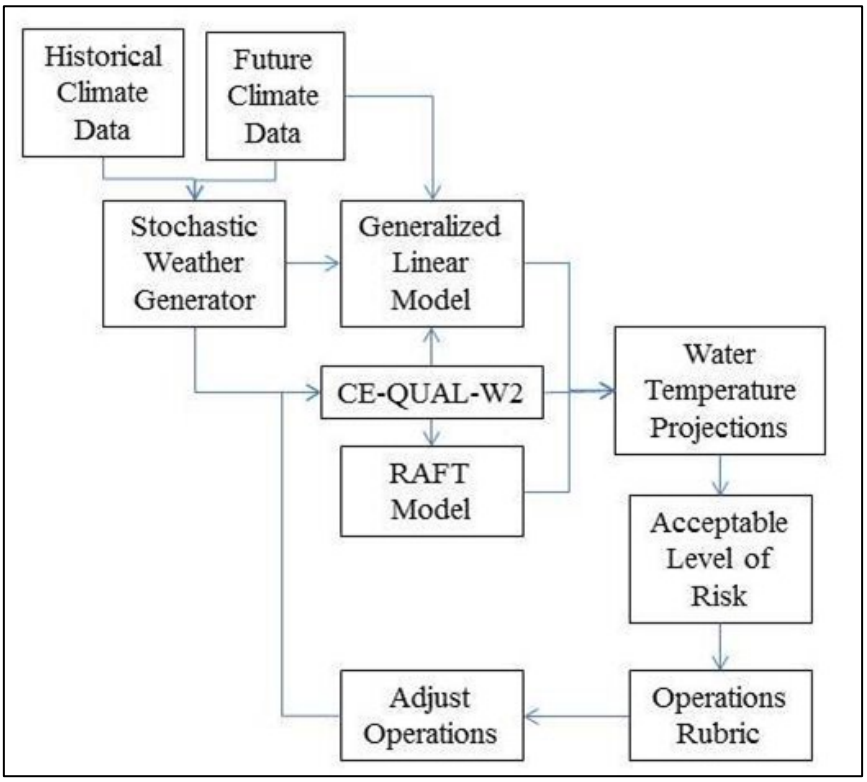

Figure 1.3: Flow chart of the integrated framework.

Here, a basic description of each subsequent chapter presents the integration of the multiple modeling systems:

Chapter 3 – Statistical Model: Seasonal Application
[submitted to Journal of Hydrologic Engineering]
A semi-parametric weather generator is developed using both unconditional (historical) and conditional (biased to future climate conditions) resampling. The weather generator simulations are then coupled with the generalized linear models for stream temperature attributes to develop future scenarios of water temperature at a downstream compliance point. Median daily flow and temperature releases are used in the statistical model.

Chapter 4 – Statistical Model: Multi-Decadal Application
[accepted in Water Resources Research]
Additional generalized linear models are developed for an unregulated basin in Washington State to indicate the applicability to other locations. In this case, the future climate conditions are derived from an application of the Variable Infiltration Capacity model using downscaled global climate model simulations.

Chapter 5 – Coupling of GLM and CE-QUAL-W2: Validation
[submitted to Environmental Modeling and Software]
The stochastic weather generator scenarios are coupled with the CE-QUAL-W2 model to generate flow and temperature releases from Shasta Dam. Single year simulations are performed for years exhibiting particular climate conditions (i.e., hot, dry, wet, cool) and use observed tributary inputs and Shasta Dam releases to generate simulated temperature releases at Shasta Dam for input to the generalized linear models. Comparison with the observations in the selected years is used to validate the model.

Chapter 6 – Coupling of CE-QUAL-W2 and RAFT
[in process]
The RAFT model is forced using the upstream boundary conditions from Chapter 5 for a particular year, the hot year of 2003. The model performance is validated against observations from that year and then compared to the performance of the generalized linear models.

Chapter 7 – Coupling of GLM and CE-QUAL-W2 (Operations Rubric)
[submitted to Journal of American Water Resources Association process]
Similar to Chapter 5, the weather generator scenarios are used to force the CE-QUAL-W2 model; however, the median flow releases at Shasta Dam are used as input to the generalized linear models instead of observed flow releases to mimic standard operations under the given unconditional or conditional climate scenario. This allows investigation of alternative operations through the application of a rubric for decision-making based on stream temperature forecasts from the coupled system. Both the individual years from Chapter 5 and the fully stochastic approach are evaluated to validate the approach. Evaluation of the alternate operations is performed using various metrics, including cold water storage, additional water usage, and number of violations.

The final chapter in the document contains a summary of the results and future directions for research, including a synopsis of an ongoing project as part of the National Oceanic and Atmospheric Administration's Sectoral Applications Research Program (NOAA SARP) to improve streamflow estimation for CE-QUAL-W2.

2 WATER TEMPERATURE MODELING

The health and productivity of aquatic ecosystems are highly sensitive to stream temperature [Caissie, 2006; Webb et al., 2008]. Temperature fluctuations induce changes in metabolic rates, concentrations of key water quality parameters (e.g., dissolved oxygen), biotic assemblages, and life cycle processes (e.g., spawning, migration, mortality) [Brown and Greene, 1992]. Since changes in stream temperature are closely tied to meteorological and hydrological conditions, any modification in the variability and mean state of the existing hydroclimate should have a corresponding effect on aquatic ecosystems [Smith and Lavis, 1975]. In response, multiple research efforts have been focused on the prediction of stream temperature [e.g., Bartholow, 2003]. This chapter provides a background on stream temperature modeling, a review of prior modeling efforts in the Central Valley region of California in the Sacramento River, and details on the models specific to the work of the dissertation.

2.1 Study Area

The Central Valley region of California is composed of the San Joaquin and Sacramento River watersheds and their many tributaries. The watersheds provide important environmental, economic, and social resources, including: recreation, habitat for fish and wildlife, water supply, hydropower, flood control, and navigation, among other significant economic drivers to California's economy. Since the mid-20th century, construction of dams have blocked historical spawning grounds for anadromous fishes and altered the flow and water quality regimes in downstream river reaches. The impact on water temperatures and its related influence on the Chinook salmon and steelhead populations are of particular concern. In response to declining populations of anadromous fishes in the Sacramento River, both the winter- and fall-run of Chinook salmon are listed on the endangered and threatened species lists, respectively. In fact, in

2008-2009, the California Department of Fish and Game halted commercial and recreational fishing on the river, resulting in multi-million dollar economic losses and thousands of unemployed personnel. In response, regulators have imposed water temperature requirements or objectives that restrict the operation of upstream reservoirs (e.g., Keswick and Shasta Dams on the Sacramento River). Mathematical modeling of water temperature, therefore, has become an important tool for operation of system reservoirs. As such, the Bay Delta Modeling Forum [Deas and Lowney, 2000] developed a document with the objective to "provide an overview of stream and reservoir modeling, review historical and current temperature modeling work in the Central Valley, identify basic temperature prediction concepts, present the required field and other physical data, and define the role of temperature modeling in addressing current biological problems." This document underlines the need and interest in mathematical modeling tools within the Sacramento River watershed and provides a concise reference for specific models within the basin.

2.2 Mathematical Modeling

There are generally two types of stream temperature models applied: (1) physically-based models (rooted in the solution of fluid flow and heat transport equations) and, (2) empirical models (relying on the correlation strength between meteorology and stream temperature). Deterministic models have been applied extensively to address a variety of problems and issues [Carron and Rajaram, 2001; Jobson and Keefer, 1979; Jobson, 1980; Sinokrot and Stefan, 1993]. Highlighting the advantage of physically-based models in the ability to estimate the spatial and temporal distribution of water temperature at fine scales over small domains, Jobson and Keefer [1979] evaluated a highly transient flow regime in the Chattahoochee River near Atlanta, Georgia, finding that the impact of timing of releases had a significant effect on the downstream

response in water temperatures. More recently, Carron and Rajaram [2001] built on the work of Jobson and Keefer [1979] to evaluate the impacts of variable releases on downstream temperature in the Green River. Jobson [1980] introduced a coupled Eulerian and Langrangian (i.e., semi-Langrangian) framework in a hydrodynamic model to assess the impact of evaporation on water temperature within a concrete canal in California. Similarly, Sinokrot and Stefan [1993] evaluated the effects of solar radiation/shading and wind sheltering on water temperature fluctuation. While physical models are excellent for evaluating the energy budget and for better understanding the dynamical properties of water under specific regimes, they are typically restrictive for performing regional simulations or for predicting changes at longer time scales (e.g., years to decades) due to extensive requirements of data and computing power [Brock and Caupp, 1996; Carron and Rajaram, 2001; Taylor, 1998]. Physical models can be adapted for larger domains [e.g., Null et al., 2012]; but, usually results in a reduction in temporal resolution. Detailed, high resolution, continuous model input is required including inputs of system geometry, meteorological forcing, and hydrological forcing; these data are often unavailable, inconsistent, or of poor quality.

Often, the availability of high-resolution geographic data for a watershed is unavailable or limited, relegating the modeler to a statistical regression methodology [e.g., Mohseni et al., 1998; Webb et al., 2003, 2008]. Statistical methods are appropriate at larger spatial and temporal scales, as they offer the benefit of computational efficiency [Benyahya et al., 2007]. Empirical models typically consist of regressions between stream temperature and environmental conditions, such as air temperature which is driven by the joint dependence of each on solar radiation [Benyahya et al., 2007]. Thus, these models are easily integrated with output from other modeling systems (e.g., hydrologic models forced with input from global climate models

(GCMs)), which provides an opportunity to apply projected changes in hydroclimate directly, rather than making discrete adjustments (say, increasing air temperatures by 2°C) to understand model sensitivity to input changes. Statistical models are limited regarding temporal resolution, in that they are appropriate for application at daily or weekly time steps [Mohseni et al., 1998]. At shorter time steps, Mohseni et al. [1998] found that autocorrelation within the stream temperature time series makes regression increasingly difficult. However, more recent methods [Caldwell et al., 2013a], apply spatiotemporal disaggregation techniques with reasonable results for generating hourly estimates of stream temperature.

Both deterministic and empirical methods have advantages and limitations in predicting stream temperature. The following sections describe the physical (i.e., dynamic) properties of stream temperatures and factors which affect the fluctuations of water temperature. In addition, brief descriptions of the modeling systems employed in the Sacramento River as part of the current project are described. The chapter concludes with the over-arching framework which integrates both deterministic and empirical models to develop a decision support system for managing water temperatures in the Sacramento River Basin.

2.3 Factors Affecting Water Temperature

Water temperatures in rivers are generally affected by four factors: (i) atmospheric conditions; (ii) topography; (iii) stream discharge; and, (iv) streambed [Caissie, 2006]. The atmospheric conditions are primarily responsible for the heat exchange processes that take place at the water surface, while the topography can influence the local atmospheric conditions and provide shading effects. The stream discharge is dependent on river hydraulics and impacts stream temperature through heating capacity (volume of water) and mixing, including tributary and other inflows and streambed heat exchange. These factors act in a bulk on thermal conditions

of rivers such that high air temperature, lack of shading and low discharge should result in higher water temperature values and vice versa; however, there are also smaller scale influences on the spatial and temporal variability of water temperatures.

In general, the mean daily water temperature increases in a downstream direction (Figure 2.1), with groundwater fed headwaters cooler than water downstream which has been influenced by several diel cycles of warming/cooling [Benson, 1953]. These large-scale variations are non-linear and rates can differ by orders of magnitude between small, shallow and large, deep rivers [e.g., Torgersen et al., 2001; Zwieniecki and Newton, 1999]. Smaller spatial scale variability can be observed at the confluence of rivers, in deep bedrock pools, or at localized groundwater seepages. As mentioned, cyclical meteorological patterns can affect the temporal variability of water temperature through solar exposure and related air temperature effects. The magnitude of variation is directly proportional to the heating capacity (i.e., volume) of water. In addition, a seasonal pattern exists which follows a general sinusoidal function [Ward, 1963; Webb et al., 2003].

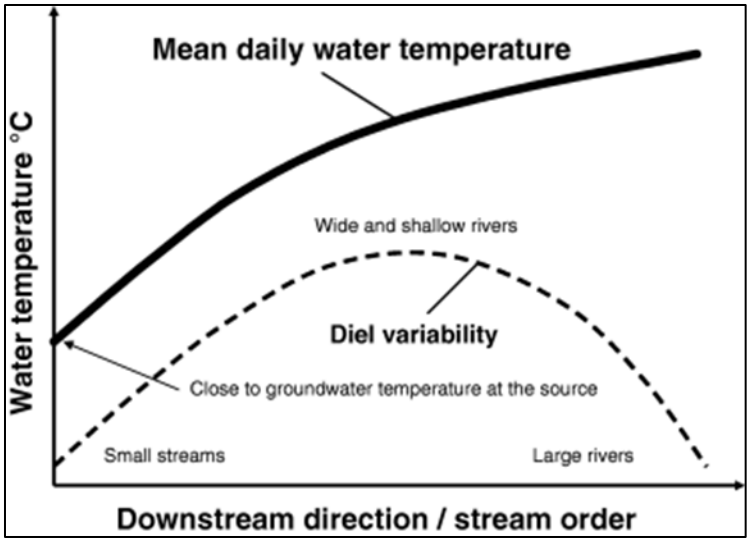

Figure 2.1: Mean daily and diel variability of water temperature as a function of stream order/downstream direction (extracted from Caissie [2006]).

2.4 Theory

In order to capture the complex interactions of meteorology, geography, discharge, and the streambed, mathematical models must consider the theoretical (i.e., physical and dynamical) properties of water temperature, most importantly heat transfer and transport. Most water temperature models focus on the laws of conservation of energy. The first law of thermodynamics (conservation of energy) states that energy can neither be created nor destroyed, but rather converted from one type to another. For lakes and rivers, this is typically expressed as Equation 2.1:

$$Q_{net}=Q_{sw} + Q_{atm} + Q_b + Q_l + Q_h + Q_g \,, \qquad (2.1)$$

where Q_{sw} is short-wave (i.e., solar) radiation, Q_{atm} is downwelling long-wave (i.e., atmospheric) radiation, Q_b is upwelling long-wave (i.e., backscatter from water surface), Q_l is latent heat flux, Q_h is sensible heat flux, and Q_g is conduction between the water and the bed. The sign convention is positive for heat entering the water and negative for heat leaving. A complete

description of the individual parameters and related equations is provided in Deas and Lowney [2000]; and, a schematic of the heat balance equation is reproduced here as Figure 2.2.

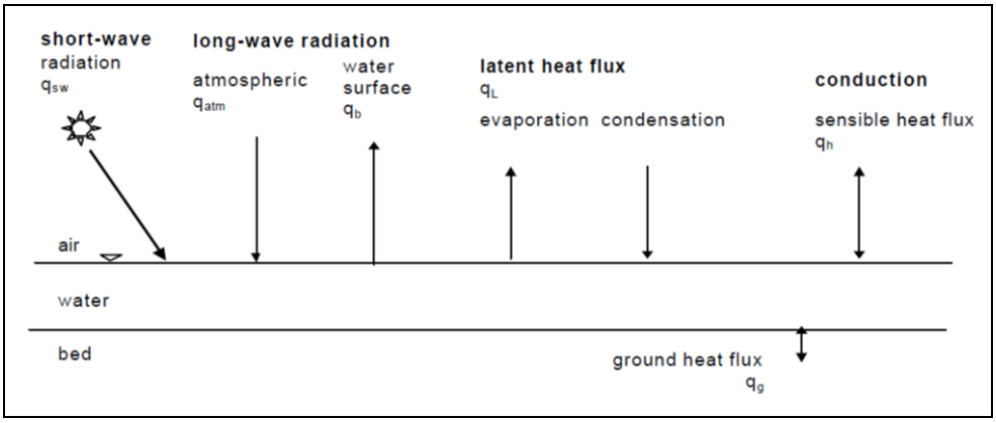

Figure 2.2: Source and sinks of heat energy (extracted from Deas and Lowney [2000]).

While this simplistic representation of stream temperature is valid for an infinitesimally small parcel (i.e., point source) of water, it neglects the effects of mixing and other source inputs of thermal energy to the system (e.g., tributaries, effluent, canals, etc.). For that reason, one must consider the heat transport mechanisms of advection and diffusion/dispersion. Advection is the bulk movement of a tracer (here, heat) with the main flow. As the tracer moves downstream, it spreads simultaneously in all directions through diffusion and dispersion. The longitudinal transport is typically defined as the x-direction, with lateral transport in the y-direction, and vertical transport in the z-direction. Molecular diffusion, or the random motion of tracer in a solution, is described by Fick's Law as proportional to the heat gradient, which is typically not included in water temperature modeling of rivers through elimination in scale analysis. Turbulent diffusion is similar in that the solute (i.e., heat) moves relative to fluctuations in velocity, which can be approximated by a statistical relationship to Fick's Law. Finally, dispersion occurs due to changes in velocity, for example across the channel, which leads to

mixing. The fate and transport of heat in a river can be described by the three-dimensional advection-diffusion equation, as in Equation 2.2:

$$\frac{\partial T}{\partial t} + u_x \frac{\partial T}{\partial x} + u_y \frac{\partial T}{\partial y} + u_z \frac{\partial T}{\partial z} = \frac{\partial}{\partial x}\left(D_x \frac{\partial T}{\partial x}\right) + \frac{\partial}{\partial y}\left(D_y \frac{\partial T}{\partial y}\right) + \frac{\partial}{\partial z}\left(D_z \frac{\partial T}{\partial z}\right) + \frac{Q_{net} A}{\rho_w C_s V} \quad , \qquad (2.2)$$

-A- ---------B---------- ----------C---------- -D-

where t is time, x is longitudinal (streamwise) distance, y is lateral distance, z is vertical distance, T is water temperature, D_i is the coefficient of diffusion in each direction, A is the surface area, V is the volume, Q_{net} is the net energy from Equation 2.1 above, ρ_w is the density of water, and C_s is the specific heat of water. Equation 2.2 describes the local change in temperature at time t (term A) as a function of: (term B) heat transported in the bulk flow, (term C) mixing processes, and (term D) the net heat flux at the air- and bed-water interfaces. Since most streams mix vertically before laterally, the vertical terms are often eliminated in Equation 2.2 to simplify the equation, giving a two-dimensional heat balance as Equation 2.3:

$$\frac{\partial T}{\partial t} + u_x \frac{\partial T}{\partial x} + u_y \frac{\partial T}{\partial y} = \frac{\partial}{\partial x}\left(D_x \frac{\partial T}{\partial x}\right) + \frac{\partial}{\partial y}\left(D_y \frac{\partial T}{\partial y}\right) + \frac{Q_{net} A}{\rho_w C_s V}, \qquad (2.3)$$

where T is now the depth-averaged temperature. Additional simplification is possible to a one-dimensional form of Equation 2.3, given that careful consideration is given to the application at hand. Fick's Law in term b indicates that the turbulent diffusion is proportional to the gradient in temperature across a particular axis. In point source locations, at confluences of tributaries or where effluent may be entering the river, this gradient may be quite large; however, in general, the atmospheric forcing acts in a distributed manner along the downstream axis which results in fairly small lateral differences, allowing the removal of the y-direction terms yielding the one-dimensional form as Equation 2.4:

$$\frac{\partial T}{\partial t}+u_x\frac{\partial T}{\partial x}=\frac{\partial}{\partial x}\left(D_x\frac{\partial T}{\partial x}\right)+\frac{Q_{net}A}{\rho_w C_s V} \qquad (2.4).$$

Finally, dispersion often plays a small role in one-dimensional water temperature models (except in cases such as pollutant discharges) and the distributed nature of the atmospheric forcing dampens this effect. The "bulk flow" version of the equation then becomes Equation 2.5:

$$\frac{\partial T}{\partial t}+u_x\frac{\partial T}{\partial x}=\frac{Q_{net}A}{\rho_w C_s V} \qquad (2.5).$$

The system of partial differential equations (PDEs) in these equations can be solved analytically if Q_{net} is described by an equation that is easily integrated in time and space. Expressions for these energy budget equations are complex PDEs themselves and, therefore, require simplification. For example, Edinger et al. [1974] and others have expressed the net heat input as a function of an overall heat exchange coefficient and the equilibrium temperature (i.e., the temperature at which Q_{net} equals zero in Equation 2.1). One example of the formulation is

$$Q_{net}=K\left(T_e-T\right) , \qquad (2.6)$$

where K is the heat exchange coefficient and T_e is the equilibrium temperature. Values for K and T_e may be formulated using a variety of methods.

The heat exchange budget equations can then be solved analytically through reduction to ordinary differential equations using an assumption of complete vertical and transverse mixing or by applying finite differencing schemes (e.g., Taylor series expansion) to simplify the PDEs to equations with analytical solutions. The specifics of the river temperature models used in the dissertation are described more fully in Section 2.5.1 (i.e., the deterministic RAFT model) and Section 2.5.3 (i.e., the statistic-based, generalized linear model).

Unlike rivers and streams, the heat budget equation for lakes/reservoirs more often includes consideration of the vertical distribution of heat. The rate of change of heat content is determined by fluxes at the air- and bed-water interfaces, but also from heat transfer from inflows and outflows (i.e., tributaries and releases, respectively). Heat exchange is dominated by processes occurring at the surface, with the exception of solar radiation, which passes through the entire water column, attenuating with increasing depth and turbidity. While the heat load is determined by solar radiation, longwave radiation, and sensible and latent heat flux in a reservoir, the distribution of heat is driven by fluid motion within the reservoir. Wind is the primary driver here, especially in the upper section of the lake where solar radiation has the maximum impact in water temperatures. This results in increasing water temperatures in this surface layer through the summer with colder, denser water with increasing depth. Stratification occurs with thermocline development and most mixing occurs in the upper layer with minimal fluid motion within the cold pool, except near tributary or other inflows where depth dependent mixing occurs relative to the thermal stratification (i.e., thermal stability) of the reservoir. The effects of these inflows and outflows are typically defined through a relationship with volume, bulk flow, and residence time. Additional specifics are provided in Section 2.5.2, where the two-dimensional reservoir model for Shasta Lake (i.e., CEQUAL-W2) used in the dissertation is described.

2.5 Integration of Deterministic and Statistical Models

Three water temperature models are applied in the current study. The first three subsections describe the set-up for each of these models. Chapter 7 will lay out the over-arching framework which integrates these models in the development of a decision support tool for mitigating high stream temperatures on the Sacramento River.

2.5.1 RAFT Model

The River Algorithm for Forecasting Temperatures (RAFT) model was developed by Pike et al. [2013] and a full description of the model can be found in their publication. For completeness, a brief description of the model is provided here.

The RAFT model merges the desirable features of previous models into a robust framework. RAFT utilizes the details of the state-space frameworks of Bravo et al. [1993], Yearsley [2009], and Boyd and Kasper [2003]. Each of these models has limitations pertaining to: the neglect of flow coupling, tributary inputs, bed processes, and spatially variable meteorology [Bravo et al., 1993]; consideration of only advection and environmental heat exchange [Yearsley, 2009]; and, lack of data assimilation capability [Boyd and Kasper, 2003]. The RAFT model expands on these works and Georgakakos et al. [1990] by linking flow, water temperature, and bed temperature dynamics in a state-space framework with three modules. The three modules include water temperature, streambed temperature, and flow dynamics.

The hydrodynamic model consists of an advection-dispersion equation describing the downstream movement of heat, coupled to a one-dimensional hydrologic routing model to describe the movement of water downstream. Pike et al. [2013] assume the lateral and vertical temperature gradients in the channel are negligible and apply a one-dimensional equation with unsteady, non-uniform dynamics (Equation 2.7):

$$\frac{\partial T}{\partial t} = -V\frac{\partial T}{\partial x} + \frac{1}{A}\frac{\partial}{\partial x}\left(D_x\frac{\partial T}{\partial x}\right) + \frac{1}{A}S, \qquad (2.7)$$

where the parameters are water velocity (V), channel cross-sectional area A, and a thermal diffusion coefficient D_x. The term S represents the sum of heat sources and sinks that affect the channel water temperature and is defined as Equation 2.8:

$$S=\frac{W}{c_w\rho_w}\Phi_{air}+\frac{P}{c_w\rho_w}\Phi_{bed}+\frac{q_{in}}{\Delta x}(T_{in}-T)-\frac{q_{out}}{\Delta x}(T_{out}-T), \qquad (2.8)$$

where W is channel width, P is the wetted perimeter, q_{in} and T_{in} are incoming flow and temperature, q_{out} and T_{out} are outgoing flow and temperature, and c_w and ρ_w are the heat capacity and density of water, respectively. The heat movement across the water-air (Φ_{air}) and water-streambed (Φ_{bed}) interfaces are represented in the first two terms on the right hand side of Equation 2.8. The air and bed influences are kept separate here to account for the forcing variables being one-way and two-way causality, respectively, for these fluxes. The hydrologic routing is accomplished through a one-dimensional Muskingum-Cunge formulation due to its prior application in unsteady, non-uniform flow by Boyd and Kasper [2003] and in state-space applications [e.g., Georgakakos et al, 1990]. The RAFT model involves converting these governing equations into linearized state-space form and assimilating observations via use of a Kalman filter and closes the energy budget equation through time and space using a robust semi-Langrangian numerical scheme. The details of these procedures can be found in Pike et al. [2013].

The model utilizes gridded input data including: (a) meteorological time series of solar radiation, long-wave radiation, air temperature, dew point temperature, and wind speed with optional entries for cloud cover and atmospheric pressure; (b) channel geometry; and, (c) flow and tributary time-series at the upstream boundary and along tributaries. The meteorological data is derived from the combined Weather Research and Forecasting (WRF) and Terrestrial Observation and Prediction System (TOPS) model. The WRF-TOPS framework integrates operational satellite data, ground-based monitoring data, microclimate mapping, and physical and ecosystem models, with an industry-standard numerical weather prediction model to

generate estimates of each atmospheric variable and can be run in hindcast or predictive mode. The bathymetric data were developed using HEC-RAS model calibration procedures. The flow and water temperature requirements were derived from point observations from at sites along the river at reservoir release sites. Additional details on model validation and performance can be found in Pike et al. [2013].

For the application in the dissertation, the RAFT model incorporates point data uniformly across the gridded domain for meteorology, which is based on the hourly observation site at Redding, California, with adjustment to a location representative of Shasta Dam. The boundary condition inputs include the simulated flow and water temperature releases using the CE-QUAL-W2 model.

2.5.2 CE-QUAL-W2

Hanna et al. [1999] utilized the CE-QUAL-W2 model (W2) to simulate the effects of temperature control device operations on in-reservoir vertical temperature profiles and, hence, biotic assemblages. While the reference from Hanna et al. [1999] provides specifics on the calibration, verification, and application of W2 in Shasta Lake, the details of the model set-up are limited. Here, a summary from Wells and Cole [2000] is provided.

The W2 model is a two-dimensional, hydrodynamic and water quality model developed by the U.S. Army Corps of Engineers and maintained/distributed through Portland State University [Cole and Buchak, 2005; Cole and Wells, 2011]. Because the model assumes lateral homogeneity, it is best suited for relatively long and narrow water bodies exhibiting primarily longitudinal and vertical water quality gradients. The W2 model is capable of predicting water surface elevations, velocities, temperatures, and a number of water quality constituents. Water is

routed through a computational grid, where each cell is a completely mixed reactor at each time step. Geometrically complex water bodies can be represented through multiple branches and cells. Hydraulic structures can also be modeled as spillways and pipes.

The model uses several assumptions and approximations to simulate hydrodynamics, transport, and water quality processes. The model solves for gradients in the longitudinal and vertical directions and assumes lateral gradients are negligible. This assumption may be inappropriate for water bodies with significant lateral variations. Turbulence is modeled through eddy coefficients of which the user must decide which scheme is most appropriate for an application. An algorithm for vertical momentum is not included and results may be inaccurate in water bodies with significant vertical acceleration. Water quality processes are extremely complex and the model uses simplified approaches to reach solutions. The model is limited by the quality and availability of input data which includes meteorological data, inflow and outflow discharge, water temperature and/or other quality variables, and calibration data. Bathymetry is a two-dimensional numeric representation of a water body which is represented as longitudinal bands and vertical slices. The model set-up from Hanna et al. [1999] is applied in the dissertation. Specifically, a calibrated version of the W2 model, Version 3.7, which includes segmentation for five branches of inflows: the Pit River, Squaw Creek, McCloud River, Sacramento River, and Backbone Creek Inlet (Figure 2.3). The W2 model of Shasta Lake uses measured bathymetry derived from U.S. Geological Survey, pre-dam elevation contours, observed meteorological data at hourly increments from Redding, California adjusted to the elevation of Shasta Dam, and inflow/outflow data and temperature data from the U.S. Bureau of BOR at Shasta Dam and U.S. Geological Survey. A water balance is applied to maintain mass continuity due to differences in computed inflow and tributary inputs.

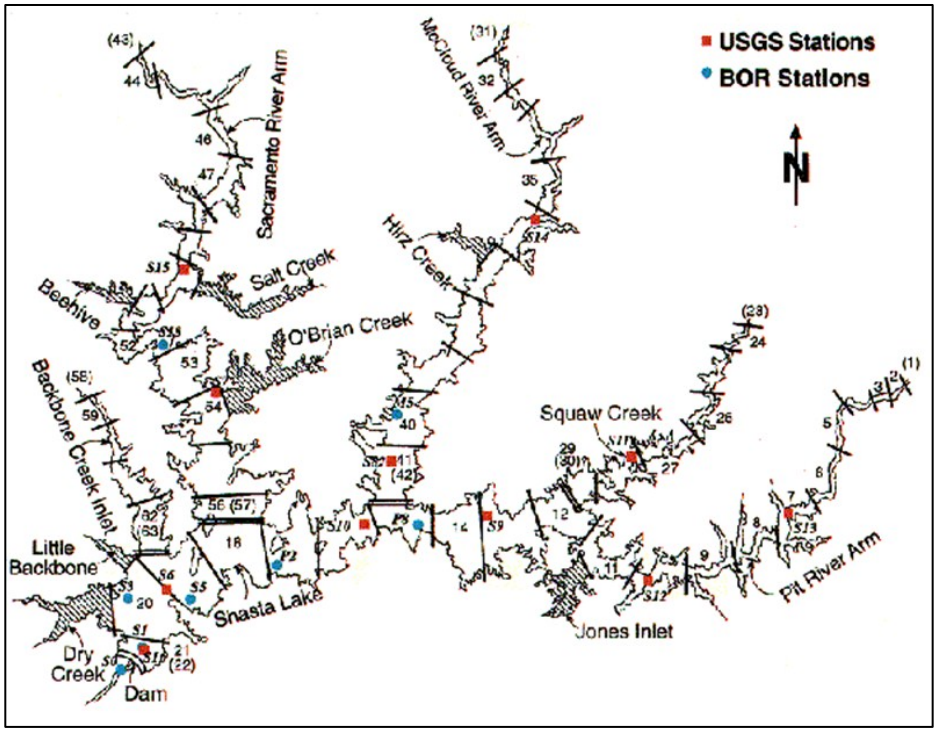

Figure 2.3: Shasta Lake CE-QUAL-W2 model segmentation from Hanna et al. [1999].

2.5.3 Generalized Linear Model

In this dissertation, we offer a generalized linear modeling (GLM) framework with local polynomial method for function estimation, to provide predictions of a range of daily water temperature attributes. The generalized linear modeling framework is a statistical model, which capitalized on the strong correlation of water temperature with hydrometeorological variables, specifically air temperature and streamflow, among other variables.

In a GLM, the response or the dependent variable Y can be assumed to be a realization from any distribution in the exponential family with a set of parameters [McCullagh and Nelder, 1989]. A smooth and invertible link function transforms the conditional expectation of Y to a set of predictors (Equation 2.9).

$$G(E(Y)) = f(X) + \varepsilon = X\beta^T + \varepsilon\,, \qquad (2.9)$$

where $G(.)$ is the link function, X is the set of predictors or independent variables, $E(Y)$ is the expected value of the response variable, ^{T} is the transpose operator, and ε is the error assumed to be normally distributed with variance (σ_ε). In a linear model (the standard linear regression), the function $G(.)$ is identity and Y is assumed to be normally distributed. Depending on the assumed distribution of Y, there exist appropriate link functions [McCullagh and Nelder, 1989]. The model parameters, β, are estimated using an iterative weighted least squares method that maximizes the likelihood function as opposed to an ordinary least squares method in linear modeling. The GLM can be used to model a variety of response variables – for skewed variables with a lower bound of 0 such as daily maximum water temperature or daily water temperature range, the Gamma distribution assumption of Y and its associated link function is appropriate; for number of hours of temperature exceedance, the Poisson distribution and its associated link functions can be used; for probability of exceedance, a binomial distribution and its link function (i.e. logistic regression) is the approach. We refer the readers to McCullagh and Nelder [1989] for information about a variety of distributions, link functions, and parameter estimation.

To obtain the best set of predictors for the model there are objective criteria such as the Akaike Information Criteria (AIC) or Bayesian Information Criteria (BIC) – both of which penalize the likelihood function based on the number of parameters [Venables and Ripley, 2002]. Models are fit using all possible subsets of predictors and also link functions; for each, the AIC and BIC are computed and the model with lowest AIC or BIC is selected as the 'best model'. Models can also be tested for significance against a null model or an appropriate subset model using a chi-squared test. Here, BIC is used as it tends to be slightly more parsimonious compared to AIC.

The function f in Equation 2.9 is linear and fitted to the entire data and, therefore, can miss capturing "local" nonlinearities. To address this, we used a nonparametric approach based on local polynomials [Loader, 1999] to fitting f. In this, the function is estimated 'locally' for any desired point x. The small set of neighbors (αN; N is the total number of data points and α is a value in the range of 0 to 1) to x is identified and to this a polynomial of order p is fitted. Thus, we used the fitted polynomial to estimate the response variable Y at the desired point x. This process is repeated for any estimation point. Note that if α and p are set to 1 then this collapses to the linear functional model in Equation 2.9. In this regard, the local polynomial provides an additional degree of flexibility to the GLM framework. The choice of α and p are obtained using a Generalized Cross Validation criteria (GCV) that is similar to AIC. The GCV can be used to obtain the local polynomial parameters (α and p) and the best set of predictors [e.g., Regonda et al., 2005]; however, we fit the local polynomials to the best predictor set obtained from BIC using the global fit. This hybrid approach is preferred for computational efficiency. A large number of predictors are considered based on prior research and knowledge of the system – they include the water and air temperatures and hydrologic characteristics of the previous and current day.

The independent variables selected for model fitting are chosen to mimic the complex dynamics incorporated in the more sophisticated deterministic models. For example, both maximum and minimum air temperature are included to capture the influence of diel temperature variability and the temperature feedbacks on evapotranspiration processes. Precipitation is included as a proxy for cloud cover and its influence on solar radiation impacting the system. The upstream discharge and temperature release variables serve as advection and mixing parameters in the statistical model. For completeness, the prior day variables are included to

account for the pre-existing state of the hydro-thermodynamics on the river and migration time of thermal inputs from the upstream boundary condition on temperature at downstream locations.

3 STATISTICAL MODEL: SEASONAL APPLICATION

Water releases from Shasta Dam into the Sacramento River in California are influenced by the short- and long-term needs of many socioeconomic factors including, but not limited to, agriculture, urban use, flood mitigation/control, and environmental concerns. The Endangered Species Act (ESA) requires that sufficient water is released to protect downstream thermal habitat for listed species, such as salmon and steelhead. In order to make efficient decisions of water release in the face of limited water availability, skillful projections of water temperature attributes are crucial. To this end, we offer a generalized linear modeling (GLM) framework with local polynomial method for function estimation, to provide predictions of a range of daily water temperature attributes - maximum daily water temperature; daily temperature range; number of hours of threshold exceedance; probability of threshold exceedance/non-exceedance. These attributes are varied in nature (i.e., discrete, continuous, categorical etc.) and GLM provides a general framework to modeling all of them. A suite of predictors that impact water temperatures are considered, including current and prior day flow, water temperature of upstream releases, air temperature, and precipitation. A two-step model selection is proposed – first an objective method based on Bayesian Information Criteria (BIC) is used in a global model to select the best set of predictors for each attribute; then the parameters of the local polynomial method for the selected best set of predictors are obtained using Generalized Cross Validation (GCV). Daily weather ensembles from stochastic weather generators are coupled to the GLM models to provide ensembles of water temperature attributes and consequently, the probability distributions to obtain risk estimates. We demonstrate the utility of this approach to modeling water temperature attributes at a compliance point on the Sacramento River below Shasta Dam. Regulations on the dam depress the water temperature forecasting skill – to show this we present

skillful results from applying the approach to an unregulated location in the Pacific Northwest. The proposed method is general, can be ported across sites and can be used in climate change studies.

3.1 Background

River water temperatures downstream of reservoirs are influenced by water operations (release volumes and temperatures) and downstream atmospheric conditions. In making water release decisions, water managers must take into account constraints on available resources, such as total reservoir volume and cold water pool storage. In the late summer and fall, water temperatures in the Sacramento River in California's Central Valley can get too warm for native salmon, and water resource managers at Shasta Dam adjust the water release volume and temperature in attempts to maintain the downstream temperatures below certain compliance thresholds. However, they are working within the constraints of the available resources, and the primary management issue is the maintenance of the cold water storage in the reservoir and its availability throughout multiple seasons. Releasing too much cold water during the early and mid-summer can exhaust the cold water pool, resulting in increased thermal stress during late summer and early fall when fish are particularly vulnerable. Therefore, to enable the most efficient management of the available resources it is essential to have effective modeling and forecasting of downstream temperature attributes. Modeling efforts that effectively incorporate climate forecast information are needed to provide adequate guidance for making decisions at a variety of time scales (i.e., sub-daily to decadal). An integrated modeling framework has been developed to address the spatial and temporal limitations of the current decision support system on the Sacramento River [Danner et al., 2012; Pike et al., 2013]. The framework includes short-range forecasting for day-to-day operations, but is currently limited to 72 hour forecasts. In this

chapter, we present the development of a seasonal component to the framework that provides managers with monthly to seasonal forecasts of key water temperature attributes and probabilistic estimates of risk of meeting or exceeding predetermined thresholds of each attribute.

Recent advances in water temperature monitoring and modeling have facilitated the collection, analysis, and understanding of the complexity of water temperature behavior [Dunham et al., 2005; Isaak, 2011; Webb et al., 2008]. These concepts and theories are essential to the development of comprehensive models of water temperature. In general, water temperature models fall into two groups: deterministic and empirical. Deterministic models employ an energy budget approach by simulating water temperature through fluid flow and heat transport equations [e.g., Brock and Caupp, 1996; Carron and Rajaram, 2001; Taylor, 1998]. These models capture the physical processes of water temperature dynamics through consideration of unsteady flow, advective-dispersive transport of heat, and heat flux across the air-water and water-sediment interfaces. These models require input of detailed data on system geometry, flow, and climate. In addition, detailed data on physical attributes of the river are needed in order to robustly calibrate and validate the models. Furthermore, they are computationally intensive which can be a deterrent for operational agencies with limited expertise.

Empirical models, in contrast, generally consist of fitting regression models to daily water temperature as a function of air temperatures and streamflow [e.g., Bogan et al., 2006; Caissie et al., 2001; Neumann, et al., 2003]. These models rely on the strong correlation between air and water temperature which is driven by the joint dependence on solar radiation [Benyahya et al., 2007]. Such statistical models typically capture variability over large geographic extents

(e.g., long stretches of river) and also offer the benefits of computational efficiency and the ability to quantify uncertainty [Benyahya et al., 2007]. At daily or weekly time steps, statistical models have the ability to capture water temperature variability; however, at shorter time steps (e.g., hourly), the autocorrelation within the water temperature time series makes the regression increasingly difficult [Mohseni et al., 1998]. Empirical modeling techniques, therefore, offer a distinct advantage at longer time scales (i.e., seasonal), while deterministic models are preferred at short (i.e., sub-daily) time scales.

While regression models (mostly linear) have been the staple of modeling average daily water temperatures [e.g., Neumann et al., 2003], they are not suitable for modeling other skewed, discrete and binary attributes of daily water temperature such as probability of threshold exceedance and number of hours of exceedance. The generalized linear modeling (GLM) framework described in Section 2.5.3 provides a flexible alternative to modeling a variety of variables. Furthermore, weather and seasonal climate forecasts can be integrated quite easily for use in operational planning [e.g., Neumann et al., 2003, 2006; Towler et al., 2010a, 2010b]. Recently, GLMs have been used in stochastic weather generation [Furrer and Katz, 2007], waste water quality modeling [Weirich, et al., 2011], and in climate applications [Chandler, 2005; Chandler and Wheater, 2002].

3.1.1 Motivation

Managing river temperatures for the protection of coldwater fishes requires understanding and forecasting of a variety of attributes. In addition to the average daily water temperature, these fish are sensitive to acute maximum temperatures and prolonged exposure to higher temperatures [e.g., Myrick and Cech, 2001; Myrick and Cech, 2004; van Vleck et al., 1988]. Thus, forecasts of these attributes are needed for water resource managers to efficiently

plan the releases from reservoirs so as to optimally manage the cold water supply. However, empirical water temperature models focus mainly on average daily water temperature, ignoring the key attributes described above. To address this crucial need, we propose a GLM-based framework that can incorporate ensemble seasonal climate forecasts and model various water temperature attributes. Our motivation for developing this flexible framework comes in large part from the application on the Sacramento River, which we describe in detail below. We follow this with a description of the methods. We then show results from application to the study region – validation of the approach and combining it with seasonal climate forecasts. In the summary and discussion we provide thoughts for improvements and other applications of this modeling approach.

3.1.2 Study Site

The Sacramento River below Shasta Dam is the largest river in California (Figure 1.1). Over the past 150 years, water resources modifications, such as agricultural development, deforestation, damming, and channeling for flood mitigation, have led to substantial changes in temperature and flow in the Sacramento River [Deas et al., 1997; Moyle and Randall, 1998; Reisner, 1986]. Historically, the Sacramento River yielded large volumes of cold water during the winter/spring and smaller volumes of warmer water during the rest of the year [Myrick and Cech, 2000]. The river currently supports four salmon runs and one steelhead run. Shasta Dam has cut off access to critical spawning and rearing habitat but allowed cooler water releases during the critical late summer season to mitigate low flow and high water temperature [SFEP, 1992; van Vleck et al., 1988; Yates et al., 2008]. To protect the remaining salmon populations in the Sacramento River, a temperature target of 13.3°C was established for habitat between

Keswick Dam and Red Bluff Diversion Dam (Figure 1.1) [Bettelheim, 2001; Hallock and Fisher, 1985].

The installation of a temperature control device (TCD) on Shasta Dam during mid-1990s improved the capability of maintaining cool downstream water temperatures by enabling the release of water from different levels within the thermally stratified reservoir. With this level of control, managers attempt to conserve the cold water supply as late in the season as possible, and release it in the late summer/early fall when upper reservoir temperatures are already approaching the compliance limit. As a result, downstream water temperatures are now a combined function of operations and hydrometeorology. Inclusion of the daily flow and water temperature releases in any statistical modeling efforts may partially account for these operations as the volume of water released and respective temperature ultimately advect downstream and alter the thermal properties of the river.

While the resolution of the water management decision support tools for the Sacramento River has improved in recent years [Danner et al., 2012], the current forecasts are limited to 72 hours and are only applicable for day-to-day operations. These methods also fail to provide a measure of uncertainty and risk at longer time scales particularly in considering the potential impacts of future climate. We have developed a flexible GLM-based method that uses local polynomials to model and predict a key set of seasonal water temperature attributes: daily temperature maximum (DTX), daily temperature range (DTR), probability of threshold exceedance (POE), and number of hours of exceedance (NHE). This method will provide a simpler and complementary tool to the short-term water temperature models being developed for the Sacramento River [Pike et al., 2013]. We applied the model to the Balls Ferry compliance

point on the Sacramento River (Figure 1.1), a key management target for meeting temperature objectives on the river [BOR, 2004].

3.2 Methods

3.2.1 Generalized Linear Models

Local polynomial based GLMs have been used recently for seasonal streamflow forecasting [e.g., Bracken et al., 2010; Grantz et al., 2005; Regonda et al., 2006], flood frequency estimation [Apipattanavis et al., 2010c], and turbidity threshold exceedance modeling [Towler et al., 2010a, 2010b]. Here we build on these by modeling the four daily water temperature attributes (DTX, DTR, POE, and NHE) at Balls Ferry. We applied the threshold temperature of 13.3°C, as this is the current compliance target for protecting ESA-listed salmon on the Sacramento River. DTX is a critical indicator for the severity of high water temperatures on any given day; however, depending on the magnitude of DTX, there is opportunity for fish to adapt provided that there is a large diurnal range (DTR) and/or that the hours above that threshold are minimal (NHE). The probability of exceedance (POE) measures whether the mean daily temperature exceeds the threshold, and therefore serves as a measure of compliance. Together they provide a comprehensive prediction of the water temperature conditions and thus, help in better planning of reservoir operations.

3.2.2 Incorporating Seasonal Climate Information

When using the GLM models for seasonal water resources planning, daily air temperature and precipitation for the season are required. The hydrologic variables such as streamflow can be prescribed as a decision variable or optimized such that the optimal solution of flow and temperature releases result in the fewest number of exceedances and least volume of

cold water usage [Neumann et al., 2006]. Stochastic weather generators can provide ensembles of daily weather variables. There is a rich literature on traditional weather generators and nonparametric weather generators based on *K*-nearest neighbor time series bootstrap [see Furrer and Katz, 2008; Lall et al., 1996; and, references therein, for a review of traditional weather generators and nonparametric methods]. The *K*-nearest neighbor based stochastic weather generators [Rajagopalan and Lall, 1999; Yates et al., 2003] have been enhanced with the addition of Markov Chains [Apipattanavis, 2007] and labeled the semi-parametric weather generator (SWG). In this, a daily weather for day '*t*' is based on weather vector on day '*t-1*' and the precipitation states on days '*t-1*' and '*t*'; *K*-nearest neighbors of the weather vector on day '*t*' are obtained from historical days within a small window centered on day '*t*' and one of them is resampled using a weight function that gives more weighting to the nearest neighbor and least to the farthest [Lall and Sharma, 1996]. This weather generator has also been applied to crop modeling and agriculture planning [Apipattanavis et al., 2010a; Podesta et al., 2010], as well as, highway construction delays [Apipattanavis et al., 2010b]; we have implemented this for the study region. The SWG can be applied to generate a variety of daily weather sequences for a desired season of any length based on historical data, 'unconditional generation', or based on probabilistic seasonal climate forecasts, 'conditional generation'. These are described in the above references. Using the SWG, daily weather sequences are generated which are then incorporated in the GLM models to obtain ensembles of various water temperature attributes, and ultimately, cumulative distribution functions (CDFs). Using the CDFs, it is possible to compute the probability of exceeding threshold values for each water temperature attribute over the seasonal planning horizon by calculating the area under each CDF curve relative to any appropriate threshold value(s). Water managers will then be informed of the relative change in

risk for the upcoming season relative to climatology. We used the observed mean values from the window of July to September for the period 1994-2007 and from the same window in 2008, predicted and observed to be both warmer and drier than normal, to indicate the utility of seasonal forecasts information in operations as hypothetical planning scenarios.

3.3 Model Evaluation

We applied the model framework using the daily water temperature data at Balls Ferry and daily weather data from the Redding Airport, Redding, California (Figure 1.1), for the period 1994-2007. Daily and hourly streamflow data, and release volume and release temperature from Shasta Dam are also available for this period [CDEC, 2011]. From the hourly water temperature data, we computed DTX, DTR, POE and NHE for each day. Daily meteorological values from Redding [NCDC, 2011] and Shasta Dam release temperature and flow served as predictors for each variable for each month (Table 3.1). We then evaluated the predictive skill of the fitted GLM models using a cross validation model. For this procedure we randomly excluded ten percent of the data, fitted the model using the remaining data, and predicted the excluded values. We computed root mean square error (RMSE) for this prediction and repeated the process 250 times.

We generated ensembles of daily weather from the SWG; and, with the fitted GLM models, we generated ensembles of the water temperature attributes. We used the observed daily streamflow and release temperatures on the selected days as surrogates for standard operating procedures. Thus, generated attributes are displayed as boxplots along with the corresponding mean values from the observations. This exercise is designed to demonstrate the ability of capturing the historic variability of water temperature attributes. We generated a total of 100 simulations of daily weather, each 14 years in length.

Table 3.1: Subset of the predictors selected for the four water temperature attributes by month[1,2,3].

Month/ Season	NHE	POE	DTR	DTX
Jan	Intercept Only *2, 0.50, < 0.01, NA*	Intercept Only *2, 0.70, < 0.01, NA*	pcp,tx,tn,pcp1,tn1,q1 *2, 0.07, < 0.01, 0.22*	tx,tn,q,tw,tx1,tn1,tw1 *2, 0.07, < 0.01, NA*
Feb	Intercept Only *1, 0.50, < 0.01, NA*	Intercept Only *2, 0.55, < 0.01, NA*	tx,tn,q,tx1 *2, 0.05, 0.12, 0.18*	tx,tn,tw,tn1 *2, 0.05, < 0.01, NA*
Mar	pcp,tn,tw,pcp1,tx1,tn1,tw1 *2, 0.50, 0.15, 0.14*	Intercept Only *2, 0.70, < 0.01, NA*	pcp,tx,tn,q *1, 0.55, 0.11, 0.66*	tx,q,tw,pcp1,tx1,tn1,tw1 *2, 0.06, < 0.01, < 0.01*
Apr	pcp,tx,tn,tw,tn1,q1,tw1 *2, 0.50, 1.73, 0.68*	tx *2, 0.55, 0.11, 0.03*	pcp,tx,tn,q *1, 0.70, 0.12, 0.58*	tx,tx1,tn1,q1,tw1 *2, 0.06, < 0.01, < 0.01*
May	pcp,tx,tn,q,pcp1,tx1 *2, 0.50, 2.84, 0.14*	pcp,tx,tn,tw,pcp1,q1,tw1 *2, 0.55, < 0.01, 0.35*	pcp,tx,tn,q,tx1 *2, 0.05, 0.01, 0.17*	tx,q,tx1 *2, 0.95, < 0.01, 0.02*
Jun	tx,tn,q,tx1,tn1,tw1 *1, 0.50, 2.73, 0.53*	tw *1, 0.50, 0.05, 0.25*	pcp,tx,tn,pcp1,tx1,q1 *2, 0.31, 0.03, 0.07*	tx,tn,q1,tw1 *2, 0.05, < 0.01, 0.48*
Jul	tx,q,tw,tn1 *2, 0.95, 2.58, 0.36*	Intercept Only *2, 0.65, 0.08, 0.23*	pcp,tx,tn,q *2, 0.40, 0.03, 0.48*	q,tw *1, 0.05, < 0.01, 0.53*
Aug	pcp,tn,q,tw,tw1 *2, 0.90, 1.57, 0.48*	Intercept Only *2, 0.50, 0.03, 0.05*	pcp,tx,tn,tx1 *1, 1.00, 0.08, 0.15*	pcp,tx,q,tw,tw1 *2, 0.05, < 0.01, 0.03*
Sep	pcp,tx,tn,tw,tx1,q1,tw1 *2, 0.65, 2.61, 0.55*	tn,q1,tw1 *2, 0.75, 0.45, 0.54*	pcp,tx,q,tx1 *2, 0.55, 0.02, 0.50*	tx,tw,tx1,tw1 *2, 0.05, < 0.01, 0.22*
Oct	pcp,tn,q,tw,tx1,q1,tw1 *1, 0.50, 4.75, 0.57*	tn,tw,tx1 *2, 0.50, 0.58, 0.60*	pcp,tx,tn,tw *2, 0.85, 0.03, 0.72*	tx,tn,tw,tw1 *2, 0.05, < 0.01, 0.21*
Nov	pcp,tx,tn,tx1,tw1 *2, 0.50, 3.17, 0.66*	tx,tn,tw,tx1,tw1 *2, 0.75, 0.32, 0.66*	tx,tn *1, 0.25, 0.09, 0.60*	tx,tn,tx1,tw1 *2, 0.05, < 0.01, 0.07*
Dec	pcp,tw,pcp1,tn1 *1, 0.50, 0.02, 0.85*	pcp,tn1,tw1 *2, 0.85, < 0.01, 1.00*	pcp,tx,tn,q,tx1 *2, 0.06, < 0.01, 0.02*	tx,tn,tw,tx1,q1,tw1 *2, 0.07, < 0.01, 0.99*
JAS	pcp,tx,tn,q,tw,tx1,tw1 *2, 0.50, 2.11, 0.61*	tx,q1,tw1 *2, 0.50, 0.24, 0.44*	pcp,tx,tn,tx1,tw1 *2, 0.97, 0.05, 0.27*	pcp,tx,q,tw,tw1 *2, 0.02, < 0.01, 0.36*

1 Variables listed are daily values of precipitation (pcp), maximum air temperature (tx), and minimum air temperature (tn) at Redding, CA; and, water temperature (tw) and flow released (q) from Shasta Dam. Variables appended with a "1" indicate prior day values.

2 Water temperature attributes include number hours of exceedance (NHE), probability of exceedance (POE), daily temperature range (DTR), and daily maximum temperature (DTR).

3 Bottom line of values provide the polynomial order, alpha, GCV, and R^2 separated by commas. R^2 was computed only for values above the thresholds provided in Table 2.

We examined the effects of climate on water temperature attributes by using the conditional SWG simulations as input into the GLM framework. We use the four conditional simulations for the period July through September [Caldwell and Rajagopalan, 2011] to generate CDFs for each of the four predicted water temperature attributes. We considered dry (D), hot (H), very dry (VD), and very hot (VH) conditional scenarios and compare these to the observed or climatological (CL) distribution functions to indicate changes relative to climate forecast input. In particular, we used the seasonal climate forecast issued by the International Research Institute for Climate and Society in June 2008 for the summer of 2008 (July through September) for the dry and hot scenarios (Figure 3.1) to conditionally generate daily weather sequences for the summer season and, consequently, the distribution functions of water temperature attributes.

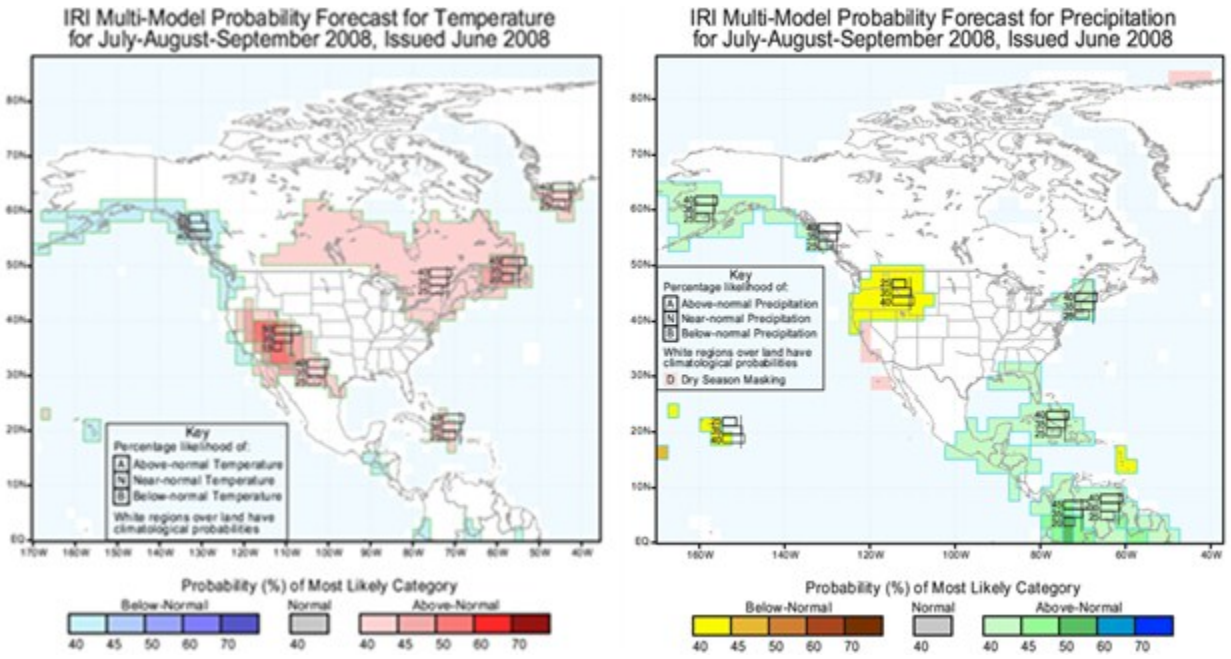

Figure 3.1: Probabilistic seasonal climate forecasts of temperature (left) and precipitation (right) for the period July through September 2008 (issued in June 2008) as applied in the dry and hot conditional scenarios for the weather generator.

3.4 Results

We applied the developed methods for the entire year; however, the primary months of concern for cold water pool management stretch from May through October. Here, we focus our results on a portion of the summer months (July-September) when the water temperatures on the Sacramento River are the highest and have the greatest management implications. We fitted the best (based on BIC or AIC) local polynomial GLM for each water temperature attribute by month using a suite of ten predictor variables – identifying the best subset of predictors and the local polynomial parameters for each (Table 3.1). For a number of cases the parameters α and p deviate from 1, indicating local nonlinear features. Subset selection for NHE and POE indicate the intercept only fits during the months of January and February when no or very few days exceed 13.3 °C. In addition, POE has an intercept that only fits during the months of July and August, where the complement is true and most days exceed 13.3 °C. In general, the subset selections for NHE include more predictors compared to other water temperature attributes, due to the fact that this is somewhat of a noisy variable relative to others. We also note that in many cases prior day values are often selected as one of the variables to account for the pre-existing state of the system.

During the period of July-September, scatterplots with a local polynomial smoother indicate DTR is linearly proportional to maximum air temperature up to 30 °C, after that reaches an asymptote at DTR ~2.5 °C (Figure 3.2a). There is an upper limit to the diurnal range once maximum air temperature reaches 30 °C. NHE is poorly correlated to daily mean water temperature releases at Shasta for temperatures less than 8 °C (Figure 3.2b), but linearly proportional for values above 8 °C. Such linear and non-linear features also exist for other water

temperature variables (not shown), which underscores the utility of the application of a local polynomial GLM.

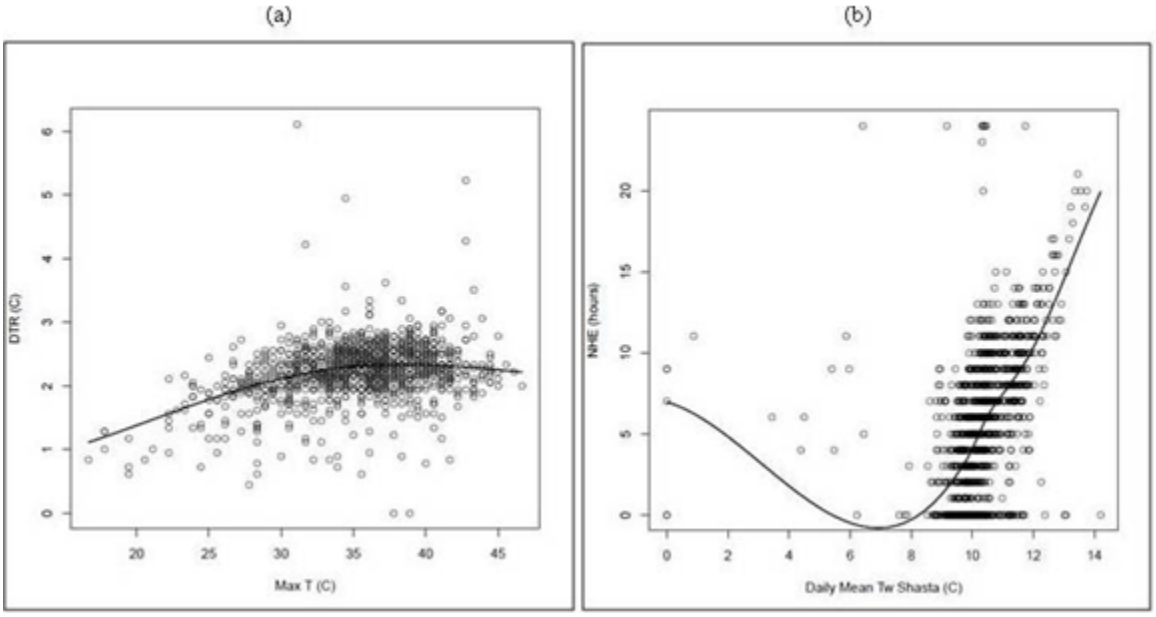

Figure 3.2: Scatterplots of (a) DTR and maximum air temperature and (b) NHE and daily mean water temperature release at Shasta for the season of July through September. The local estimation curve is plotted to indicate local non-linear features in the data.

The model is generally able to predict the observations of the four daily temperature attributes during the July-September period with R^2 values ranging from 0.27 (for DTR) to 0.61 (for NHE) (Figure 3.3). The NHE is well modeled, with the exception of an under estimation for higher observed hours of exceedance, especially 15 hours and beyond (Figure 3.3a). The probability of exceedance (Figure 3.3b) too is under estimated (i.e., lower probability values when there is exceedance). The predictions of DTR values greater than 2.5°C are under estimated (Figure 3.3c) and somewhat less so in the case of DTX (Figure 3.3d) for values beyond 16 °C. DTR and DTX are influenced by the clustering of values in the observed data between 1-3 °C and 13-15 °C, respectively.

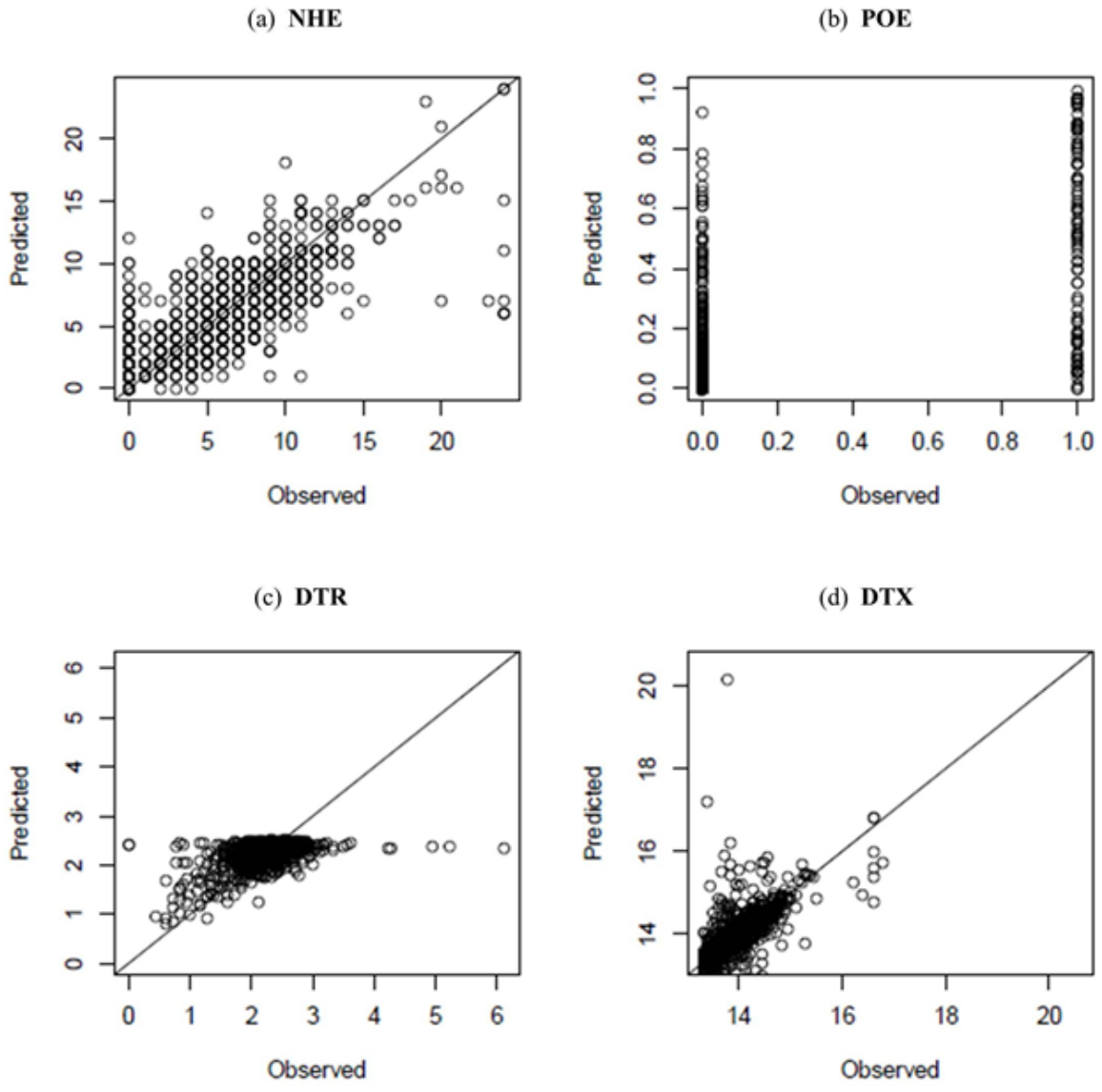

Figure 3.3: Comparison of observed and predicted values from the GLM for (a) NHE in hours; (b) POE in probability; (c) DTR (°C); and, (d) DTX (°C) for the season of July through September.

To test the predictive skill of the models, we computed the RMSE in a cross validation model. We excluded 10% of the observations at random. These values were predicted from the remaining values and repeated 250 times. Skill is generally best early in the year (January to June) for NHE and POE with higher RMSE values during the summer and fall seasons (Figure 3.4a and Figure 3.4b). For DTR and DTX, mean RMSE values are highest during the winter and spring when flood control and snowmelt runoff are more dominant drivers of water temperatures

than meteorology or standard operations (Figure 3.4c and Figure 3.4d). Variability in the RMSE, however, is low during the summer months for DTR and DTX, except for August for DTX, indicating a greater level of confidence in the predicted values. The mean RMSE values consistently range between 0 and 1 °C for DTR and DTX, which may be a tolerable threshold for seasonal planning efforts.

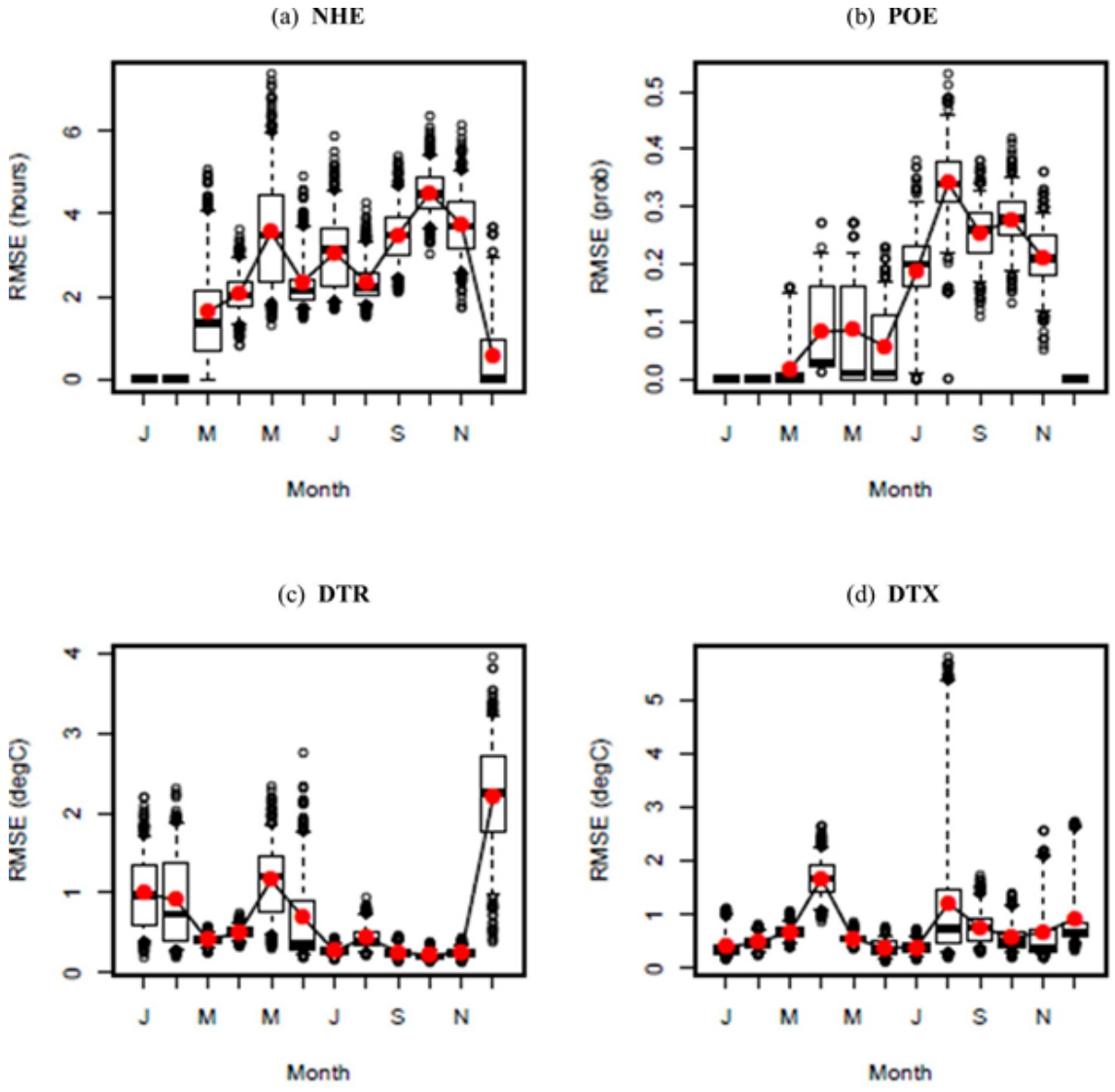

Figure 3.4: Cross validation model results for (a) NHE; (b) POE; (c) DTR; and (d) DTX by month. Observed climatological means of each variable (black line with overlaid red points) are shown. Boxplots provide the median as horizontal black line, box is the interquartile range, whiskers indicate 5th and 95th percentiles, and hollow points indicate values outside the whiskers.

3.4.1 Water Temperature Attributes: Unconditional Ensembles

We used the SWG to generate ensembles of daily weather sequences – i.e., 'unconditional' simulations. We used these in the GLM model to generate ensembles of daily water temperature attributes and displayed them as boxplots for each month along with the observed monthly mean values. The weather generator ensembles provide a rich variety in the water temperature attributes that adequately capture the historical mean (Figure 3.5).

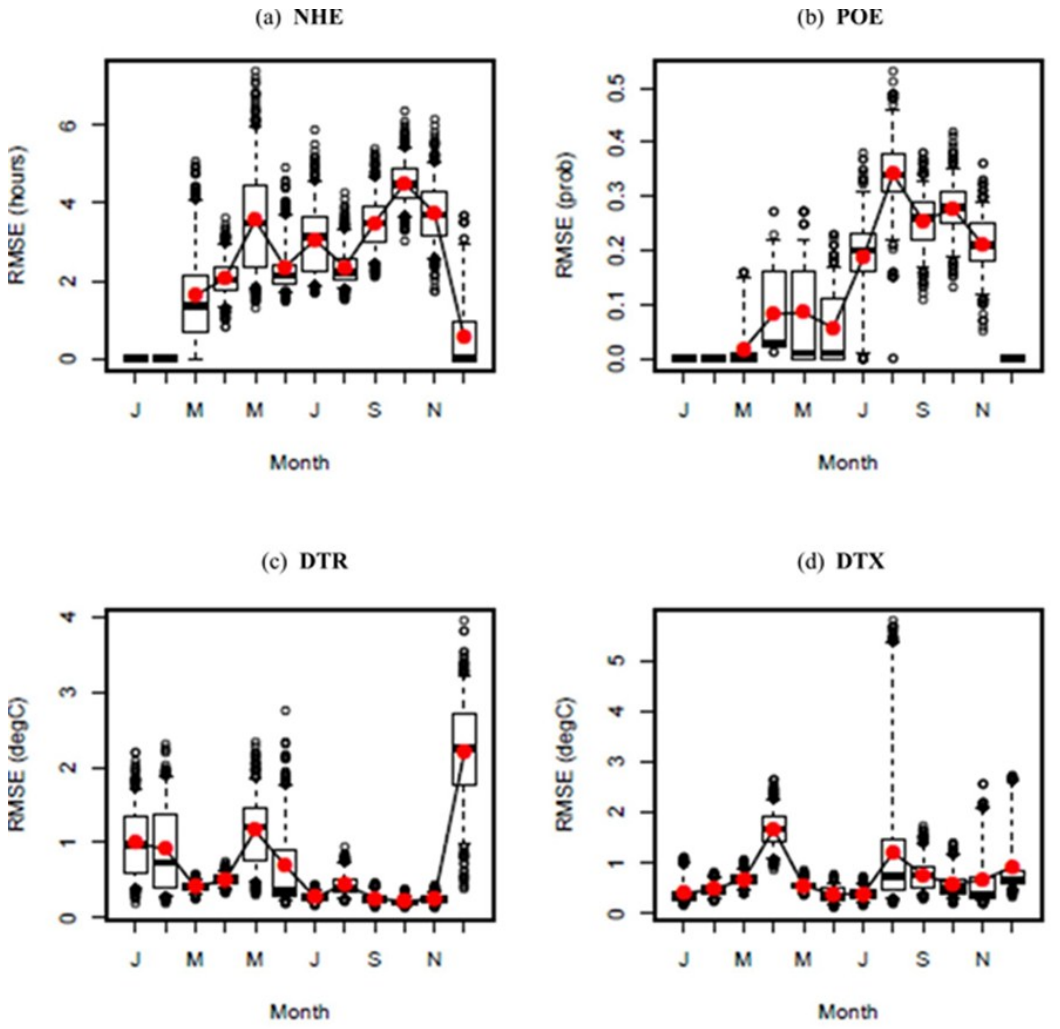

Figure 3.5: Comparison of observed and unconditional simulations of (a) NHE; (b) POE; (c) DTR; and, (d) DTX using the GLM coupled with the SWG by month. Observed climatological means of each variable (black line with overlaid red points) are shown. Boxplots of unconditional simulated values provide median as horizontal black line, box is the interquartile range, whiskers indicate 5th and 95th percentiles, and hollow points indicate values outside the whiskers.

Exceptions include: (i) under-estimation of NHE during the months of April through June, and over-estimation in October (Figure 3.5a); and, (ii) under-estimation of POE during the months of September and October with over-estimation in November (Figure 3.5b). Any biases in the DTR and DTX are not discernible (Figure 3.5c and Figure 3.5d). These scenarios reach beyond the observed record and offer an avenue to apply probabilistic approaches in seasonal water temperature management. This indicates that the coupling of a SWG to the local polynomial GLM approach to predict and simulate water temperature attributes is quite robust.

3.4.2 Water Temperature Attributes: Conditional Ensembles

We generated conditional daily weather sequences for the July-September period for the four climate scenarios (D, VD, H and VH) described earlier. For the D and H scenarios, we used forecasts for 2008 (seen in Figure 3.1). We combined the generated daily weather ensembles with the local polynomial GLM to provide ensembles of water temperature attributes and the respective CDFs from the ensembles and climatology (Figure 3.6). The steepness of the slope of a CDF curve can be interpreted as a larger contribution to the cumulative probability across a given range of values; the probability of falling between the values is determined by the difference cumulative probability values on the y-axis. For example, at NHE less than 3 hours and greater than 12 hours, all of the CDFs of NHE during warmer and drier conditions (colored) indicate enhanced risk compared to climatology (black) (Figure 3.6a). The largest risk of NHE > 12 hours occur in the very hot conditional simulations with a probability of ~0.40, compared to the other conditional simulations (~0.20) and climatology (<0.10). Similarly, the conditional runs indicate an increased risk of POE compared to climatology (Figure 3.6b). The very hot simulation estimated the greatest shift in POE with the steepest slope at POE values > 0.60 compared to other curves. There is an increased probability of decreased diurnal range (DTR) in

the conditional simulations, as expected in a hotter regime – this can be seen by the CDFs being shifted to lower DTR values relative to climatology (Figure 3.6c). Likewise, there is an increased risk of higher DTX (Figure 3.6d) compared to climatology.

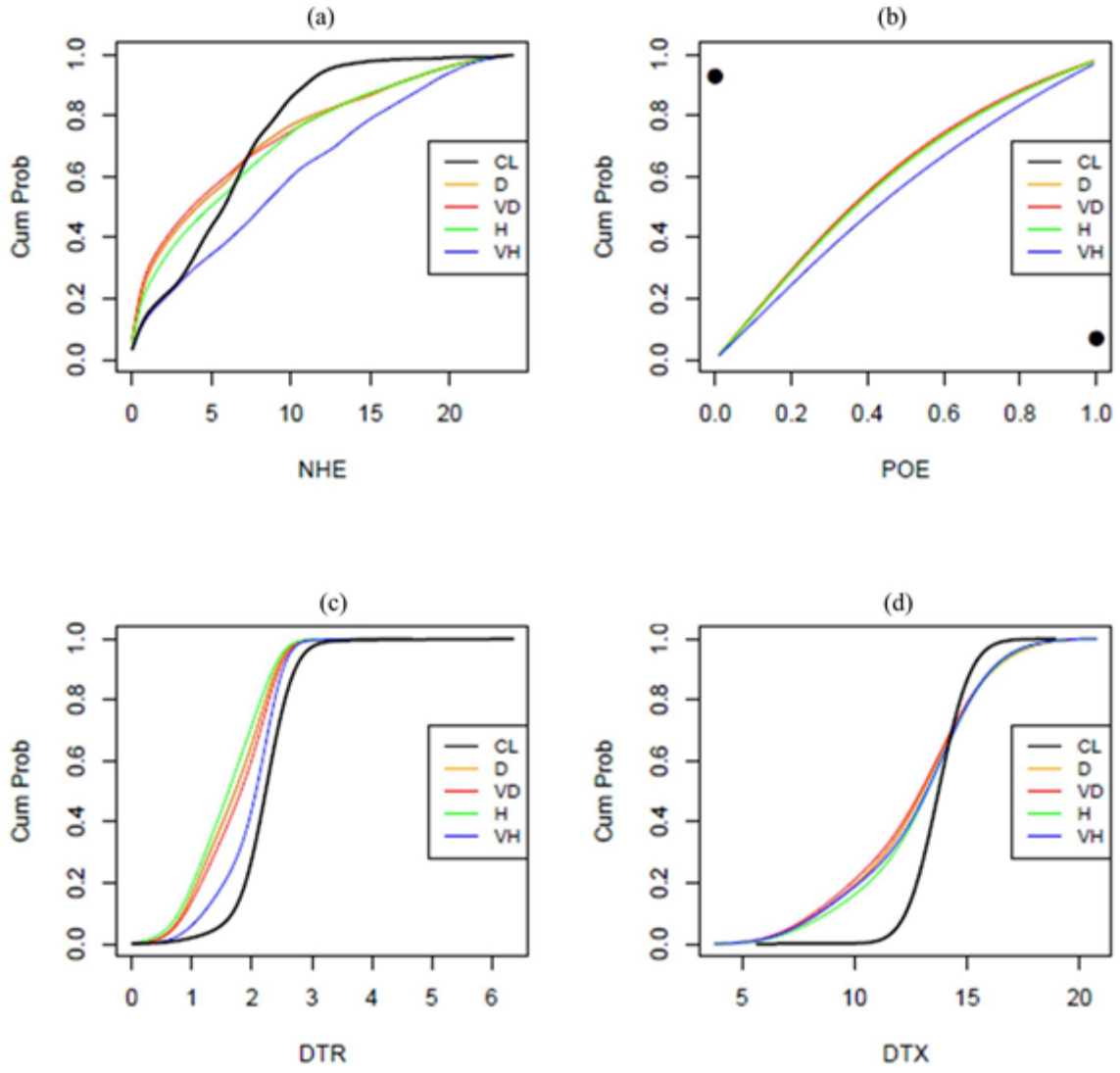

Figure 3.6: Cumulative distribution functions for the season of July through September for (a) NHE; (b) POE; (c) DTR; and, (d) DTX for the observed climatology (CL), dry (D), very dry (VD), hot (H), and very hot (VH) conditional simulations.

As described in the comparison to climatology, these exceedance probabilities can provide an indication of risk with respect to thresholds relevant for management by computing the area under the curve relative to a threshold value, for example the climatological mean for the period of interest. Using values from 2008 as a reference (Table 3.2), we examined the

relative change in risk compared to climatology. The findings are summarized as a bar plot, whereby the probability of exceeding climatological means of each variable are shown relative to the probabilities from each conditional simulation (Figure 3.7).

Table 3.2: Probabilities of threshold criteria computed from the CDFs in Figure 3.6. Threshold values correspond to July through September seasonal means in 2008.

Variable/Threshold	CL	D	VD	H	VH
NHE > 13.4	0.04	0.17	0.17	0.17	0.28
POE > 0.79	0.15	0.12	0.12	0.12	0.17
DTR > 2.33 C	0.17	0.26	0.25	0.27	0.22
DTX > 14.78 C	0.17	0.23	0.23	0.24	0.24

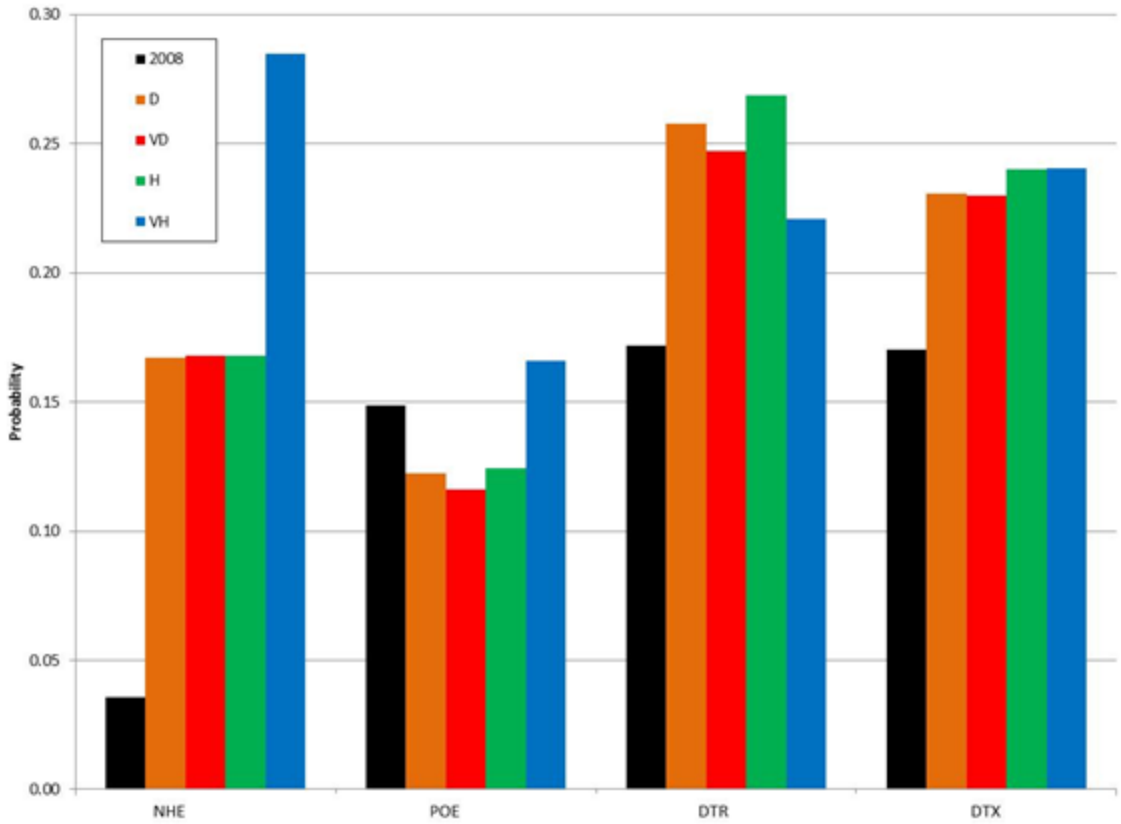

Figure 3.7: Probabilities of threshold criteria (from Table 3.2) for the observed (2008), dry (D), very dry (VD), hot (H), and very hot (VH) conditional scenarios.

All of the conditional scenarios provide increased risk of NHE greater than 13.35 hours, indicating a tendency for more days with mean water temperature above 13.3 °C (Table 3.2). In addition, there is a decreased risk of POE above 0.79, except for the very hot scenario (Table 3.2 and Figure 3.7). Increased risk is noted for DTR < 2.33 °C, which would suggest that recovery time for fish will be diminished during hotter or drier than normal conditions if mean water temperatures are high, regardless of the magnitude of the climate shift. Despite the fact that the GLM model generally under-estimates higher values of DTX (Figure 3.3), increases in risk of DTX > 14.78 °C are evident for all conditional scenarios (Table 3.2 and Figure 3.7).

3.5 Summary and Discussion

We have developed a complementary statistical modeling tool using local polynomial based GLMs that provides monthly to seasonal forecasts of key water temperature attributes and probabilistic estimates of risk of meeting or exceeding predetermined thresholds of each attribute. The GLM framework can model a variety of variables such as discrete, binary, and continuous, among others. For example, we fitted models to predict a variety of water temperature attributes such as number of hours of exceedance (discrete), probability of temperature exceeding a threshold (binary), and daily maximum water temperature and daily water temperature range (both continuous). We fitted models for each month and for each variable separately using a large pool of predictor variables based on atmospheric variables (e.g., temperature, precipitation from current and previous day) and water variables (e.g., flow, temperature from previous day). Based on cross validated skill scores, the models performed well, especially during the summer months of interest. We applied the stochastic weather generator (SWG) to generate ensembles of daily weather sequences in an unconditional manner (i.e., assuming all of the historical years are equally likely) and conditional manner (based on

probabilistic seasonal climate forecast). We also generated local polynomial GLM ensembles of water temperature attributes. We found that these ensembles were consistent with the seasonal forecast, demonstrating the ability of the proposed methodology to provide projections of water temperature attributes before the start of the season. The ensembles of water temperatures provide the estimates of risk of exceeding various compliance thresholds. These risk estimates can be of immense help to water managers in making plans for additional water or changes in operations before the start of the season to help mitigate water temperature risk in a sustainable manner.

Our integration of the GLM and SWG allows investigation of the relative change in risk of meeting temperature criteria at Balls Ferry by performing both unconditional and conditional simulations. As a proof of concept, the threshold values from 2008 were used to indicate relative changes of risk captured by the conditional scenarios (Figure 3.7). For NHE, DTR, and DTX, the forecasts issued in June 2008 would have been sufficient to convey an increased risk of meeting or exceeding the thresholds from Table 3.2; however, a highly skewed forecast – like that offered in the very hot scenario – would have been required to suggest a POE value of 0.79 for the three-month period. Though not applied in the current study, the flows and water temperature releases associated with each conditional scenario could be adjusted from the observed values used in the GLM to modify the predicted values of each water temperature attribute. For example, operators could apply a designated 90-day flow and temperature regime derived from historical data (i.e., a prior extremely hot or dry years) to adjust the predicted values from the GLM until the relative risk is reduced to a climatological value or other acceptable level. In essence, multiple flow and temperature regimes could be applied through the GLM to determine an optimal solution for reducing cold water usage and maintaining temperatures downstream.

Atmospheric variables are typically well-correlated with water temperatures, particularly during the summer months when solar radiation is at a maximum. In addition, water temperature is generally inversely proportional to flow as larger volumes of water take longer to warm and cool. The skill of the GLM is directly proportional to the strength of these correlations between the hydrometeorological predictors and the water temperature at Balls Ferry. During the summer months, the water temperatures on the Sacramento River are also strongly influenced by the temperature and volume of water released from Shasta Dam. The interactions between the environment and operations are highly non-linear and, therefore, the local polynomial based GLM is capable of predicting the response in temperature attributes. Predictor variables from the prior day state of the hydrologic system improve the model fits by including residence time of water release impacts and persistence into the model (i.e., if the prior day water temperatures are cool, there is a natural tendency for today to also be cool.

Since water management (e.g., power generation) may involve sub-daily management of releases [Carron and Rajaram, 2001], the GLM might be even more effective during the summer months if sub-daily dam operations were included in the model fitting process, along with specific information on releases from the temperature control devices on Shasta Dam. Unfortunately, these data are either unavailable, discontinuous, or require reconstruction using detailed hydraulic modeling efforts. To some degree, this relationship was included in the GLM through the mean daily flow and water temperature released at Shasta. We applied this framework to modeling stream temperatures in the Methow River basin, an unregulated system in the State of Washington [Caldwell et al., 2013a], to assess the impact of climate change on fish habitat. Results from an unregulated system (Chapter 4) indicate that model predictions are very good in comparison to the current application (Figure 3.3). This indicates that the

methodology is portable to other watersheds and can provide improved skill when water management impacts are minimal.

Water projects in the western United States have fundamentally altered temperature regimes in major rivers, particularly downstream of large dams. While dams such as Shasta can selectively release colder water to meet downstream temperature criteria, the current operations approach does not have sufficient forecasting capabilities. High resolution water temperature models have been developed to improve forecasting; but, these models are limited to forecasts of hours to several days, and cannot provide seasonal-scale planning guidance in a timely manner, unless coupled with input from statistical models.

Protection of the native cold water fish in the Sacramento River is a challenge in this highly altered river system. Careful and innovative management strategies are needed, as any additional changes in water temperature in response to climate could result in conditions that favor non-native species [May and Brown, 2002]. Yates et al. [2008] suggest that future warming in air temperatures of 2 – 4 °C could lead to additional threshold temperature exceedances, particularly in August and September of drought years. In addition, maintaining the cold pool in Shasta Lake would be difficult through the summer and fall [Yates et al., 2008]. As such, additional research is needed to improve seasonal forecasts of water temperatures during the critical summer and late fall period. Future modeling efforts, therefore, should concentrate on additional predictors such as observed dam operations. Integration of the GLM with hydraulic models of Shasta Lake would also be beneficial by ensuring upstream criteria within the reservoir are met and by providing an input for flow and temperature release information to the GLM, as opposed to the use of a surrogate such as the simulated flow and temperature values

from the SWG. Optimization techniques could then be applied directly to monitor cold water storage and both in-lake and downstream habitat.

This chapter of the dissertation was submitted in June 2013 to the American Society of Civil Engineers' Journal of Hydrologic Engineering as an article entitled 'Statistical Modeling of Daily Water Temperature Attributed on the Sacramento River'. The article is under review at the time of publication of the dissertation and is listed as Caldwell et al. [2013b] in the Bibliography.

4 STATISTICAL MODEL: DECADAL APPLICATION

4.1 Abstract

Management of water temperatures in the Columbia River Basin (Washington) is critical because water projects have substantially altered the habitat of Endangered Species Act (ESA) listed species, such as salmon, throughout the basin. This is most important in tributaries to the Columbia, such as the Methow River, where the spawning and rearing life stages of these cold water fishes occurs. Climate change projections generally predict increasing air temperatures across the western United States, with less confidence regarding shifts in precipitation. As air temperatures rise, we anticipate a corresponding increase in water temperatures, which may alter the timing and availability of habitat for fish reproduction and growth. To assess the impact of future climate change in the Methow River, we couple historical climate and future climate projections with a statistical modeling framework to predict daily mean stream temperatures. A *K*-nearest neighbor algorithm is also employed to: (i) adjust the climate projections for biases compared to the observed record and (ii) provide a reference for performing spatiotemporal disaggregation in future hydraulic modeling of stream habitat. The statistical models indicate the primary drivers of stream temperature are maximum and minimum air temperature and streamflow and show reasonable skill in predictability. When compared to the historical reference time period of 1916-2006, we conclude that increases in stream temperature are expected to occur at each subsequent time horizon representative of the year 2020, 2040, and 2080, with an increase of 0.8 ± 1.9 °C by the year 2080.

4.2 Background

The health and productivity of aquatic ecosystems are highly sensitive to stream temperature [Caissie, 2006; Webb et al., 2008]. Temperature fluctuations induce changes in metabolic rates, concentrations of key water quality parameters (e.g., dissolved oxygen), biotic assemblages, and life cycle processes (e.g., spawning, migration, mortality). Since changes in stream temperature are closely tied to meteorological and hydrological conditions [Smith and Lavis, 1975], modification of the variability and mean state of the existing hydroclimate should have a corresponding effect on aquatic ecosystems.

In response, multiple research efforts have been focused on the prediction of stream temperature under multiple future climate conditions [e.g., Mantua et al., 2010; Null et al., 2012; Webb et al., 2008]. Often, these models focus on geographical regions (e.g., Pacific Northwest) which require a hydrologic system with large spatial (sub-basin to watershed scale) and temporal (daily to weekly) resolutions [Ficklin et al., 2012; Mantua et al., 2010; Null et al., 2012]. These models typically couple hydrologic models with stream temperature models to inform broad decisions on the magnitude and general spatial extent of climate-related impacts on thermal properties of rivers and streams. Null et al. [2012] coupled the Water Evaluation and Planning System (WEAP21) hydrologic model with the Regional Equilibrium Temperature Model (RTEMP) physical temperature model, while Ficklin et al. [2012] modified the temperature model in the Soil and Water Assessment Tool. Mantua et al. [2010] coupled output from the Variable Infiltration Capacity (VIC) model with the statistical stream temperature model of Mohseni et al. [1998] to simulate weekly stream temperature.

The incorporation of the hydrologic forcings into stream temperature models has been shown to improve the predictability of models [Lowney, 2000; van Vliet et al., 2011; Webb et

al., 2003]. For example, Ficklin et al. [2012] improved on an existing stream temperature model by including the contributions of multiple source water constituents (e.g., groundwater, snowmelt, surface runoff, in-stream flow) to the thermal dynamics for seven watersheds across the western United States. In addition, they adjusted the input air temperatures, precipitation, snowmelt, and groundwater to evaluate the sensitivity of stream temperature to hydroclimate changes.

The complexity of any modeling system, however, is usually directly related to the required level of quality and continuity of input data sets. There are generally two types of stream temperature models applied in assessing future climate impacts: (1) physically-based models (rooted in the solution of fluid flow and heat transport equations) and, (2) empirical models (relying on the correlation strength between meteorology and stream temperature). The advantage of physically-based models is the ability to estimate the spatial and temporal distribution of stream temperature at fine scales over small domains; therefore, they are typically restrictive for performing regional simulations or for predicting changes at longer time scales (e.g., years to decades) due to extensive requirements of data and computing power [Taylor, 1998]. Physical models can be adapted for larger domains as described previously [e.g., Null et al., 2012]; but, usually results in a reduction in temporal resolution. Detailed, high resolution, continuous model input is required including inputs of system geometry, meteorological forcing, and hydrological forcing. In unregulated systems, these data are often unavailable, inconsistent, or of poor quality.

For these data sparse situations, stream temperatures are often modeled using statistical regression [e.g., Mohseni et al., 1998; Webb et al., 2003; Webb et al., 2008]. Statistical methods are appropriate at larger spatial and temporal scales, as they offer the benefit of computational

efficiency [Benyahya et al., 2007]. Empirical models typically consist of regressions between stream temperature and environmental conditions, such as air temperature which is driven by the joint dependence of each on solar radiation [Benyahya et al., 2007]. Thus, these models are easily integrated with output from other modeling systems (e.g., hydrologic models forced with input from global climate models (GCMs)), which provides an opportunity to apply projected changes in hydroclimate directly, rather than making discrete adjustments (say, increasing air temperatures by 2°C) to understand model sensitivity to input changes. Statistical models are limited regarding temporal resolution, in that they are appropriate for application at daily or weekly time steps [Mohseni et al., 1998]. At shorter time steps, Mohseni et al. [1998] found that autocorrelation within the stream temperature time series makes regression increasingly difficult.

In this chapter, we present the first statistical modeling effort to apply future hydroclimatological changes at sub-daily time scales (i.e., hourly) with spatial resolutions at the sub-reach scale (i.e., meters). The proposed approach seeks to bridge the gap between daily values and the hourly requirements of high-resolution hydraulic modeling efforts. For example, this type of high-resolution data is essential for assessing the influence of mitigation efforts (e.g., channel dredging, riparian zone refurbishment) that seek to alleviate future climate impacts on stream temperature. As such, we develop a flexible statistical modeling framework that is capable of providing input at high spatial and temporal resolution to these models. We couple a generalized linear model (GLM) [McCullagh and Nelder, 1989] at the daily time scale with a *K*-nearest neighbor (*K*-nn) resampling algorithm, which provides a bias-correction function and allows disaggregation of daily values to hourly estimates of stream temperature. While we focus on the generation of a daily mean state variable (i.e., mean daily stream temperature), the modeling framework provides the opportunity to predict daily variables with a variety of

distributions (i.e., continuous, logistic, discrete), such as daily maximum stream temperature, exceedance/non-exceedance of a particular thermal threshold, and number of hours exceeding that threshold, respectively. The computational efficiency of the statistical models allows the future projections of stream temperature to extend to decades, where physically-based models are currently restrictive at the prescribed spatial and temporal resolution.

We test the methodology in the Methow River basin in the State of Washington in a roughly 1 kilometer reach near the confluence of the Methow and Chewuch Rivers (Figure 4.1). The area of interest is described in the subsequent section (Section 4.3) along with the datasets available. The coupled GLM-VIC statistical modeling framework, *K*-nn methodology, and disaggregation technique are presented in Section 4.4. Application and results from the proposed framework including stream temperature projections for three future time periods (2020s, 2040s and 2080s) are described in Section 4.5. Chapter conclusions along with a discussion of model uncertainty under the proposed framework are summarized in Section 4.6.

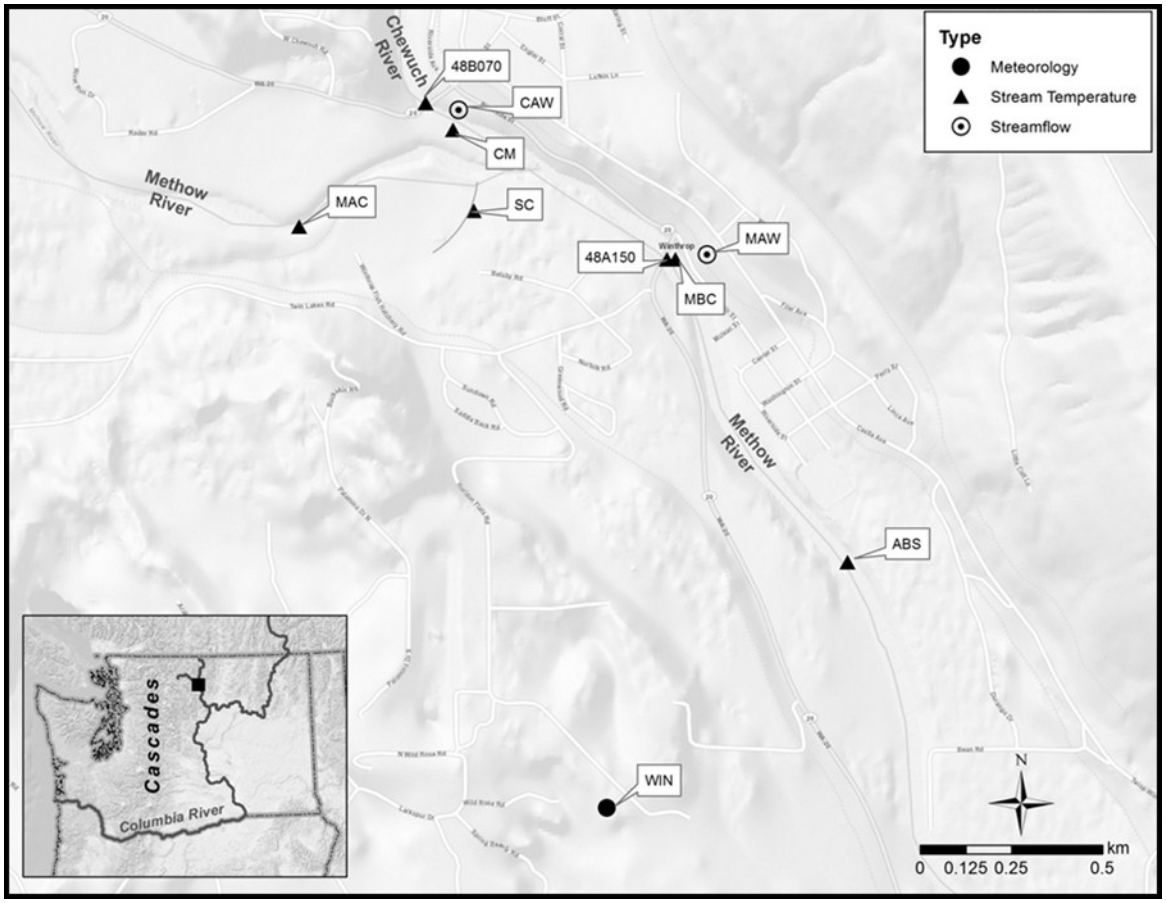

Figure 4.1: Map of the confluence of the Methow and Chewuch Rivers. Observation sites near Winthrop, Washington, are indicated. Inset shows the location of the study area (black box) relative to the State of Washington.

4.3 Study Area

The Methow River in Washington (see Figure 4.1) offers prime spawning habitat for salmon and other cold-water fish. It is a tributary to the Columbia River system and offers a natural setting with generally unregulated flow. During the summer months, streamflow in the Methow River is typically low (less than approximately 25 cubic meters per second (cms)), resulting in both higher thermal vulnerability and cutoff side channels that limit the habitat available to these fish. Being unregulated, there is an inability to mitigate these high temperatures through upstream water releases. Under these circumstances, mitigation efforts rely heavily on stream restoration projects and riparian zone refurbishment.

Future climate projections which indicate increasing air temperature in the western United States suggest the potential for increasing stream temperatures in response to changes in hydrology (i.e., snowmelt, streamflow) and additional heating [e.g., Ficklin et al., 2012; Mantua et al., 2010]. To assess the impacts of climate change in the Methow River, a statistical modeling framework is developed for generation of daily projections of stream temperature. The framework is unique in that it must provide the ability to generate sub-daily meteorological forcings and hydrologic boundary conditions to be integrated with an hourly time-step, two-dimensional hydraulic model for predicting spatial variations of stream conditions and the impacts of various mitigation efforts.

In this chapter, observations of stream temperature and environmental conditions (i.e., air temperature, precipitation, and streamflow) are used to develop statistical models of daily mean stream temperature for the Methow River near Winthrop, WA. The location is situated at the confluence of the Methow and Chewuch Rivers, which corresponds to the site of an ongoing hydraulic modeling project. Therefore, there is a need for hourly boundary condition inputs at locations upstream of the confluence, including temperature and flow projections.

4.3.1 Data

Statistical models of stream temperature require hydrometeorological data as input. Typical hydrometeorological variables include maximum/minimum air temperature (T_{ax} and T_{an}, respectively), precipitation (P_p), and streamflow (Q). The quality and quantity of the data are two primary indicators of the level of skill that can be expected from the models. For the current study, there is a limited set of water temperature data which requires a subset of data from the period 2005 to 2011.

This research uses two types of data: observed and simulated. The observed data includes stream temperature, T_s (the independent variable for the model), and, T_{ax}, T_{an}, P_p, and Q (the dependent variables). Once the models are developed using observed time series, the simulated model outputs (see Section 4.3.1.5) from the VIC model can be integrated to produce future scenarios of T_s. This section describes the individual datasets by providing the metadata associated with each and quality control employed prior to use. The locations of the observed data are shown in Figure 4.1.

4.3.1.1 Stream Temperatures

Near the confluence of the Methow and Chewuch Rivers, a total of seven T_s time series are available (Table 4.1). The sources of these data include the United States Forestry Service (USFS), US Bureau of Reclamation (BOR), Wild Fish Conservancy (WFC), and Washington State Department of Ecology (DOE). It should be noted that while the period of records and frequencies in Table 4.1 would indicate a wealth of data at these sites, none of the gauges provide continuous observations throughout the period of record, with most measurements occurring during the warm season. Quality control of the T_s data was performed by the respective operating agencies and, therefore, additional quality control was not performed prior to use.

Table 4.1: Metadata for T_s observation sites.

Site	Stream	ID	Entity	Period of Record	Frequency
Above Chewuch	Methow	MAC	USFS	06/30/2005 - 10/21/2010	sub-daily to 30 minute
Spring Creek	Spring	SC	USFS/BOR/WFC	07/02/2009 - 10/25/2010	hourly to 30 minute
Above Barkley Silo	Methow	ABS	USFS/BOR/WFC	11/26/2009 - 10/04/2010	sub-daily to hourly
Chewuch Mouth	Chewuch	CM	USFS/BOR/WFC	06/01/2005 - 04/05/2011	sub-daily to 30 minute
Below Chewuch	Methow	MBC	USFS	06/07/2005 - 10/13/2009	hourly
Hwy 20 Bridge at Winthrop	Methow	48A150	DOE	10/08/2007 - 09/08/2008	monthly
Hwy 20 Bridge at Winthrop	Chewuch	48B070	DOE	10/08/2007 - 09/08/2008	monthly

The period of 16 July 2010 to 04 October 2010 was the only time frame which had overlapping, primarily continuous, sub-daily data for more than two sites. Only four of the seven sites (i.e., Methow Above Chewuch (MAC), Spring Creek (SC), Above Barkley Silo (ABS), and Methow Below Chewuch (MBC)) are available during that time, reiterating the data availability in that portion of the Methow is highly limited and restricts the use of physically-based models. Since the primary focus is on the prediction of water temperature below the confluence of the Methow and Chewuch, the sub-daily values of T_s at the MBC and ABS sites in Table 4.1 were averaged to create a single, daily mean time series. The daily values at the downstream site were compared to the Q at the Methow above Winthrop (MAW) site (see Section 4.3.1.2) and meteorological data at Winthrop 1WSW (WIN; see Section 4.3.1.3). This composite of daily mean T_s serves as the dependent variable in the statistical model.

The adjusted R^2 values are computed and shown in Figure 4.2 to indicate the strength of correlations between the independent variables and T_s. In general, the air temperature and flow variables show strong correlations with stream temperatures. The correlation with precipitation is near zero during the summer season Figure 4.2d); however, precipitation may serve as a surrogate for cloud cover and its related impacts on stream temperatures. Therefore, we include precipitation in the set of potential predictors, allowing a subset selection criterion (e.g., Bayesian Information Criteria (BIC)) to determine if the variable is applied in the final statistical models.

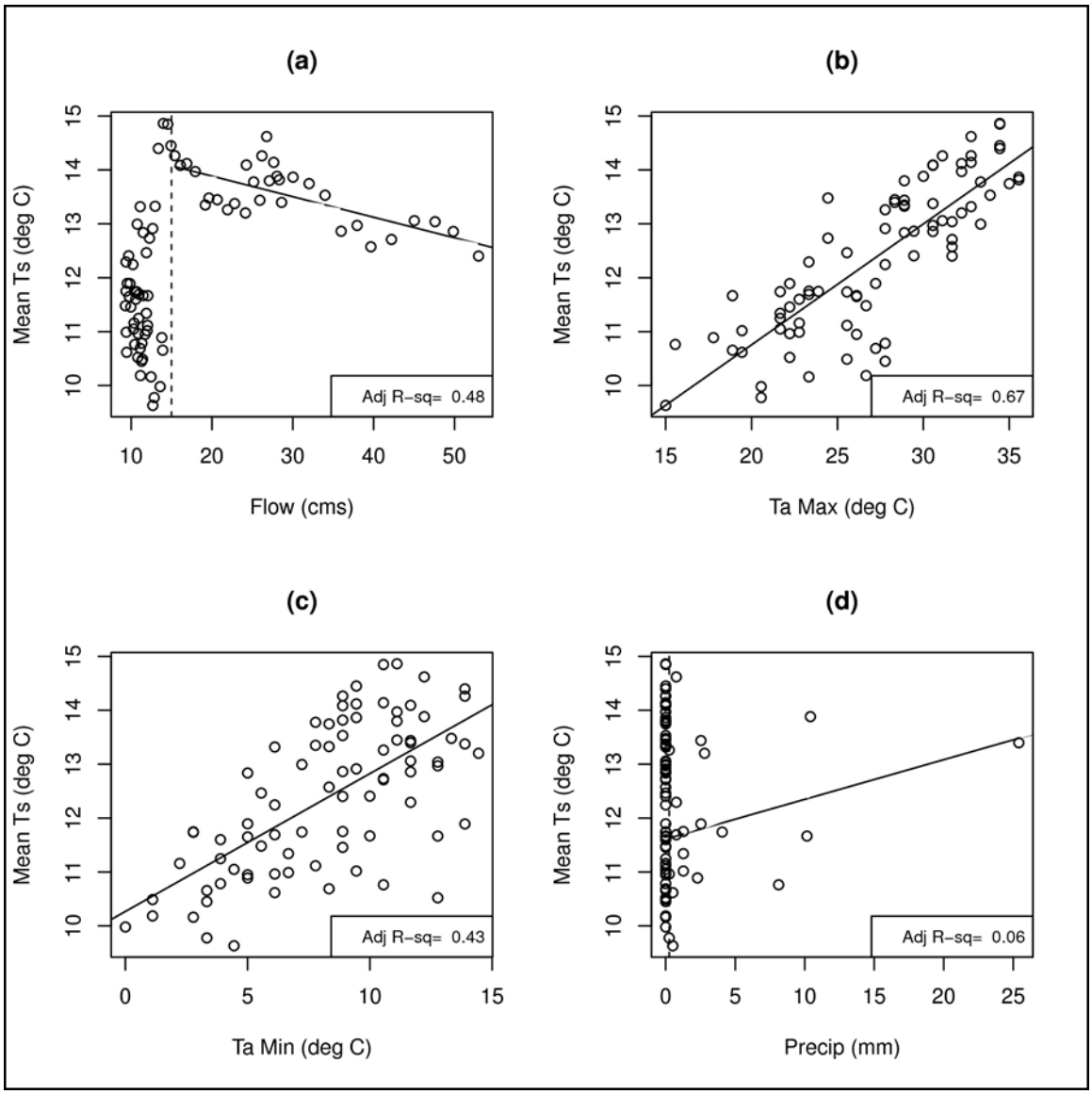

Figure 4.2: Scatterplots of hydrometeorological variables and mean *Ts* for the period 7/16/2010 to 10/04/2010 with adjusted R^2 given of linear fits for (a) streamflow above 15 cms, (b) maximum air temperature, (c) minimum air temperature, and (d) precipitation above 0.254 mm.

4.3.1.2 Streamflow

Streamflow data were gathered from the United States Geological Survey (USGS) for the overlapping period with the T_s data (i.e., 01 January 2001 to 19 May 2011). A total of three sites are available near the confluence of the Methow and Chewuch Rivers; however, only the site at Methow at Winthrop (USGS 12448500; MAW) was used. Unlike the T_s data, the measurements

are predominantly continuous, except during transmission and equipment failures. Times with missing values and equipment issues were removed from the observational time series. As can be seen in Figure 4.2a, Q above 15 cms at MAW is inversely proportional and correlated (adjusted $R^2 = 0.48$) with the T_s. The excellent continuity and quality of the MAW data can be also be seen in Figure 4.3a. The Q at MAW will serve as one of the independent variables in the model fitting described in Section 4.4.

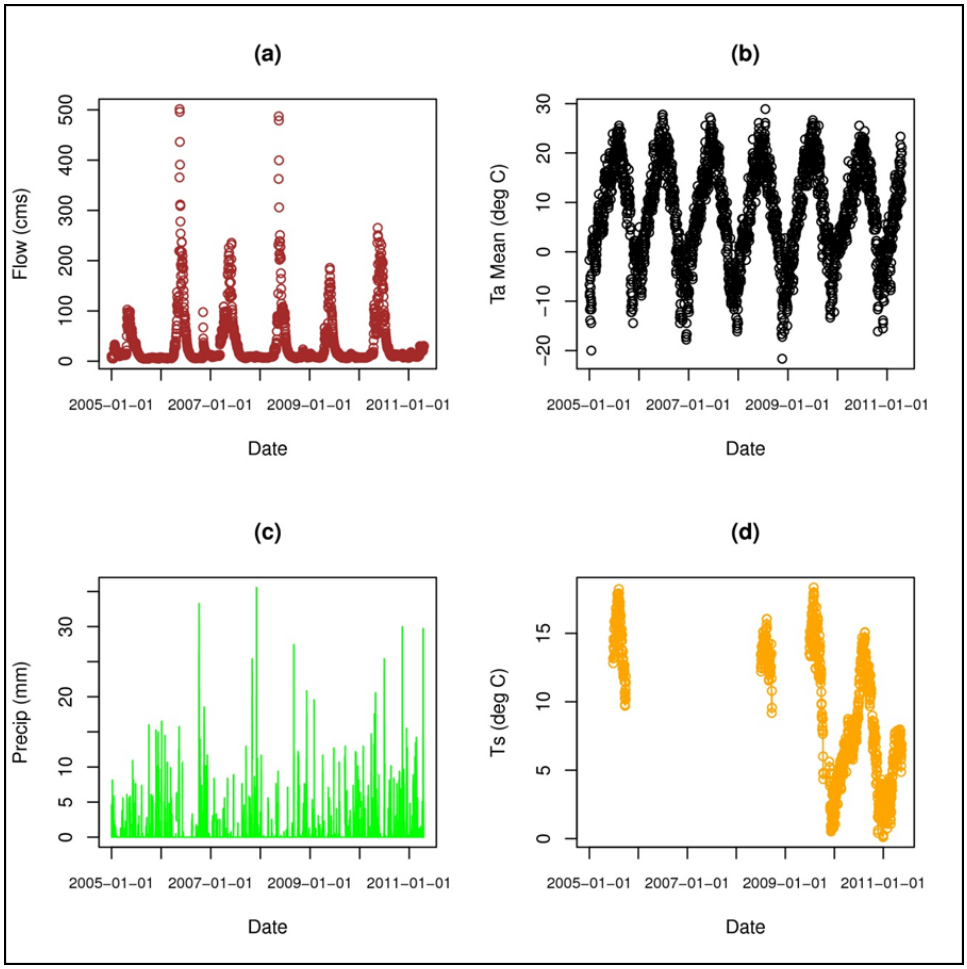

Figure 4.3: Quality controlled time series of daily hydrometeorological variables for the period 01 January 2005 to 19 May 2011. Time series of (a) streamflow, (b) mean air temperature, (c) precipitation, and (d) daily mean stream temperature are shown.

4.3.1.3 Meteorology

Daily meteorological data were collected from the National Climatic Data Center for the period 01 March 1906 to 19 May 2011 for the site at Winthrop 1WSW (NCDC 459376; WIN). The daily data included multiple meteorological variables; however, only the P_p, T_{ax}, and T_{an} values were considered. The daily meteorological data are fairly continuous, but did show some quality issues. For quality control, values that were unrealistic (e.g., T_{an} below -30 °C), missing, or entered as text (e.g., "T" for trace amounts of P_p) were removed from the record. As with the streamflow at the MAW gauge, only data for the period 01 January 2005 to 19 May 2011 were used. The quality-controlled daily meteorological time series for mean daily air temperature and P_p are shown in Figure 4.3b and Figure 4.3c. The time series for T_{ax} and T_{an} (not shown) showed similar continuity and quality.

As seen in Figure 4.2b and Figure 4.2c, air temperatures are well-correlated (adjusted $R^2 \geq 0.43$) with Ts in the Methow Basin; therefore, the values of Tax and Tan will serve as potential predictors in the statistical model development. Precipitation shows less correlation (adjusted $R^2 = 0.06$); but again, due to its relationship with cloud cover and the associated feedbacks on solar insolation on the stream, this variable is also included in the potential predictors (Figure 4.2d).

4.3.1.4 Snow Water Equivalent

In the Methow Basin, the Natural Resources Conservation Service operates a single snowpack telemetry (SNOTEL) station at Harts Pass. The daily snow water equivalent (*SWE*) for the period 01 January 2005 to 19 May 2011 were downloaded and will be used as a predictor variable in the statistical model.

4.3.1.5 VIC Model Output

The Climate Impacts Group at the University of Washington generated regional scale, future climate projections for the Pacific Northwest using ten GCMs under different emissions scenarios [Hamlet et al., 2010]. For our application, we focused on the use of the ten climate projections based on the A1B emissions scenario (Table 4.2). While B1 emissions scenarios were available, the A1B scenarios serve as a proof of concept application, which the authors consider a plausible future with little greenhouse gas mitigation until the mid-21st century. The output from the downscaled GCMs was used to develop inputs to the Variable Infiltration Capacity (VIC) [Liang et al., 1994; Liang et al., 1996; Nijssen et al., 1997] model to assess the impacts of climate change on ecological and hydrological systems in the region.

Table 4.2: List of the ten global climate models used in the A1B scenarios.

GCM
hadcm
cnrm_cm
ccsm2
echam5
echo_g
cgcm3.1_t47
pcm1
miroc_3.2
ipsl_cm4
hadgem1

The VIC model is a spatially-distributed hydrologic model that solves the water and energy balance at each model grid cell. The model initially was designed as a land-surface model to be incorporated in a GCM so that land-surface processes can be more accurately simulated; however, it is often run in standalone mode. For climate change impact studies, VIC is run in what is termed the water balance mode that is less computationally demanding than an

alternative energy balance mode, in which a surface temperature that closes both the water and energy balances is solved for iteratively. Using the University of Washington VIC applications, the water balance mode is driven by daily weather forcings of precipitation, maximum and minimum air temperature, and wind speed. Additional model forcings that drive the water balance, such as solar (short-wave) and long-wave radiation, relative humidity, vapor pressure, and vapor pressure deficit, are calculated within the model. The VIC outputs are configurable but typically include grid cell moisture and energy states through time (i.e., soil moisture, snow water content, snowpack cold content) and water leaving the basin either as evapotranspiration, base flow, sublimation, or runoff, where the latter represents the combination of faster-response surface runoff and slower-response base flow. Additional details on the VIC setup and development are well-documented in Maurer et al. [2002], Wood and Lettenmaier [2006], and Wood et al. [2004]. An overview of the Columbia Basin Climate Change Scenarios Project is currently in press, which provides additional details on the integration of the GCM output and VIC model, including implementation and calibration [Hamlet et al., 2013]. The reader is, therefore, referred to these references for further details.

For the current study, meteorological variables (e.g., T_{ax}, T_{an}, and P_p) and bias-adjusted flow (Q) were extracted from ten different VIC simulations for three future climate horizons: 2010-2039 (representative of year 2020); 2030-2059 (representative of year 2040); and 2070-2099 (representative of year 2080). Two 1/16th degree latitude-longitude grid cells were used for the extraction of data from VIC. The first location was centered at 48.46875 N, 120.15625 W, which is in close proximity to the MAW gauge. This site serves as the source for the predictor variables of meteorology and flow, with the assumption that the weather is consistent over the grid box and that the flow is accumulative over the entire watershed. The second grid location

was centered at 48.71875N, 120.65625W and contains the SNOTEL site at Harts Pass. This site serves as the source the *SWE* predictor variable; however, comparison with the observed gauge data requires an adjustment factor of 0.65 be applied to the Harts Pass gauge for direct comparison (not shown). These differences arise from point to area reduction and universal assignment of vegetative class at the grid scale in the VIC model which fails to allow for point-specific estimates of *SWE*. In addition, the same data were available from a single historical VIC model simulation. The VIC output provides historical projections at daily time steps for the period 1916 to 2006 for a total of 91 years of daily data, which serves as a reference period. The VIC output is also provided as a time series of 91 years of data representative of the three future climate horizons of 2020, 2040, and 2080.

4.4 Methods

In this study, mean daily T_s is modeled as a function of T_{ax}, T_{an}, and P_p at the WIN meteorological site; daily mean Q at the MAW gauge, and daily *SWE* at the Harts Pass gauge. This section will describe the methodology for developing the GLM and the *K*-nn technique used to perform bias-adjustment of the VIC scenarios prior to application in the statistical modeling framework, including disaggregation (Figure 4.4).

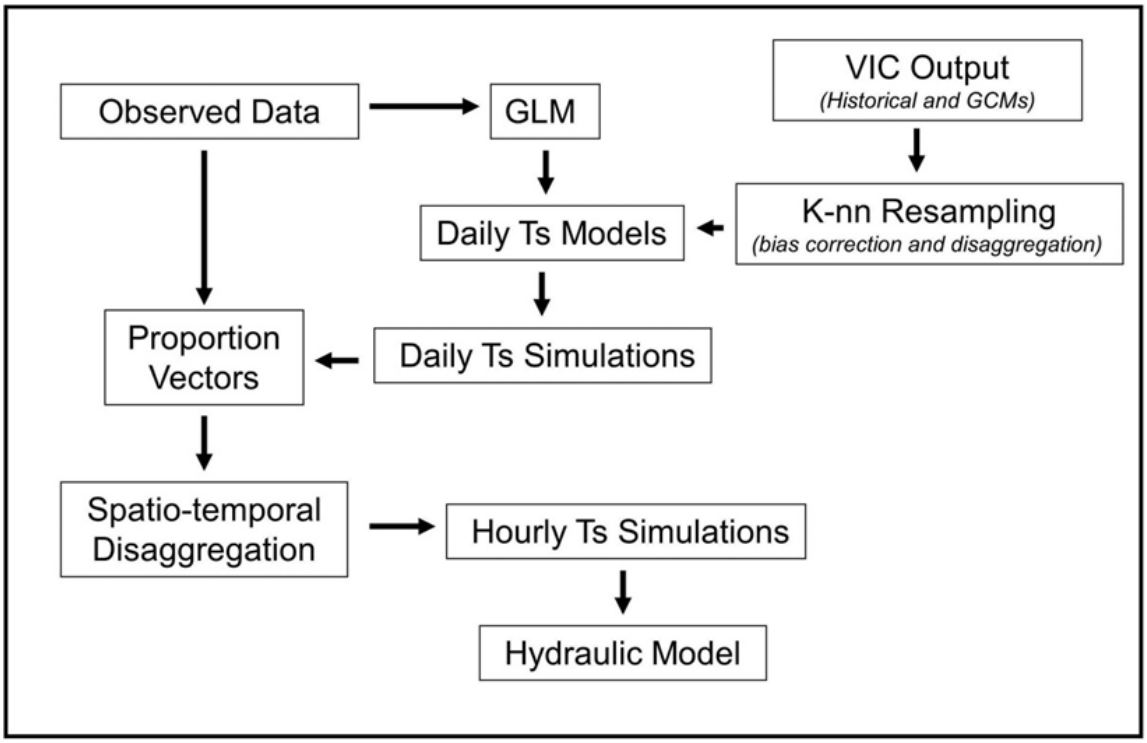

Figure 4.4: Flow chart of the statistical framework.

4.4.1 Generalized Linear Models

A flexible statistical framework has often been applied in the assessment and prediction of many water quality variables [Neumann et al., 2003; Neumann et al., 2006; Towler et al., 2010a, 2010b]. Neumann et al. [2003, 2006] used regression to model the daily maximum T_s, while Towler et al. [2010a, 2010b] incorporated the generalized linear model (GLM) into a seasonal risk analysis of meeting turbidity requirements for a water supplier in the Pacific Northwest. Section 2.5.3 [also in Caldwell et al., 2013a, 2013b] advanced the work of Neumann et al. [2003, 2006] by predicting multiple T_s characteristics (e.g., daily T_s range and probability of exceedance) using a GLM coupled with a stochastic weather generator to assess the seasonal risk to salmon fisheries. The current application builds on the work of the previous chapter by integrating the output from the VIC hydrologic model to generate future T_s scenarios to assess

the impact of climate change on fisheries in the Methow River. T reader is referred to Chapter 3 and Section 2.5.3 for further details on the methodology of the generalized linear model.

To obtain the best set of predictors for the model there are objective criteria such as the Akaike Information Criteria (AIC) or Bayesian Information Criteria (BIC) – both of which penalize the likelihood function based on the number of parameters [Venables and Ripley, 2002]. Models are fit using all possible subsets of predictors and also link functions; for each, the AIC and BIC are computed and the model with lowest AIC or BIC is selected as the 'best model'. We used BIC in this study as it tends to be slightly more parsimonious compared to AIC. This subset selection procedure accounts for correlation between independent variables. Models can also be tested for significance against a NULL model or an appropriate subset model. For our case, we compare the GLM model to a simple linear regression model, typical in statistical models of stream temperature [Benyahya et al., 2007], where the daily mean stream temperature is function only of daily mean air temperature.

4.4.2 K-Nearest Neighbor Resampling

Since the output from the VIC model spans a much longer period of record than observed, a *K*-nearest neighbor (*K*-nn) resampling algorithm [Rajagopalan and Lall, 1999; Buishand and Brandsma, 2001] is employed to select days from the historical record that are representative of the hydrometeorological conditions in the model output. The *K*-nn algorithm is a method for classifying objects based on closest training examples in a feature space. To account for the shifting hydrology and meteorology throughout the year, the training examples (or observed weather and flow vectors) are selected from a 30-day window on either side of the current Julian date. In our case, there are typically 6 years of data (2005-2011) with a total of 61 potential neighbors from each year. The length of this window of time can be adjusted by the user, but

should maintain the general statistics of the hydroclimate for that time of year. Here, we selected 30 days to account for potential shifts in the seasonality of snow accumulation and melt. For example, if the current Julian day is 31 (i.e., 31 January), first the weather-flow vector is extracted from the current VIC run. The potential neighbors are then 01 January to 01 or 02 March (depending on leap year) from each year 2005 through 2011. The Mahalanobis distances between the daily VIC and the potential neighbors' weather-flow vectors from the observed record (i.e., 01 January 2005 to 19 May 2011) are computed [e.g., Yates et al., 2003]. After ordering the distances from closest to farthest, each neighbor is prescribed a weight based on the cumulative sum of $1/K$ with the closest neighbor receiving the highest weight. A neighbor is then selected at random based on weight; the index of that neighbor is used to extract the associated weather-flow vector from the observational record. The selected weather-flow vector (i.e., neighbor) from the historical record is then used to replace the VIC model output prior to use as predictors in the statistical modeling framework. An additional benefit of the *K*-nn algorithm is selection of particular dates, which can be used to disaggregate the daily simulations to hourly.

4.4.3 Spatio-temporal Disaggregation

Hourly hydrometeorological inputs are required for the two-dimensional hydraulic model being developed at the BOR. Since the GLM models predict daily T_s at the MAW site, spatial disaggregation is required to distribute the daily hydrometeorological variables to two synthetic upstream boundary condition locations: upstream Methow (MUS) and upstream Chewuch (CUS). CUS is assumed to represent a location near the site of the CM T_s measurements; MUS is assumed to represent a location near the site of MAC T_s measurements. In addition, the downstream location (MDS) is assumed to represent the location of the MBC and ABS T_s observations. Henceforth, we will use the CUS, MUS, and MDS abbreviations for clarity. The

daily values then must be disaggregated temporally to generate inputs for the hydraulic modeling system. Since the quality and availability of continuous, daily and sub-daily measurements in the Methow River Basin were severely limited, we perform the spatial and temporal disaggregation by developing proportion vectors at the daily and hourly time scale, using the methods employed in Nowak et al. [2010]. Nowak et al. [2010] applied a non-parametric stochastic approach to disaggregation of annual flow values via K-nearest neighbor resampling of daily proportion vectors which captured the observed statistics quite well. We further this approach by using both hourly and daily proportion vectors for both streamflow and stream temperature.

Daily mean T_s values are computed for three locations (MUS, MDS, and CUS using the sub-daily and daily measurements at four sites (i.e., ABS and MBC for MDS; MAC for MUS; and, CM for CUS) from the period 01 January 2005 to 31 December 2011. If all three sites do not have a daily mean, then the period mean is used at each of the sites. The proportion of each upstream, gauge relative to the downstream gauge is calculated to yield the daily temperature proportion vectors (DTPV). Only 329, of a possible 2555, DTPVs are unique (Figure 4.5). The mean values for CUS (1.05) and MUS (0.93) approach one but signify that the Chewuch is generally warmer than the Methow inflows due to differences in riparian cover and flow.

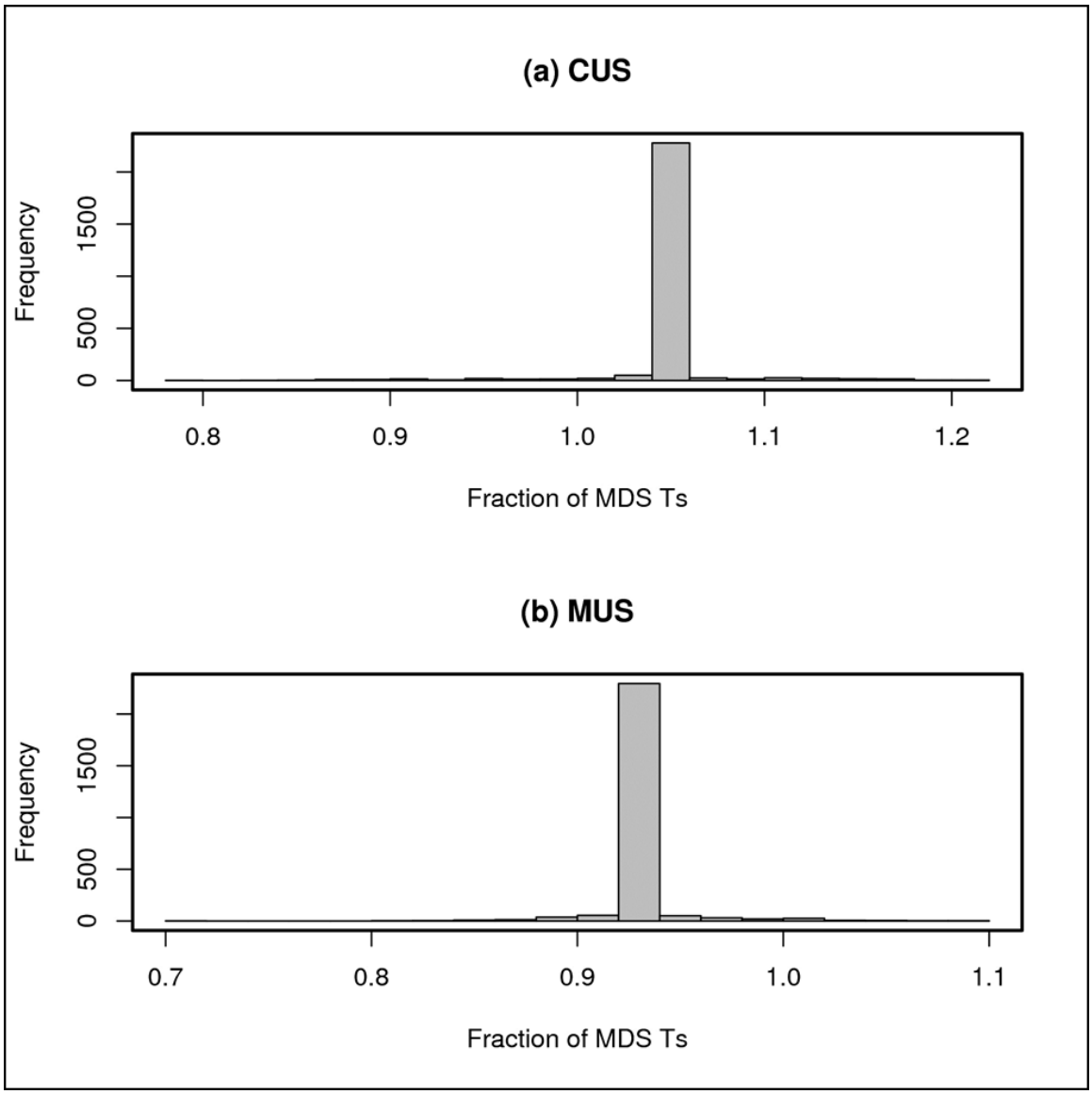

Figure 4.5: Histograms of the daily temperature proportion vectors for the (a) Chewuch Upstream and (b) Methow Upstream sites, shown as a fraction of the daily mean stream temperature downstream.

The hourly T_s proportion vectors (HTPVs) use the available hourly T_s measurements at the same sites. For each day of the calendar year (1 – 365), the hourly mean T_s is calculated. At least one of the sites must be reporting for a given hour; otherwise, the monthly mean for that hour is imposed. Separate HTPVs are calculated as the fractional contribution of each hour to the daily sum for days 1 to 365 at the two upstream and one downstream site to account for the impact of flow differences between the tributaries and the cumulative flow downstream. The

variety of diurnal fluctuations inherent in the HTPVs at each site can be seen in Figure 6. Using the corresponding date (or its Julian day of the year) picked during the *K*-nn resampling, the appropriate proportion vectors for both spatial and temporal disaggregation can be selected for distributing the predicted value from the GLM to both upstream points at hourly time steps. Validation statistics for the spatiotemporal disaggregation technique are presented in Section 4.5.

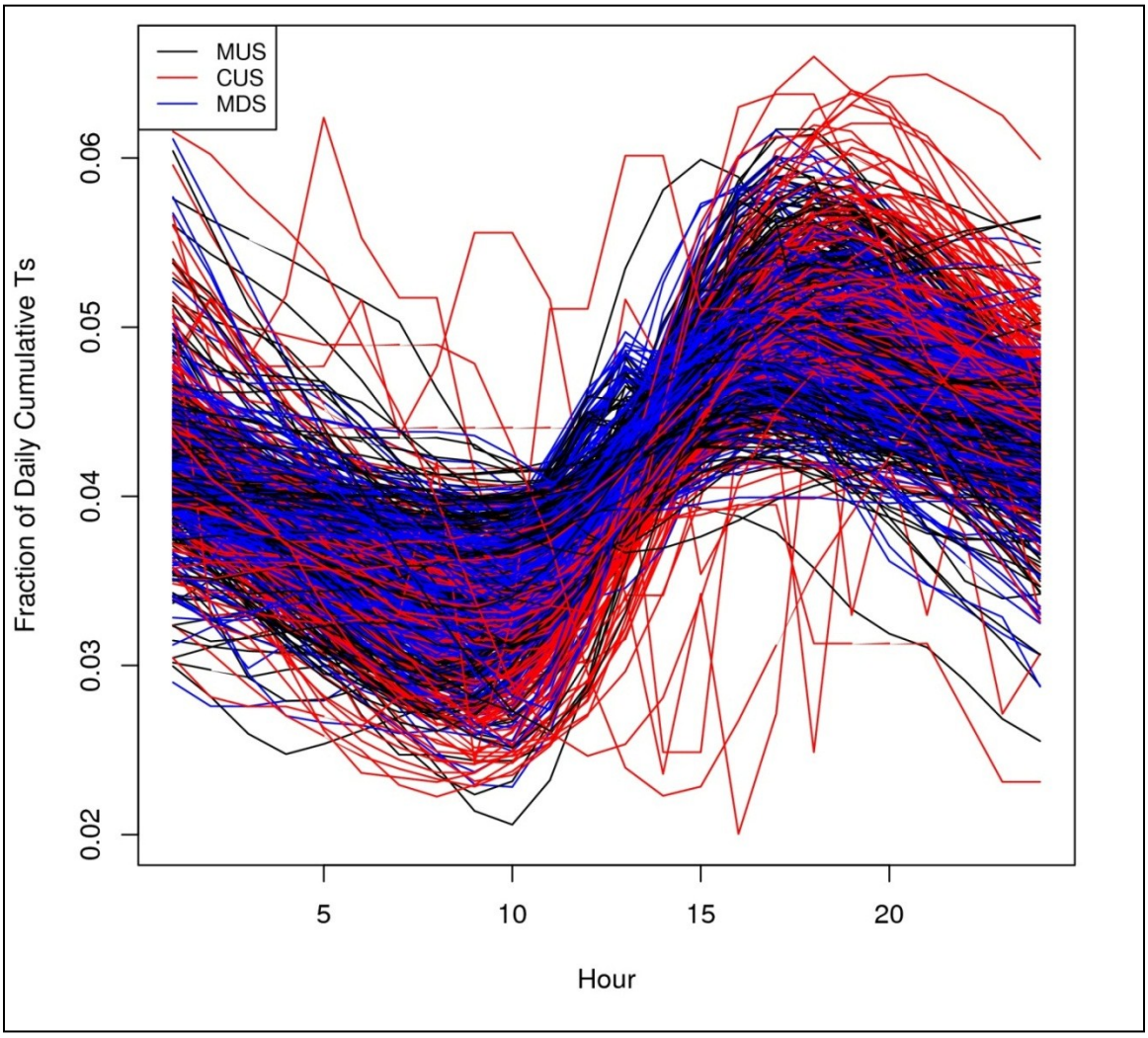

Figure 4.6: Hourly stream temperature proportion vectors for the Methow Upstream (MUS), Chewuch Upstream (CUS), and Methow Downstream (MDS) sites, shows as fractional values of the daily accumulative stream temperature.

4.5 Results

4.5.1 Statistical Model Development

Since the statistical model is predicting the mean daily T_s at the downstream location, only the sites at MBC and ABS were used to create a composite daily T_s time series for the period 01 January 2005 to 19 May 2011. A total of 738 days were available during the period with observed temperatures above 0 °C; and, the highest number of days was available by month during the warm season (Figure 4.7). For the days with available T_s data, the GLM was fit by month using the hydrometeorological predictors from WIN (e.g., T_{ax}, T_{an}, and P_p), the MAW (e.g., Q) site, and the Harts Pass location (e.g., *SWE*). Therefore, there are a total of twelve statistical models, one for each month to forecast mean daily stream temperature. Using the BIC for subset selection, the preferred predictors for T_s include T_{ax}, T_{an}, and Q. Only two months (February and March) include P_p in the best subset from BIC, primarily during the rainy, cool season. The *SWE* variable is also selected during the cool season during the months of January, March, November, and December. The results of BIC subset selection can be found in Table 4.3.

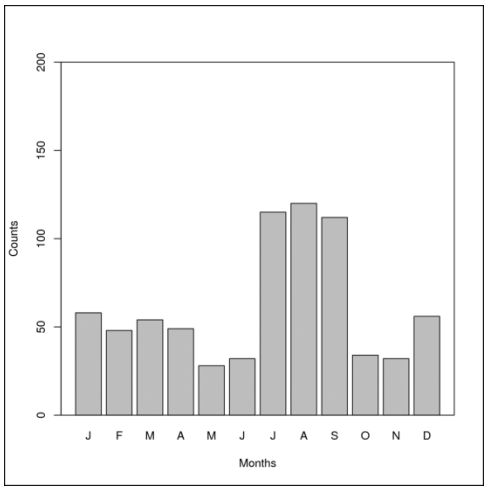

Figure 4.7: Counts of the number of days with mean daily T_s available by month during the period 01 January 2005 to 19 May 2011.

Table 4.3: Subset of predictors selected by the GLM using BIC.

Month	Predictors
Jan	*Tax, Tan, Pp, Q, SWE*
Feb	*Tax, Tan, Pp, Q*
Mar	*Tax, Tan, Pp, SWE*
Apr	*Tax, Tan, Q*
May	*Tax, Tan, Q*
Jun	*Tax, Tan, Q*
Jul	*Tax, Tan, Q*
Aug	*Tax, Tan, Q*
Sep	*Tax, Tan, Q*
Oct	*Tax, Tan*
Nov	*Tax, Tan, Q, SWE*
Dec	*Tax, Tan, P, Q, SWE*

4.5.2 GLM Verification

To test the skill of the GLM, cross-validation is performed by randomly dropping ten percent of the points over 100 iterations and computing the root mean square error (RMSE). Scatterplots of the observed vs. predicted values (Figure 4.8) and RMSE boxplots (Figure 4.9) indicate excellent skill throughout the year. To highlight the seasonal performance of the models, only relationships for January, April, July, and October are shown, though the relationships are similar in other months. Correlations are high in all months (with adjusted $R^2 \geq 0.60$); and, all are statistically significant based on a *t*-test for the significance of the correlation coefficient at significance level, $\alpha = 0.05$, such that *t* is defined in Equation 4.1 as:

$$t = \frac{r\sqrt{n-2}}{\sqrt{1-r^2}}, \qquad (4.1)$$

where *t* is the test statistic, *r* is the coefficient of correlation, and *n* is the sample size. The warm season months generally exhibit highest RMSE values, with mean RMSE approaching 0.8 °C. The largest variability in RMSE is during the months of April and July large variability in T_s

occurs due to snowmelt and high air temperatures, respectively. Lowest RMSE values in the winter are related to daily T_s that remain near 0 °C as the Methow River freezes.

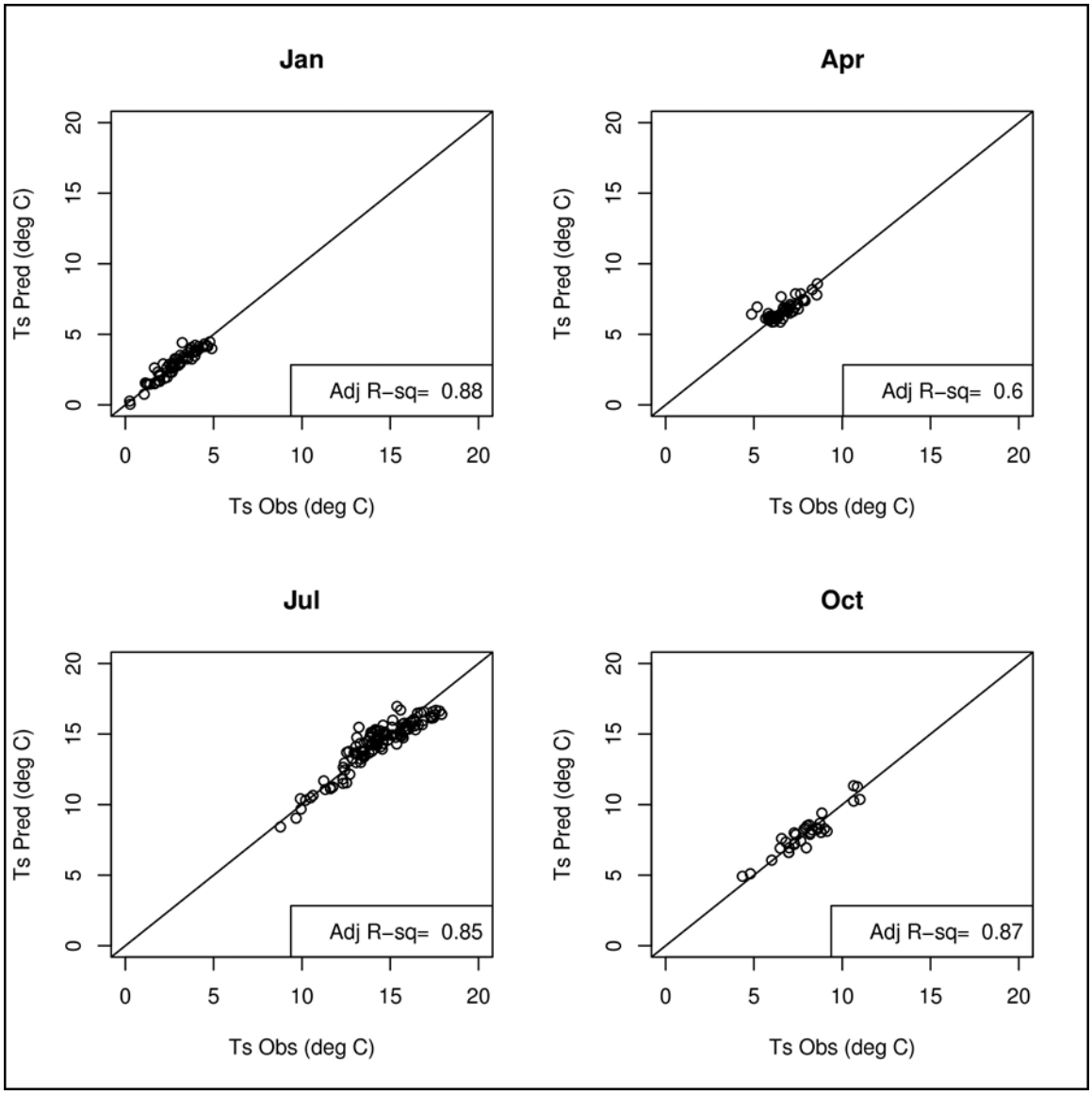

Figure 4.8: Scatterplots of observed vs. predicted values for January, April, July, and October from the GLM model fitting. The one-to-one line is overlaid for reference.

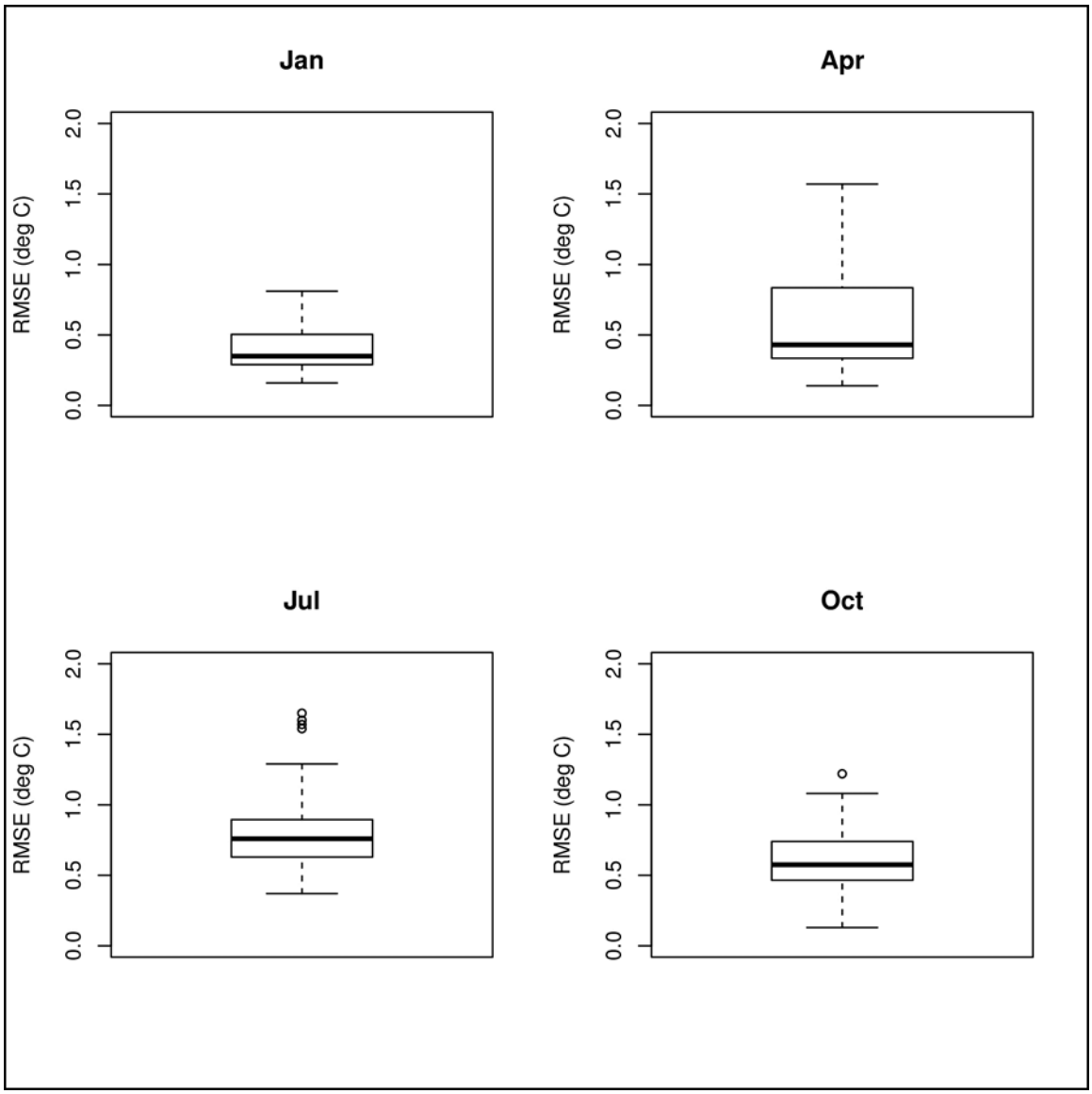

Figure 4.9: Boxplots of RMSE for January, April, July, and October from the cross-validation. Errors generally average less than 1 °C, except during the summer when mean errors approach 1.2 °C.

4.5.3 Integration of GLM and Climate Change Scenarios

Outputs from the historical climate model simulations are combined to generate a large predictor matrix of daily T_{ax}, T_{an}, and P_p (January 1915 – December 2006); Q (October 1915 to December 2006); and *SWE* (January 1915 – December 2006) for use in the GLM framework. The historical predictor matrix is the overlapping subset that covers 91 complete calendar years for the period from January 1916 to December 2006. Using the twelve monthly GLM models,

the historical predictor matrix is used to predict daily mean T_s at the MAW site. Boxplots and probability distribution functions (PDFs) of daily mean T_s for the four months representing each season (i.e., January, April, July, and October) indicate that the variability is increased in the historical simulations compared to observations (*PrV* in Figure 4.10 and Figure 4.11) when using the GLM-VIC model output without adjustment. Similar results are observed for other months (not shown). To address the issue, we implemented a *K*-nn resampling technique as described in Section 4.4.2 to perform bias-adjustment on the VIC model output. Difference in variance and means between the observations and historical runs, both with VIC and adjusted using *K*-nn, were tested using an *F*-test and the appropriate *t*-test, respectively. Results indicate that while the variance is similar at the 95% confidence level for the VIC runs, there is a significant deviation in the mean. On the other hand, the variance is reduced in the *K*-nn simulations (a known limitation to *K*-nn); however, the simulated mean daily stream temperatures are approximately 50 percent closer to the observed values than in the VIC alternative. Both the *K*-nn and the VIC simulations of daily mean stream temperature under-estimate the mean. The center location and shape of the resulting boxplots and PDFs related to the *K*-nn simulations match much more closely with the observed distributions (see *PrK* in Figure 4.10 and Figure 4.11). As a result, the bias-adjusted VIC output then serves as input to the monthly GLM models.

The future climate projection scenarios are processed in the same manner. First, climate change predictor matrices are developed for each of the 30 coupled VIC scenarios. Then, the *K*-nn resampling is applied to each predictor matrix to generate new bias-adjusted matrices, which are used to predict daily mean T_s through the GLM (not shown).

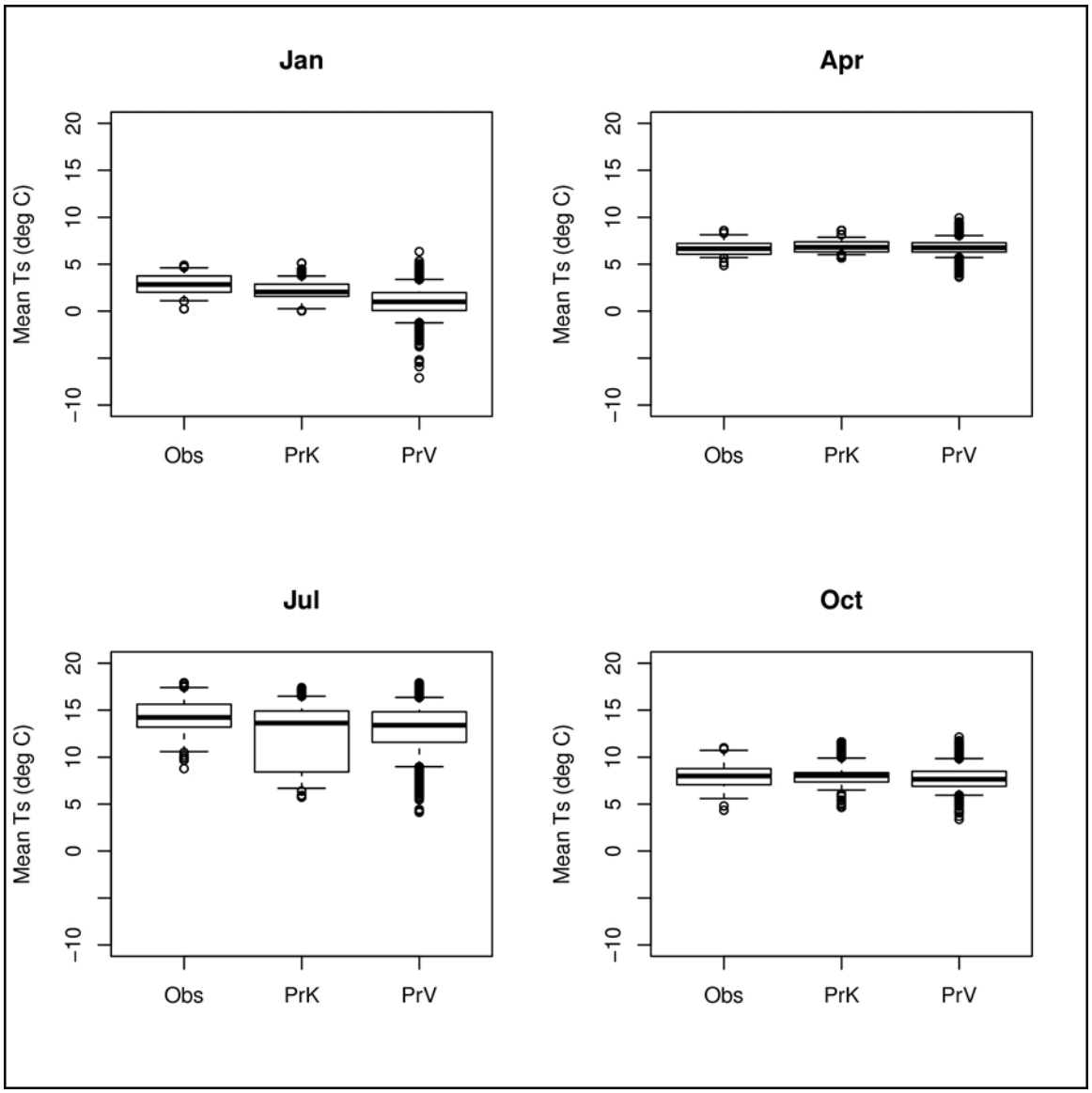

Figure 4.10: Boxplots of observed (*Obs*) vs. predicted values of mean stream temperature for January, April, July, and October when using the historical simulation as input to the GLM, using the historical VIC (*PrV*) simulations compared to the bias-adjusted, *K*-nn simulations (*PrK*).

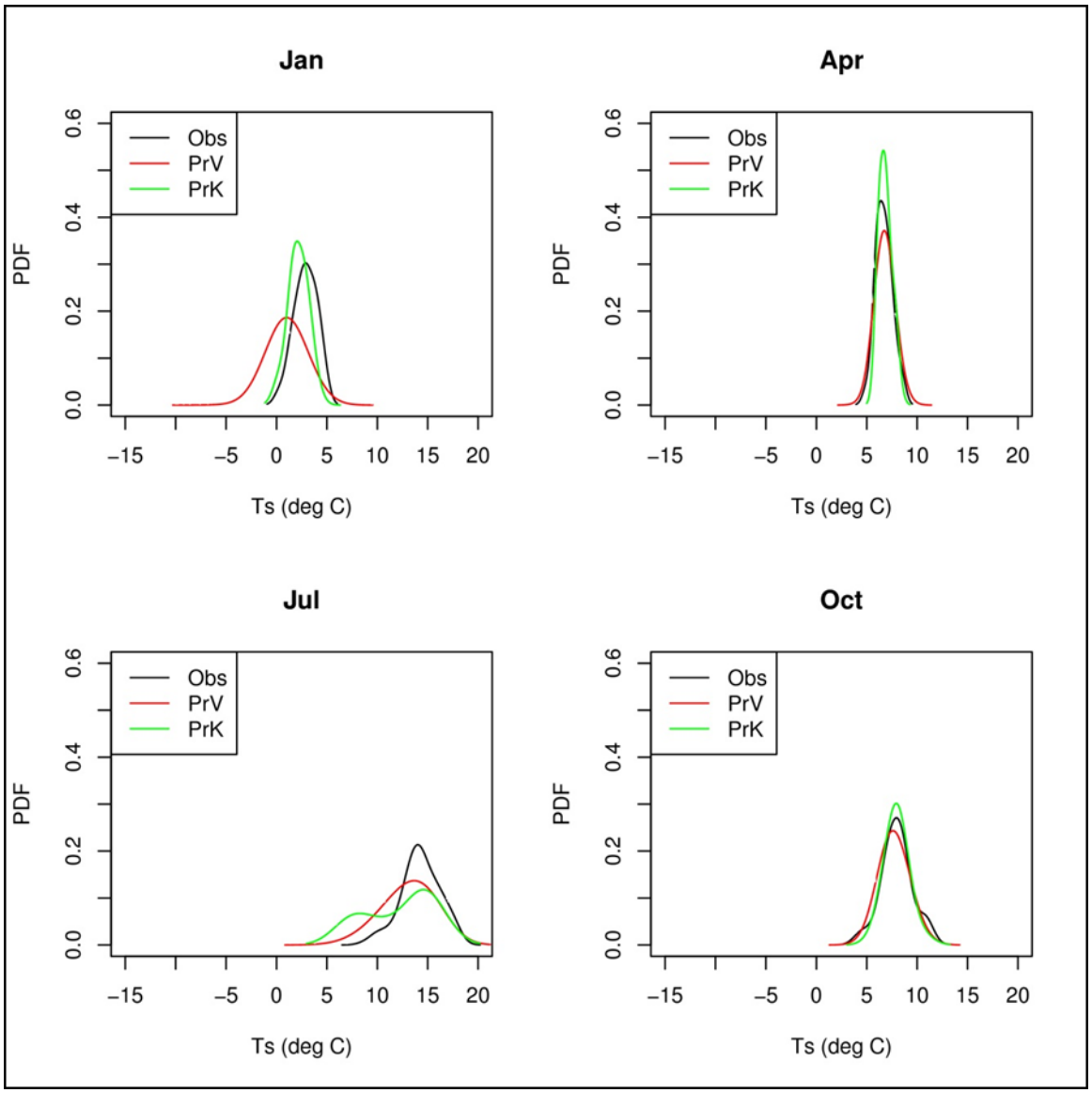

Figure 4.11: Probability density functions (PDFs) of daily mean stream temperature for observed (*Obs*; black) vs. predicted with historical VIC (*PrV*; red) and predicted with bias-adjusted *K*-nn VIC output (*PrK*; green).

4.5.4 Validation of the Integrated VIC-GLM Model

To assess the performance of the coupled VIC GLM, the mean daily stream temperature from the historical climate simulations were compared to daily values at each site using the following statistics: Nash-Sutcliffe coefficient [NS; Nash and Sutcliffe, 1970]; ratio of the root mean square error to the standard deviation of the observed data (RSR); percent bias (PBIAS),

the ratio of the sum of residual errors between the simulated and observed data and the sum of the observed data; the mean error (ME); the root mean square error (RMSE); and, the adjusted R^2 or the squared correlation between the observed and predicted values adjusted for sample size and degrees of freedom. Guidelines established by Moriasi et al. [2007] and applied in Ficklin et al. [2012] where NS > 0.50, RSR < 0.70, and PBIAS between +/- 25 percent are used to qualify the validation results as satisfactory. Comparison to the NULL model described in Section 4.4.1, indicates the GLM model exhibits increased values of NS, decreased values of RSR, equivalent absolute PBIAS and ME, and lower RMSE (Table 4.4), indicating enhanced skill over simple linear regression. In addition, the adjusted R^2 values using the GLM for the months shown in Figure 4.8 were equal to or higher than those from the NULL model, particularly in April and July when correlation was more than double (Table 4.5).

Table 4.4: Comparison of daily validation statistics between the NULL and GLM models.

Statistic	NS	RSR	PBIAS	ME (°C)	RMSE (°C)
NULL	0.96	0.19	0.1	-0.01	0.9
GLM	0.98	0.14	-0.1	-0.01	0.7

Table 4.5: Comparison of adjusted R^2 values between the NULL and GLM models.

Adjusted R^2	Jan	Apr	Jul	Oct
NULL	0.76	0.27	0.33	0.88
GLM	0.88	0.60	0.85	0.88

The robustness of a model to small changes in input parameters provides an estimate of the sensitivity of the model to individual parameters. For example, in Ficklin et al. [2012], model sensitivity was analyzed using a normalized, dimensionless sensitivity index (*I*) shown in Equation 4.2, where

$$I = \frac{(y_2 - y_1)/y_0}{2\Delta x/x_0}, \qquad (4.2)$$

where y_2 is the perturbed predicted values at $x_2=x_0+\Delta x$ and y_1 is the perturbed predicted values at $x_1=x_0-\Delta x$, y_0 is the original predicted values, and $\Delta x=x_2-x_1$.

As in Ficklin et al. [2012], we apply Δx variations of +/- 10 percent to each of the predictor variables (i.e., T_{ax}, T_{an}, P_p, Q, and SWE). The index I then represents the change in output variable (mean and variance) resulting from a change in the inputs to the model. The absolute value of I can be ranked into four classes based on level of sensitivity as given in Ficklin et al. [2012] from Lenhart et al. [2002], such that higher values indicate increasing sensitivity. We calculate the sensitivity index I for both the mean and variance of the predicted variable T_s (Table 4.6). For the prediction of the mean, *Tax* was the most sensitive parameter with *Tan* being of medium sensitivity, and the other variables found to be insensitive. Using the variance as an indicator, the variable T_{ax} was of medium sensitivity with all other variables insensitive, suggesting that the primary drivers for the mean state of T_s and its variance are air temperature related, with lesser influence from precipitation, flow, or snow water equivalent.

Table 4.6: Sensitivity indices for each of the predictor variables. High (H) and medium (M) sensitivity denoted.

Indicator	*Tax*	*Tan*	*Pp*	*Q*	*SWE*
Mean	0.21^{H}	0.11^{M}	-0.01	-0.03	-0.02
Variance	0.10^{M}	0.02	0.00	0.01	0.00

4.5.5 Validation of Spatiotemporal Disaggregation

Simulations of daily mean stream temperature using the historical VIC inputs were spatially disaggregated to both upstream points and temporal disaggregation applied at all three

locations. To test the validity of the results, the same statistics were computed using the hourly data as for the daily values, including: NS, RSR, PBIAS, ME, and RMSE (Table 4.7). While marginal results were evident for the MUS location (NS=0.50, RSR=0.70, PBIAS=-5.6), both the CUS and MDS locations were considered acceptable with NS>0.50, RSR<0.70, and PBIAS between +/- 25 percent. Scatterplots of the observed vs. predicted hourly values at each site show modest correlation with adjusted R^2 values exceeding 0.73 at CUS and MDS and 0.57 at MUS (Figure 4.12).

Table 4.7: Comparison of hourly validation statistics at the three disaggregated sites.

Site	NS	RSR	PBIAS	ME (°C)	RMSE (°C)	Adjusted R^2
CUS	0.67	0.58	-4.1	-0.60	1.8	0.73
MUS	0.50	0.70	-5.6	-0.75	2.0	0.57
MDS	0.71	0.54	-6.1	-0.90	1.5	0.81

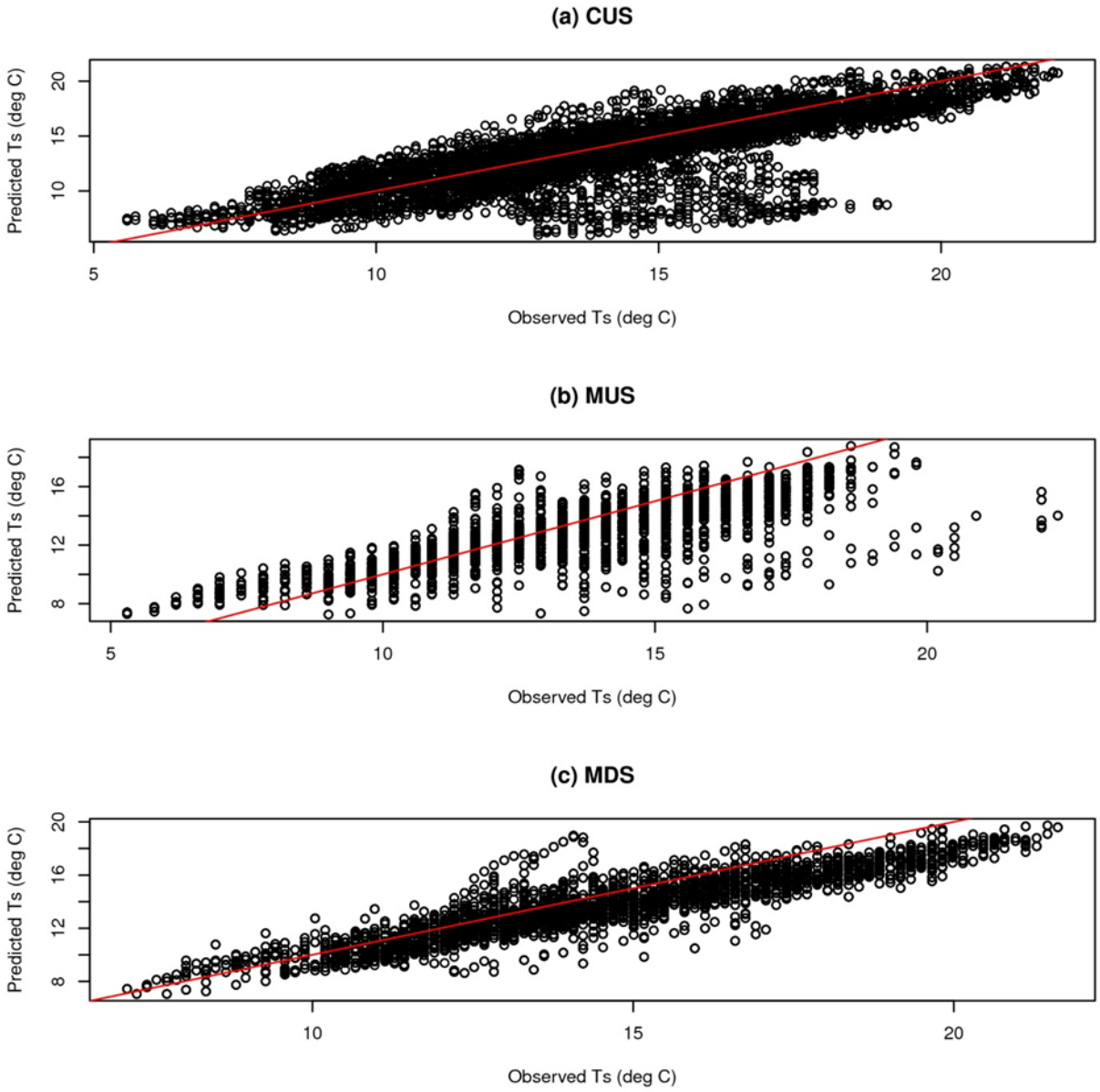

Figure 4.12: Scatterplots of observed vs. predicted values of hourly stream temperature for (a) Chewuch Upstream, (b) Methow Upstream, and (c) Methow Downstream. The one-to-one-line is overlaid in red.

4.5.6 Implications of Climate Change on Stream Temperatures

Mean daily values of T_s from each of the VIC simulations were concatenated by month and assembled to identify the mean and standard deviations (hence, confidence intervals) (

Table 4.8), as well as to show the variability in predictions. Figure 4.13 shows the boxplots for the months of June through September, the primary season of evident shifts. The ensemble means were computed for each of the future time horizons of 2020, 2040, and 2080, by averaging the results by day of each of the ten climate modeling scenarios. PDFs of each time horizon were plotted relative to the historical simulation. Mean daily T_s increases by ~2 °C during the warm season by the year 2080, with lesser magnitude positive shifts in the distribution at the 2020 and 2040 time horizons (Figure 4.14). Shifts during the cool season (see

Table 4.8) were less pronounced. These results suggest that a warming climate will likely be associated with warming Ts in the Methow River Basin. Figure 4.15 indicates that the greatest increase in mean daily T_s will occur during the summer months. Given the anticipated shift to warmer conditions in future climate, a one-tailed, unpaired t-test indicates the simulated daily mean stream temperature time series from the historical run is significantly different from the simulated values at each future period at the $\alpha = 0.05$ level. Maximum differences between the historical run and the 2080 time horizon are 2.8 ± 4.7°C (in July) and 0.8 ± 1.9 °C (annual average), respectively. The values of maximum differences between the historical run and the 2020 and 2040 time horizons range from 1.4 ± 3.5 °C (2020) to 2.4 ± 4.4°C (2040). Mean differences are 0.4 ± 1.6 °C and 0.7 ± 1.8 °C, respectively, for the 2020 and 2040 time horizons.

Table 4.8: Mean monthly daily mean stream temperature (°C) with 90% confidence interval for differences between historical and each future period in parentheses.

Month	Historical	2020	2040	2080
Jan	2.2	2.2 (±1.3)	2.3 (±1.3)	2.3 (±1.4)
Feb	3.0	3.1 (±1.3)	3.2 (±1.3)	3.2 (±1.4)
Mar	5.5	5.8 (±1.8)	6.0 (±1.8)	6.1 (±1.9)
Apr	6.9	6.9 (±0.9)	7.0 (±1.0)	7.0 (±1.1)
May	7.4	7.5 (±0.9)	7.5 (±1.0)	7.5 (±1.0)
Jun	8.8	9.4 (±2.1)	10.0 (±2.8)	10.4 (±3.3)
Jul	12.2	13.6 (±3.5)	14.6 (±4.4)	15.0 (±4.7)
Aug	14.1	14.9 (±1.5)	15.4 (±1.7)	15.5 (±1.7)
Sep	11.7	12.1 (±1.4)	12.5 (±1.5)	12.6 (±1.5)
Oct	8.0	8.1 (±1.2)	8.3 (±1.3)	8.4 (±1.2)
Nov	4.6	4.8 (±2.1)	5.0 (±2.1)	5.1 (±2.1)
Dec	3.2	3.5 (±1.6)	3.8 (±1.8)	3.8 (±1.9)

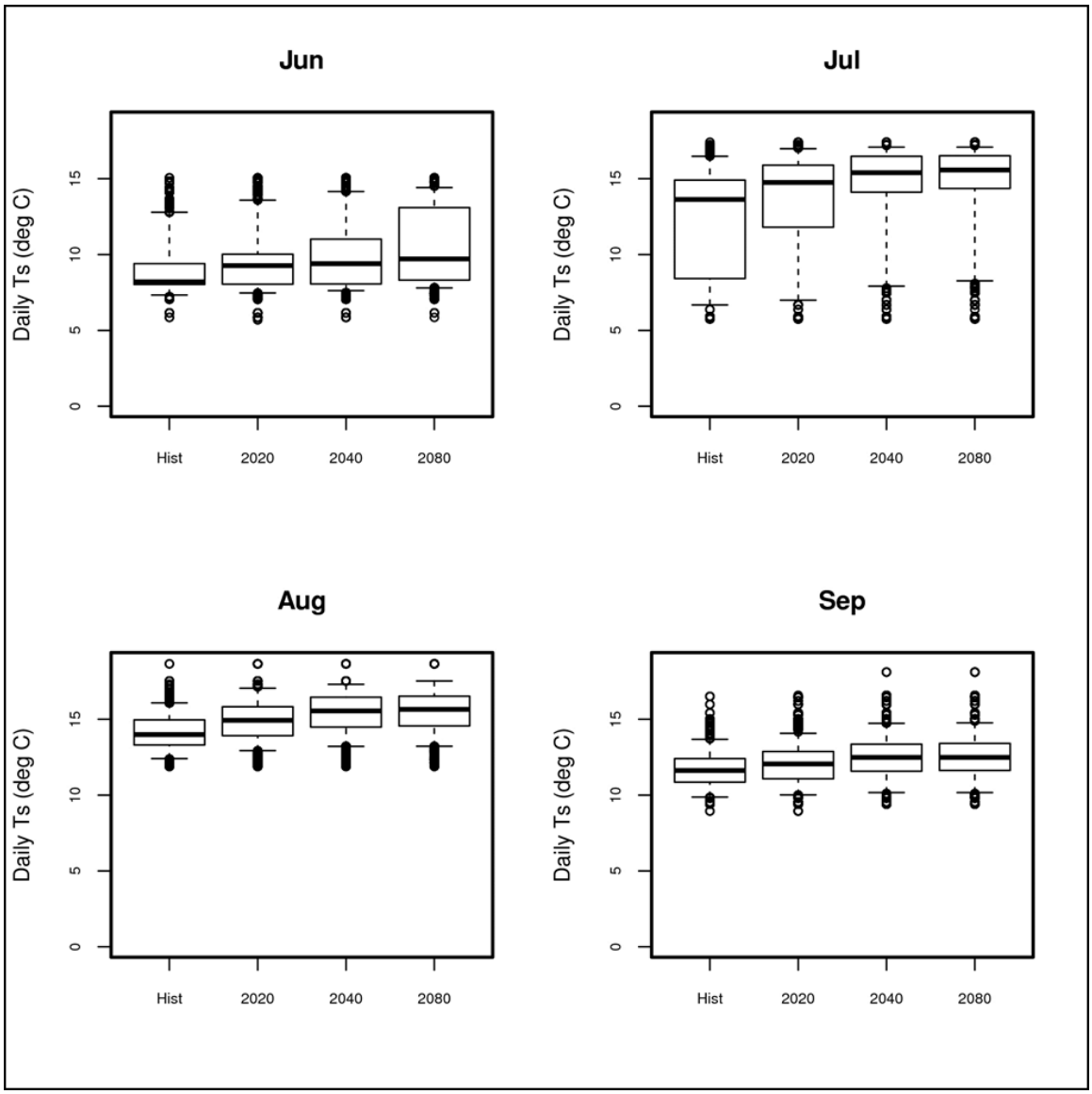

Figure 4.13: Boxplots of daily mean stream temperature for the months of June through September for the historical and each future climate horizon of 2020, 2040, and 2080, indicating the range of values predicted and uncertainty associated with each month.

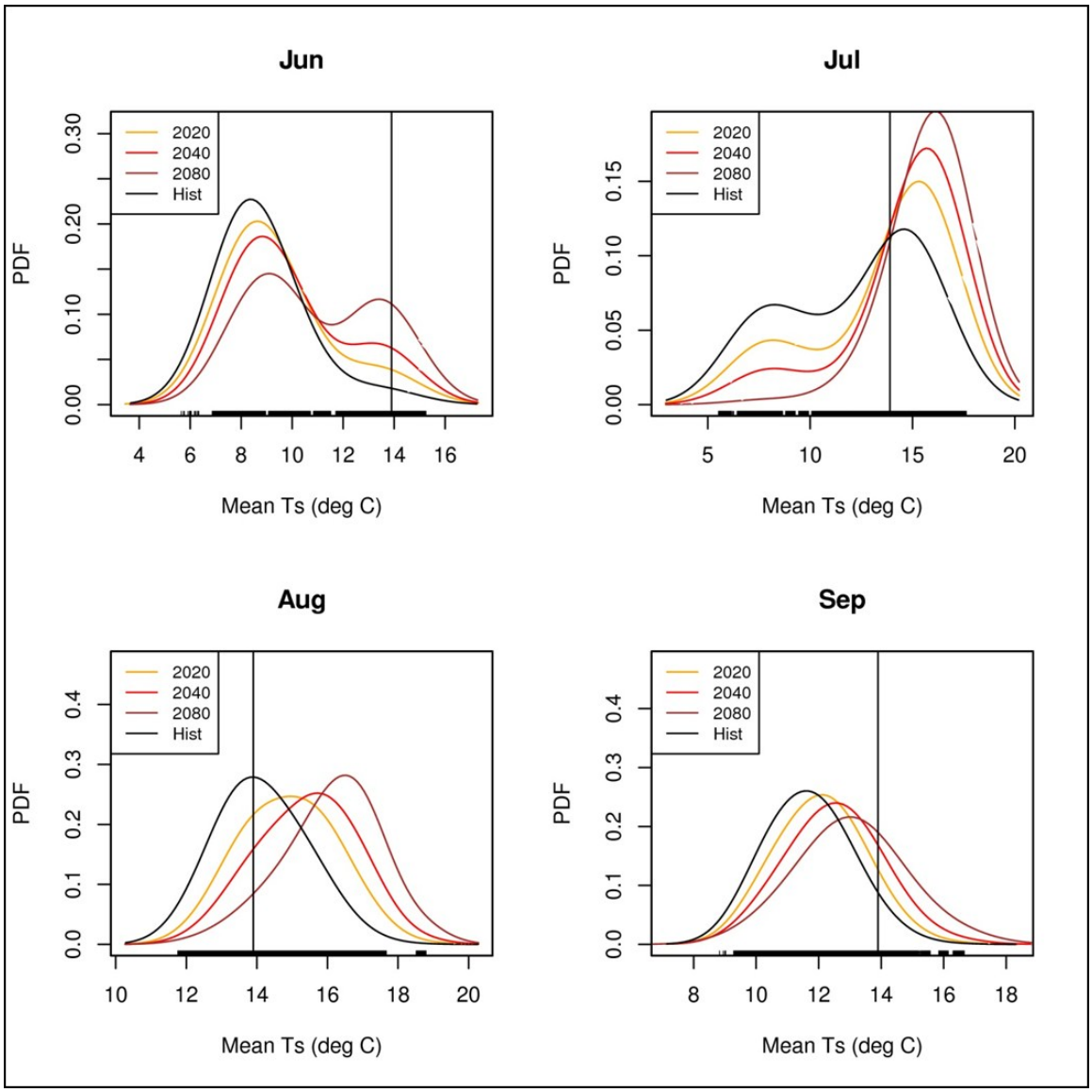

Figure 4.14: Probability density functions (PDFs) of ensemble mean values from the GLM when coupled with the VIC output using *K*-nn for the historical (black) and each future period of 2020 (orange), 2040 (red) and 2080 (dark red). Abscissa line at daily mean stream temperature of 13.9 °C indicates upper threshold used to designate properly functioning fish habitat.

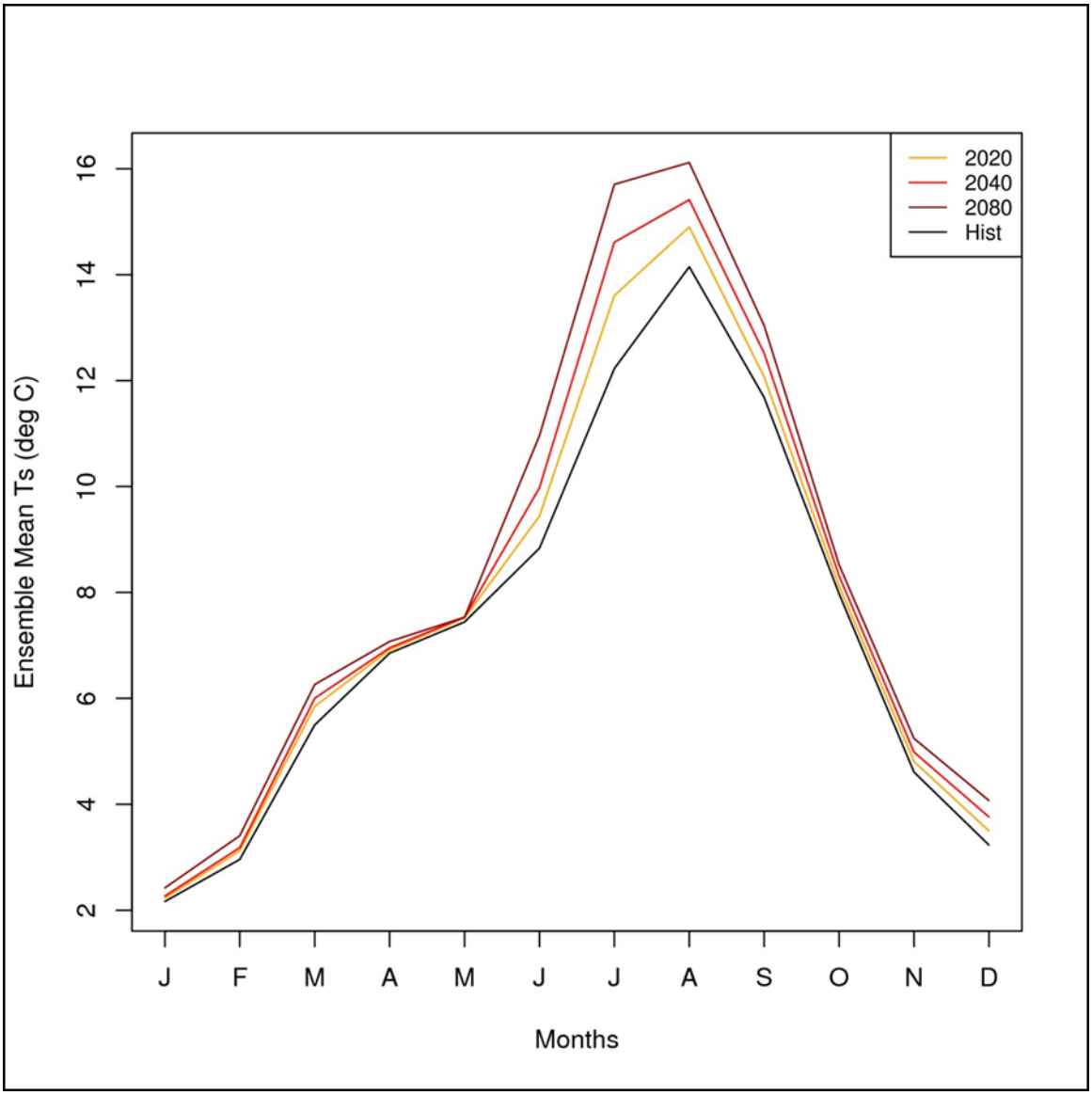

Figure 4.15: Monthly ensemble means of T_s from the GLM when coupled with the VIC output using *K*-nn for each future period of 2020 (orange), 2040 (red), and 2080 (dark red). Historical from *K*-nn shown in black.

The National Marine Fisheries Service and U.S. Fish and Wildlife Service prescribe general guidelines for T_s to assess properly functioning habitat for salmonids [Bjorn and Reiser, 1991; FWS, 1999; BOR, 2008b, Appendix I, Table I-4]. The upper limit of 13.9 °C is used to discriminate T_s that are beyond an acceptable limit, that thermal threshold at which initial effects begin to occur on salmonids, according to these two studies. Several other studies use a slightly higher value around 15 °C. The flexibility of the modeling system allows this to be a user

defined parameter as the value may differ based on species, life cycle stage of the fish, and river system. We highlight the probabilities of exceeding these values in Figure 4.14. The potential to exceed the threshold value in future climates is evident as the area under the curves is larger than historical, particularly in months June to September (Figure 4.15), with increasing impacts at each successive 2020, 2040, and 2080 time horizon, respectively. Table 4.9 shows the corresponding increases in the probability of mean daily T_s above 13.9 °C during the summer season at each time horizon. These threshold exceedances are more than 40 percent more likely during the months of July and August by the year 2080.

Table 4.9: Probability of Ts > 13.9 °C for the ensembles at each time horizon for the months of June through September.

Period	Jun	Jul	Aug	Sep
Historical	0.02	0.39	0.55	0.07
2020	0.03	0.54	0.74	0.09
2040	0.05	0.67	0.84	0.17
2080	0.11	0.85	0.95	0.27

4.6 Conclusions

The current study develops a methodology for using available daily T_s data and hydrometeorological inputs for generating statistical models of daily T_s for each month. In addition, the GLM provides a mechanism for ingesting the output from climate change scenarios to evaluate future impacts on T_s in the Methow River Basin. Despite the sparse data in the region, the statistical model fits were excellent with small values of RMSE across all months. Predicted values from the historical climate scenarios indicated that there was some limitation to skill during the winter months when data was most scarce; however, the use of a *K*-nn resampling approach improved the skill relative to using the raw output from the coupled VIC modeling

framework. As such, the *K*-nn resampling technique was applied, as well, to perform bias-adjustment on the future climate projections at each time horizon of 2020, 2040, and 2080.

The ensemble mean plots of future T_s indicated a mean annual warming of 0.8 ± 1.9°C by the year 2080 with increases relative to historical at each of the future climate horizons, all significant at the α=0.05 level. Despite the large range in the 90 percent confidence intervals, the projections remain skewed toward positive changes in stream temperature under future climate scenarios, with the primary focus during the summer months. Using a threshold T_s as a metric of viable habitat for fish, we note the increased probability of days with temperatures exceeding the threshold. The threshold of 13.9 °C is conservative due to the use of daily mean instead of instantaneous values, which suggests that the impact to viable habitat may be more profound.

Though the proposed framework provides a flexible approach to incorporate projected climate change into stream temperature modeling, there are several key uncertainties that will need to be kept in perspective while applying the methodology. There are three primary sources of uncertainty in the current study: (i) the *K*-nn resampling algorithm; (ii) the coupled VIC modeling system; and, (iii) the statistical regression. The *K*-nn resampling approach restricts sampling only from observed data, thereby possibly providing a low estimate of future climate-driven stream temperature given the assumption of warming; however, testing of the range of future values compared to historical values showed less than two percent of the daily values exceeded those from the observed record. The small fraction of projected future days that fall outside the bounds of historic observations is recognized as a potential suppression of extreme events for use in impacts analysis. In addition, future days that fall close to the bounds of the historical observations may be resampled disproportionately, resulting in reduced variability. Changes in the hydrologic character of the system (e.g., riparian vegetation) may also be

partially neglected through the limitations of the resampling approach. Since extreme events are of primary interest to impact modelers, this limitation should be considered before direct application of the approach outlined in the current study. The coupled VIC modeling system itself has several uncertainties including the process of statistical downscaling from large-scale GCM grids to finer-scale grids needed for hydrologic modeling. Also, the quality of the calibrated VIC model will govern the quality of the flow outputs. Thirdly, developing the regression models from limited data, and not being able to include variables such as the groundwater components of runoff could impact projected stream temperature results.

Subsequent modeling efforts will investigate the impact of these future scenarios on the spatial and temporal distribution of stream temperature within the confluence region of the Methow and Chewuch Rivers by using a two-dimensional hydraulic model. Therefore, we also present an efficient method for disaggregating the daily mean projections to hourly increments. While skill scores indicated satisfactory results at the CUS and MDS sites, additional calibration is required for the MUS site. This is potentially due to the limited data at that location. In an unregulated system like the Methow River, the mitigation efforts to reduce the impacts of climate change will focus on restoration projects that provide additional habitat, where suitable water temperatures can be maintained over the longest duration. Restoration efforts will focus on identifying these areas by analyzing outputs from the two-dimensional hydraulic model. We expect that these efforts will be essential in supporting healthy habitat in the Methow River Basin under climate change, particularly for cold-water fishes, such as salmon.

This chapter of the dissertation was accepted in June 2013 to Water Resources Research as an article entitled ‘Statistical Modeling of Daily and Sub-daily Stream Temperatures: Application to the Methow River Basin, Washington’; see the Caldwell et al. [2013a] reference.

5 COUPLING OF WEATHER GENERATOR AND CE-QUAL-W2

5.1 Abstract

Water temperatures have a major impact on aquatic health. This is underscored in the semi-arid regions of Western US where several factors such as increased water demand due to population growth, reduced streamflow due to extended drought in recent years, and the semi-arid climate and managed systems converge to produce acute conditions for habitat. Managed systems such as reservoirs with their cold water pool provide an opportunity to mitigate water temperature impacts. In order to mitigate water temperature effects from climate conditions with efficient water resources management, an integrated modeling approach which combines modules for water temperature, weather and reservoir release temperatures is needed. In this research, we develop such a coupled tool. The coupling consists of a stochastic weather generator to provide ensembles of weather scenarios; a hydrodynamic model to provide reservoir thermal structure and water release temperature; and a statistical water temperature model. The coupled system is demonstrated on Shasta Lake and downstream of Shasta Dam on the Sacramento River and validated by simulations for three years that are representative of cool, hot, wet, and dry conditions within the watershed. Model results are used to assess the effects of TCD operations on river thermal conditions at a downstream compliance point under variable hydroclimatological conditions. We find that the integrated modeling approach is necessary to adequately estimate the impacts to fisheries downstream; default operations yield release temperatures that predict a large number of violations downstream during the various hydroclimate conditions. Uncertainty information from this approach provides future opportunity to apply risk-based decisions to fisheries management.

5.2 Background

Water resources modifications (e.g., agricultural development, deforestation, damming, and channeling for flood mitigation) have led to changes in temperature and flow in the Sacramento River Basin (SRB) [Deas et al., 1997; Moyle and Randall, 1998; Reisner, 1986]. Historically, the SRB yields large volumes of cold water during the winter/spring and smaller volumes of warm water during the rest of the year [Myrick and Cech, 2000]. Prior to the completion of Shasta Dam in 1945 near the headwaters of the Sacramento River about 16 km north of Redding (Figure 1.1), downstream reaches in the SRB were unsuitable for salmon due to the low flow and high water temperature. The dam decreased the availability of habitat, but dam operations allowed cooler water releases during the critical late summer season to mitigate low flow and high water temperature [SFEP, 1992; van Vleck et al., 1988; Yates et al., 2008]. With a surface area of 11,940 ha, maximum depth of 157.6 m, and length of 56 km, Shasta Lake is the largest storage reservoir in California. Shasta Lake and Dam provide water for hydroelectric power generation, irrigation, municipal, and industrial uses, and recreation.

High demands from a growing population for water supply and irrigation, limited summer precipitation, and high summer air temperature and solar radiation have altered the water quality and flow patterns of the Sacramento River substantially, leading to increased risk of low flow and high water temperature, particularly in the late summer and early fall seasons [Myrick and Cech, 2002, 2004]. Population declines and extinction of native fish in the SRB have occurred concurrently with these changes [Brown, 2000; Brown and Moyle, 1993; Moyle, 1976]. For example, salmon populations have steadily declined since the late 1960s when approximately 80,000 salmon passed per year at Red Bluff [Hallock and Fisher, 1985] to the late 1990s when less than 1,500/year were observed [CDFG, 2005]. Since the late 1990s, a slight

recovery in returning salmon has been observed, though in 2008 and 2009, the SRB was closed to fishing due to the low numbers of salmon in those years. Because salmon are sensitive to water temperatures, a maximum temperature threshold of 13.3 °C (56 °F) was established [BOR, 1991a, 1991b, 2004] in a key habitat regime along a stretch of the Sacramento River from Keswick Dam to the City of Red Bluff to address sustainability of salmon populations [Bettelheim, 2001; Deas et al., 1997; Hallock and Fisher, 1985].

Protection of the native fish in the SRB continues to be a conflict between human needs for water resources and requirements of ecosystems. Careful and innovative operations strategies will be needed to address this conflict as any changes in water management in response to climate change and agricultural/urban needs could result in conditions that favor non-native species [May and Brown, 2002]. Yates et al. [2008] conclude that future warming could lead to additional threshold temperature exceedances, particularly in August and September drought years. The period of potential exceedance would increase from an average of three months during the period 1971-1998 to five months given warming scenarios of +2 and +4 °C by the mid-21st century [Yates et al., 2008]. In addition, Yates et al. [2008] found that the cold pool in Shasta Lake available for mitigating downstream water temperature would be difficult to maintain through the summer given the two warming scenarios.

In the mid-1990s, the U.S. Bureau of Reclamation (Reclamation) installed a temperature control device (TCD) at Shasta Dam to improve the capability of reservoir operators to maintain suitable water temperatures downstream of the dam for the winter-run Chinook salmon populations protected by the Endangered Species Act. Until the TCD installation in 1997, Reclamation addressed thermal criteria by releasing water through bypass outlets, instead of routing through penstocks to power generating facilities before discharge to the river. Bypassing

of the penstocks during the period of 1987 to 1996 resulted in approximately $63 million in lost power generation revenue [Saito, 1999]. In February 1997, the TCD was installed upstream of Shasta Dam (Figure 5.1), providing the opportunity to selectively withdraw from different reservoir elevations (i.e., different water temperatures within the reservoir water column) to meet thermal objectives downstream. The TCD allows ample discharge for hydropower generation cost $80 million to install. The TCD consists of a shutter structure for each of the five penstocks to the power plant. Shallow, deep, and/or intermediate withdrawals can be made using the adjustable shutters. In addition, a new low-level outlet was installed that allowed withdrawal from depths deeper than possible before TCD installation [Hanna et al., 1999].

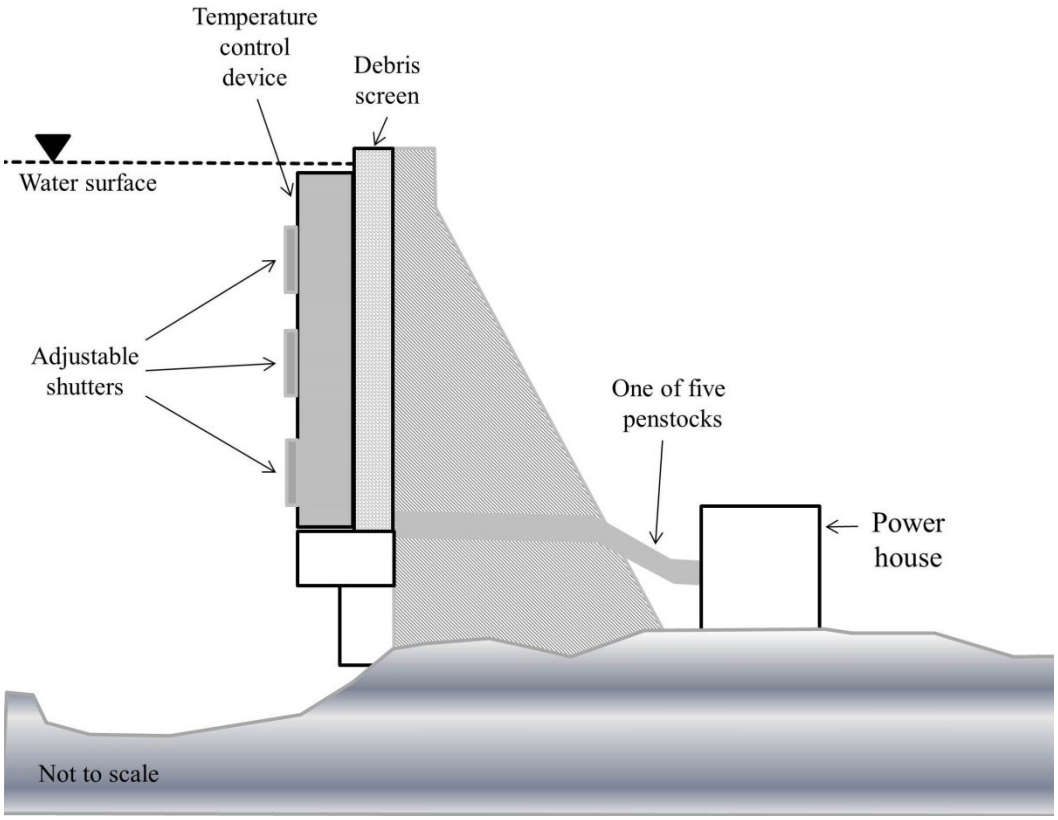

Figure 5.1: Temperature control device schematic as seen through a cross-section of Shasta Dam. Penstocks are all at elevation 249 m (adapted from Hanna et al. [1999]).

Operation of the TCD altered both the in-reservoir and downstream thermal, chemical, and, hence, biological dynamics of the system. Using coupled hydrodynamic and ecological models, the in-reservoir effects of TCD operations on water quality and biota, including fish and phytoplankton within Shasta Lake, were examined [Bartholow et al., 2001; Saito et al., 2001], and as well as the ability of the TCD to meet downstream temperature objectives [Bartholow et al, 2001; Hanna et al., 1999]. Hanna et al. [1999] found that the new TCD operations would improve the ability to meet downstream temperature targets, but the operations would have little effect on in-reservoir conditions for fish [Bartholow et al., 2001; Hanna et al., 1999; Saito et al., 1999]. Lieberman et al. [2001] also used monitoring data to evaluate the effects of the TCD on nutrients, particulate organic matter, and plankton in the Shasta Dam tailwaters and found that water quality pre- and post-installation of the TCD may potentially influence the food base, and therefore, fish production in the Upper Sacramento River. In addition, Deas et al. [1997] developed models of river temperature for the Sacramento River downstream of Shasta Dam and investigated the sensitivity of water temperature predictions to upstream boundary conditions and meteorology. These studies evaluated the effects of TCD operations on in-reservoir and downstream temperatures and fish impacts; however, they did not address the assessment of thermal conditions under variable climatological conditions.

Biological criteria for salmonid health on the Sacramento River below Shasta Dam have been set through collaboration between Reclamation and the National Marine Fisheries Service (NMFS). While a threshold temperature of 13.3 °C (56 °F) has been determined critical for meeting thermal objectives on the river [Deas et al., 1997], Reclamation and NMFS meet regularly to decide on the location of the compliance requirement [BOR, 2004]. The most upstream compliance point within the modeling domain is the Balls Ferry gauge with the most

downstream point at Red Bluff Diversion Dam. Balls Ferry is selected as the compliance point of interest since it is closest to Shasta Dam and has the highest probability of experiencing the mitigation effects of the TCD. In other words, if the temperature objectives are not met at Balls Ferry, it is highly likely that due to interaction with the atmosphere, downstream water temperatures will be warmer. The most critical period is in the late summer and fall, when cold water storage in Shasta Lake is typically low and meteorological conditions are hot and dry. During this period, there is a restriction on the river that no more than three consecutive days can exceed the mean daily water temperature threshold by 0.9 °C (0.5 °F) [BOR 1991a, 1991b]. Thus, the intent of the TCD is to reduce the magnitude and the duration of high temperature water downstream of Shasta Dam during that time.

In order to enable efficient management of the water resources system to mitigate water temperature effects from climate conditions, an integrated modeling approach which combines modules for water temperature, weather and reservoir (lake) release temperatures is needed. In this research we develop such a coupled tool. The coupling consists of a stochastic weather generator to provide ensembles of weather scenarios [Apipattanavis et al., 2007]; a hydrodynamic lake model [Hanna et al., 1999; Saito et al., 2001] to provide the lake thermal structure and water release temperature and, a statistical water temperature model [Caldwell et al., 2013b]. The coupled system is demonstrated and validated by simulations for several years since operation of the TCD began in 1997 that are representative of cool, hot, wet, and dry conditions within the watershed. Model results are used to assess the effects of TCD operations on river thermal conditions at a compliance point downstream under variable hydroclimatological conditions.

5.3 Methods

5.3.1 Proposed Coupled System and the Components

The proposed coupled system is shown in the schematic of Figure 5.2. In this, a reservoir hydrodynamic and water quality model, CE-QUAL-W2 (W2; Cole and Wells [2011]], is linked with a stochastic weather generator [Apipattanavis et al., 2007] and a statistical model of water temperature attributes using a generalized linear modeling (GLM) approach for the downstream compliance point at Balls Ferry [Caldwell et al., 2013b]. The stochastic weather generator provides multiple scenarios of daily weather that feed into both the W2 and GLM models; the W2 model provides the reservoir thermal structure and the water release temperatures that are additional inputs to the GLM model which results in forecasting of water temperature attributes at Balls Ferry. Details on the individual components of the flow chart in Figure 5.2 are provided in subsequent sections.

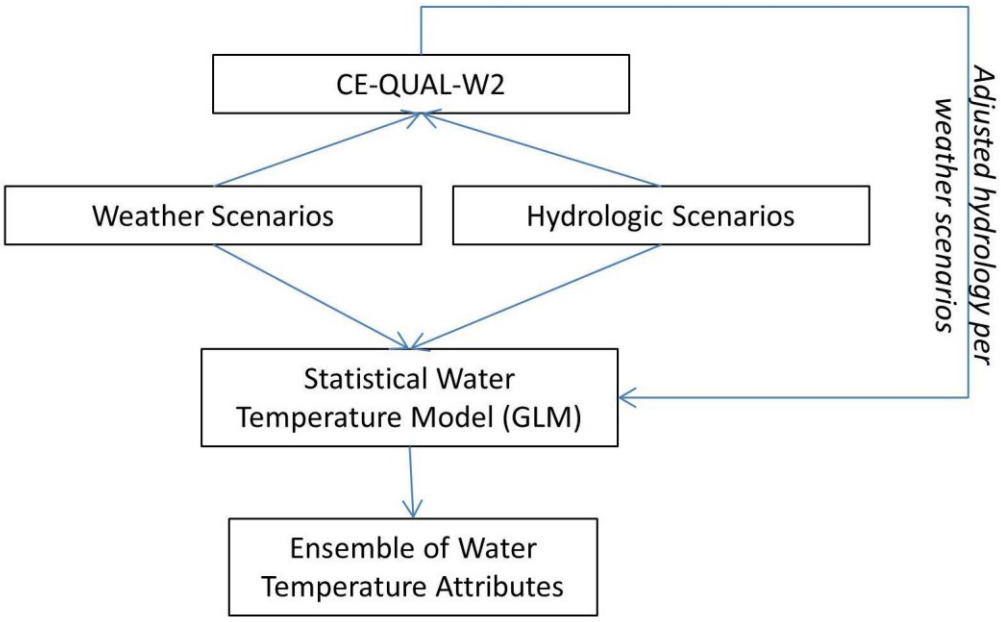

Figure 5.2: Flow chart of the modeling approach.

This modeling approach was selected for several reasons. First, meeting release temperature objectives at the reservoir potentially neglects the impact of environmental conditions and lag time between the dam and the downstream compliance point. The statistical model provides the opportunity to include atmospheric forcing and lagged predictor variables to incorporate these processes. Second, the application of stochastically-generated weather scenarios provides an opportunity to evaluate uncertainty and multiple hydroclimate regimes through conditional resampling rather than using a single input time series to the hydrodynamic model. The stochastic approach, however, fails to capture the effects of the simulated weather on reservoir conditions (i.e., in-reservoir vertical thermal structure, volume of cool hypolimnetic water, etc.) throughout the year. Without the coupling with a hydrodynamic reservoir model, the hydrologic forcing in the statistical model (i.e., release temperature and flow from Shasta Dam) assumes median values for a given Julian day. Integration with CE-QUAL-W2 allows adjusted hydrology to be generated using the stochastically-generated weather ensembles to serve as input to the reservoir model, ensuring consistency between simulated weather and water release temperature from the dam. Therefore, the third advantage of the linked modeling approach is the ability to include the reservoir thermodynamics appropriately in the statistical model input.

5.3.2 Hydrodynamic Model of Shasta Lake

Shasta Lake is a large, deep, and dendritic system with water quality characteristics that vary spatially and temporally. As such, Hanna et al. [1999] developed and calibrated a W2 model for Shasta Lake to simulate TCD operations and predict in-reservoir water temperatures. W2 is a two-dimensional hydrodynamic and water quality model that can simulate reservoir operations [Cole and Buchak, 1995]. This current study uses the model of Hanna et al. [1999] that was upgraded to version 3.7 of W2 from Cole and Wells [2011].

Reservoir geometry in the W2 model is two-dimensional and varies with depth and longitudinal distance, with lateral averaging in the third dimension (Figure 5.3). The Shasta Lake W2 model is partitioned into 63 model segments along the length of the reservoir. Model output for Shasta Lake consists of simulated vertical profiles of water quality parameters, including water temperature for each of those segments at a maximum of 51 vertical layers, ranging from 1.5m thick at the surface to 6m thick at the bottom. As seen in Figure 5.3, Shasta Lake is fed by multiple rivers and creeks. The W2 model includes five branches: Pit River, Squaw Creek, McCloud River, Sacramento River, and Backbone Creek Inlet, although flows are assumed to be zero for Backbone Creek [Saito et al., 2001].

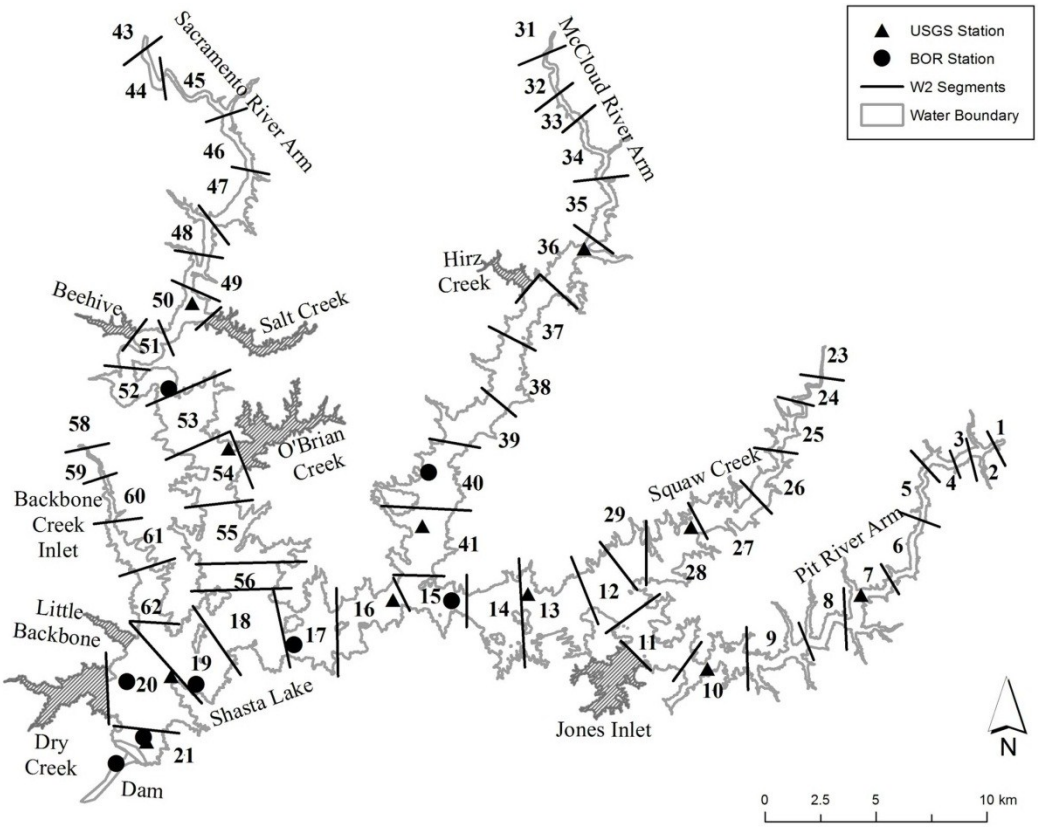

Figure 5.3: Shasta Lake segmentation map for CE-QUAL-W2 model (adapted from Saito [1999]. Model segment numbers, boundaries, and sampling stations are also indicated.

The W2 model of Shasta Lake requires the following inputs: measured bathymetry from topographic maps, initial storage and initial in-reservoir temperature, daily inflow volumes, daily inflow temperatures, daily outflow volumes, and sub-daily meteorological data. Outflow volumes and computed total inflows to Shasta Lake were provided by Reclamation for the period 1994 to present. Daily inflow volumes and temperatures were gathered from the U.S. Geological Survey (USGS) for three tributaries: Pit River (#11365000), McCloud River (#11368000), and Sacramento River (#11365000). Squaw Creek, the fourth tributary was estimated using methods in Saito [1999). Sub-daily meteorological data were not available near Shasta Dam for the period of interest; therefore, the meteorological data from the Redding Airport site were adjusted to account for elevation based on regression equations from Saito [1999]. TCD operations for the model were established using a set of decision points throughout the year based upon the release temperature target, where release temperatures are as warm as possible from November through April and cooler than temperature thresholds during May through August as applied in Hanna et al. [1999] (Figure 5.4).

The model was re-calibrated for the present study using Version 3.7 of W2 by comparing in-reservoir water temperature output with water temperature profile data collected by the USGS in 1995; the locations of those sites are also shown in Figure 5.3. Model coefficients were adjusted and investigated through sensitivity analyses to determine the effects of and appropriate values for the model's coefficients for wind sheltering (WSC), bottom heat exchange (EXH20), and light extinction (BETA). The final calibrated values for WSC (1.0), EXH20 (0.40), and BETA (0.45) were the same as in Hanna et al. [1999]. Calibration results indicate that simulations of reservoir water surface elevation at the dam in the year 1995 had a root mean squared error (RMSE) of 0.17m, percent bias of 0.02%, and adjusted R^2 of 0.999. Monthly

temperature statistics for the calibration run included RMSE in °C ranging from 0.59 (May) to 1.23 (Oct), with a mean error of +0.95 °C. The mean percent bias was -2.33%, and the mean adjusted R^2 was 0.966.

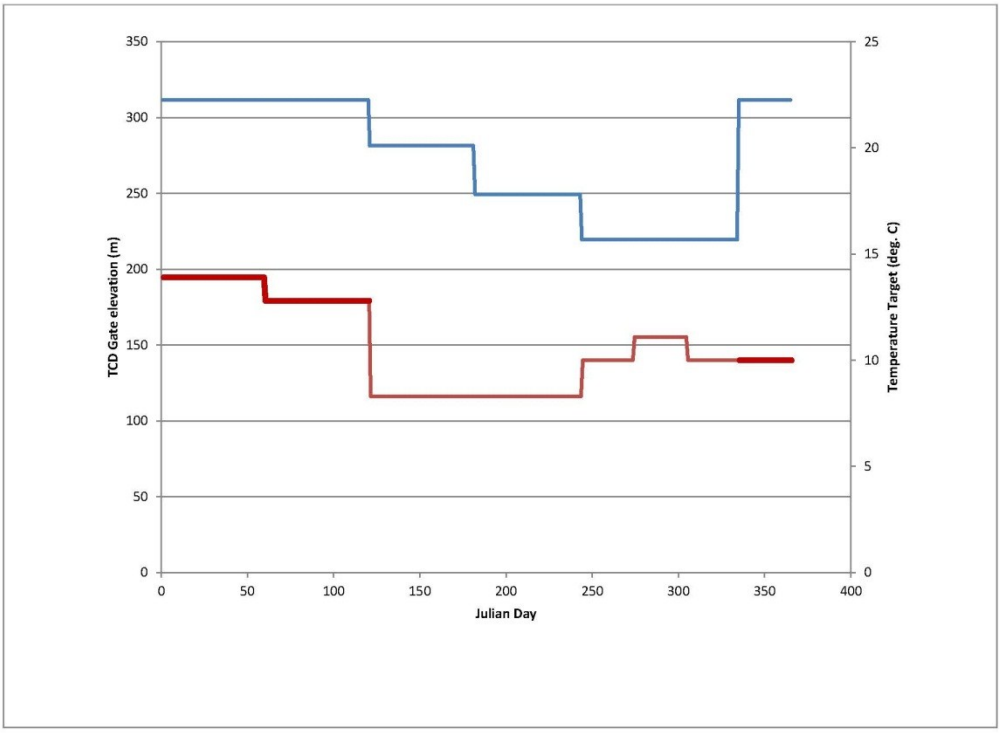

Figure 5.4: TCD gate operations and release temperature targets used in the Hanna et al. [1999] study.

5.3.3 Stochastic Weather Generator

Weather generator algorithms are typically used to produce multiple, synthetic time series of weather from finite station records of hydrometeorological variables. These time series are expected to capture the statistical properties of the historical record, such as mean, variance, skew and probability density function. Parametric and non-parametric methods have been employed to the task of stochastic weather generation [Wilks, 1999; Wilks and Wilby, 1999,

Rajagopalan and Lall, 1999]. Parametric weather generators entail modeling precipitation occurrence as a Markov Chain and conditionally modeling precipitation amounts and other weather variables such as maximum and minimum temperatures, solar radiation etc., via parametric probability distribution functions fitted to the historical data. Capturing seasonality and lagged dependence requires fitting the distributions and Markov chains separately for each month and multivariate regression model. As can be seen the computational expense is quite high by way of fitting several model parameters, furthermore, it can get unwieldy if this is to be extended for multi-site weather generation. Also, any distributional features, such as bimodality, and nonlinearity in relationships are not captured using parametric methods due to the unimodal nature of the candidate distributions and underlying assumption of linearity for the regression models (see Rajagopalan and Lall, 1999; Rajagopalan et al., 2010 for an overview of these methods).

Non-parametric methods, on the other hand, are data driven, and hence make no a priori assumptions based on distribution of the historical data or linearity. See Rajagopalan [1995] and Rajagopalan et al. [2010] for an overview of these methods for hydrologic modeling. There are several nonparametric methods of which k-Nearest Neighbor (*K*-nn) time series resampling, first introduced by Lall and Sharma [1996], is simpler and robust. The method has been expanded to multivariate weather generation [Rajagopalan and Lall, 1999], and more recently, to multiple sites [Buishand and Brandsma, 2001; Mehrotra and Sharma, 2006; Yates et al., 2003] and also to downscaling climate information [Bannayan and Hoogenboom, 2008].

The *K*-nn based stochastic weather generators [Rajagopalan and Lall, 1999; Yates et al., 2003] have been enhanced with addition of Markov Chains [Apipattanavis, 2007] and labeled the semi-parametric weather generator (SWG), which is used in this research. In SWG, daily

weather for day ‘t’ is based on the weather vector on day ‘t-1’ and the precipitation states (wet or dry) on days ‘t-1’ and ‘t’; K nearest neighbors of the weather vector on day ‘t’ are obtained from historical days within a small window centered on day ‘t’ and one of them is resampled using a weight function that gives more weighting to the nearest neighbor and least to the farthest [Lall and Sharma, 1996]. The SWG can be applied to generate a variety of daily weather sequences for a desired season of any length based on historical data (unconditional generation), or based on probabilistic seasonal climate forecasts (conditional generation). For example, if there is a forecast of 40 percent above normal temperature, 35 percent near-normal, and 25 percent below normal temperatures, the neighbor selection can pick from the respective hot, normal, and cool years at the given percentages, respectively, thus generating daily weather sequences that are consistent with the probabilistic seasonal climate forecast. The use of seasonal climate forecasts in weather generators are described in the above references. The integration of weather generators with crop models, hydrologic models and also in construction management has been well-documented [Apipattanavis, 2010a, 2010b; Hobson, 2005; Podesta et al. 2010].

In this chapter, conditional weather ensembles were generated using the SWG with both analog years and a seasonal climate forecast. For the analog years of 2000, 2003, and 2005, the SWG software of Appipatanavis et al. [2007] was adapted such that the observed meteorology, precipitation state, and precipitation transition type for the analog year were applied in the *K*-nn resampling. The neighbors selected for a given day were required to be representative of the current and prior day’s weather. For example, on January 1, 2003, a set of neighbors are selected from the historical record that are similar to the meteorological conditions on that day. Using this method, the antecedent atmospheric conditions may be coupled with the observed flow and water temperature conditions in that year to create an ensemble of hydroclimatologically-consistent

time series of atmospheric and hydrologic forcings. In addition, unconditional (33.3 percent probability in each tercile) and conditional weather ensembles (using a seasonal climate forecast of 40 percent above normal, 35 percent near normal, and 25 percent below normal air temperatures) were generated to indicate the potential application to seasonal planning during the hot year of 2003.

5.3.4 Statistical Models of Water Temperature Attributes

The availability of the W2 model provides upstream boundary conditions (i.e., Shasta Dam release temperature and volume) that serve as input to a statistical model for water temperature attributes at the downstream compliance point at Balls Ferry. The statistical model essentially predicts the change in water temperature from Shasta outfall to the compliance point as a result of the atmospheric forcing (i.e., translates reservoir operations downstream to the river portion of the Sacramento River system).

For completeness, a brief description of the GLM approach developed in Caldwell et al. [2013b] is provided. In a GLM, the response or the dependent variable Y can be assumed to be a realization from any distribution in the exponential family with a set of parameters [McCullagh and Nelder, 1989]. A smooth and invertible link function transforms the conditional expectation of Y to a set of predictors (Equation 5.1).

$$G(E(Y)) = f(X) + \varepsilon = X\beta^T + \varepsilon \qquad (5.1)$$

G(.) is the link function, *X* is the set of predictors or independent variables, *E(Y)* is the expected value of the response variable, ^{T} is the transpose operator, and ε is the error assumed to be normally distributed with variance (σ_ε). In a linear model (the standard linear regression), the function *G(.)* is identity and *Y* is assumed to be normally distributed. Depending on the assumed

distribution of Y, there exists an appropriate link function [McCullagh and Nelder, 1989]. The model parameters, β, are estimated using an iterative weighted least squares method that maximizes the likelihood function as opposed to an ordinary least squares method in linear modeling. The GLM can be used to model a variety of response variables. For skewed variables with a lower bound of 0 such as daily maximum water temperature (DTX) or daily water temperature range (DTR), the Gamma distribution assumption of Y and its associated link function is appropriate. The Gamma distribution is also valid for the daily minimum and daily mean water temperature (DTN and DTM, respectively). For number of hours of temperature exceedance (NHE), the Poisson distribution and its associated link functions can be used; for probability of exceedance (POE), a binomial distribution and its link function (i.e., logistic regression) is the approach. We refer the readers to McCullagh and Nelder [1989] for information about a variety of distributions, link functions, and parameter estimation.

To obtain the best set of predictors for the model, there are objective criteria such as the Akaike Information Criteria (AIC) or Bayesian Information Criteria (BIC), both of which penalize the likelihood function based on the number of parameters [Venables and Ripley, 2002]. Models are fit using all possible subsets of predictors and also link functions; for each, the AIC and BIC are computed and the model with lowest AIC or BIC is selected as the 'best model.' Models can also be tested for significance against a null model or an appropriate subset model using a chi-squared test. We used BIC in this study as it tends to be slightly more parsimonious compared to AIC.

The function f in Equation 5.1 is linear and fitted to the entire data, and therefore can miss capturing "local" nonlinearities. To address this, we used a nonparametric approach based on local polynomials [Loader, 1999] to fit f. In this, the function is estimated 'locally' for any

desired point x. The small set of neighbors (αN; N is the total number of data points and α is a value in the range of 0 to 1) to x is identified and to this a polynomial of order p is fitted. Thus, we used the fitted polynomial to estimate the response variable Y at the desired point x. This process is repeated for any estimation point. Note that if α and p are set to 1 then this collapses to the linear functional model in Equation 5.1. In this regard, the local polynomial provides an additional degree of flexibility to the GLM framework. The choice of α and p are obtained using a Generalized Cross Validation criteria (GCV) that is similar to AIC. The GCV can also be used to obtain the best set of predictors [e.g., Regonda et al., 2005]. However, the local polynomials are fit to the best predictor set obtained from BIC above using the global fit. This hybrid approach was applied in Caldwell et al. [2013b] and is preferred for computational efficiency. A large number of predictors are considered based on prior research and knowledge of the system, including the water and air temperatures and hydrologic characteristics of the previous and current day (see Table 3.1). In addition, a seasonal model fit for the period July through September is also provided to encompass the primary season of violations. The GLM is used to translate the release temperature and flow from Shasta Dam to the downstream compliance point at Balls Ferry, allowing the W2 model forced with the variety of future hydroclimates to determine the thermal structure in the reservoir driven by atmospheric conditions and TCD operations.

5.3.5 Multi-model Integration and Application

The data from the study region and the selected years for application is first described, followed by the steps involved in the multi-model integration. High quality measurements of hourly water temperature at the Balls Ferry gauge are available for the period 1994 to present from the California Data Exchange Center (CDEC) of the California Department of Water

Resources. Overlapping hourly discharge and water temperature release data at Shasta Dam are also available from CDEC with hourly meteorological data from the National Weather Service automated site at Redding Airport. Since the primary season of interest for fish mortality includes the summer months when water supply is low and atmospheric heating is at a maximum, the selection of years for simulation focus on the seasonal values of mean air temperature and total precipitation. During the period 1994 to present, an evaluation of meteorological data identified three years that represent dry (2005), hot (2003), and cool, wet (2000) conditions (Figure 5.5). The data from each of these years were used to generate multiple scenarios within the weather generator software while constraining the weather scenarios to best match flow conditions in the river system during the observed year.

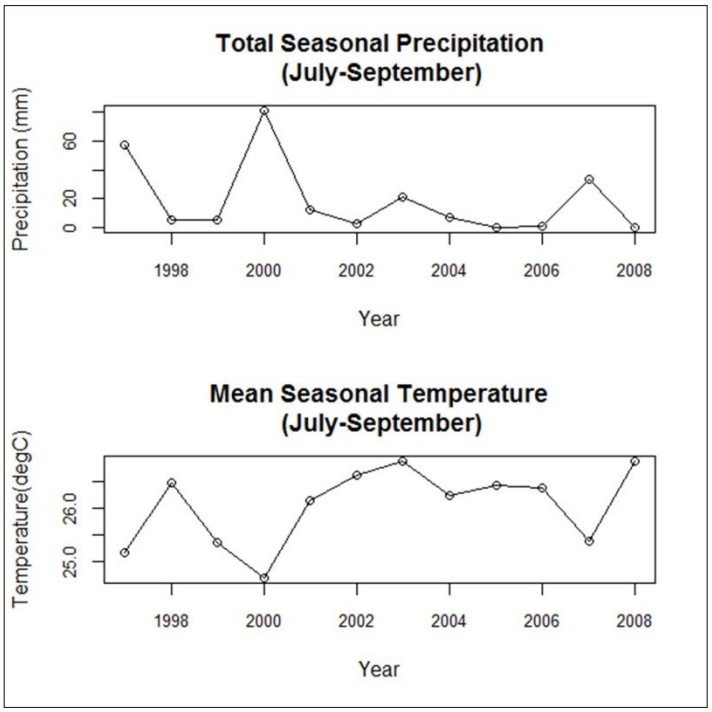

Figure 5.5: Seasonal a) total precipitation and b) mean air temperature for the period July through September at Redding, California, used for selecting different hydroclimatological regimes.

For the analog years of 2000, 2003, and 2005, the SWG weather generator was applied to generate daily for each day in these years using the observed data from the previous day. For example, an ensemble of daily weather is generated for January 2, 2000 using the observed daily weather of January 1, 2000 and the precipitation transition type between these days and so on. Thus, the produced weather ensembles, along with the daily observed flow and water temperature conditions, create an ensemble of hydroclimatologically-consistent time series of atmospheric and hydrologic forcings. For 'conditional' weather ensembles, a seasonal temperature forecast of 40 percent above normal, 35 percent near normal, and 25 percent below normal air temperatures for the year 2003 was used.

As shown in Figure 5.2, integration of the individual dynamic and statistical tools provide a coupled system that uses TCD operations and an ensemble of weather and hydrologic conditions to modify in-reservoir thermal structure. The level of release from the default TCD operations is used to extract the release temperature from the modified in-reservoir thermal profile prior to application in the GLM for prediction of the water temperature attributes at the Balls Ferry compliance point. The individual steps required include:

a) The weather generator is conditioned on one of the analog years or on a future climate forecast to provide a set of dates from the historical record

b) For each simulated date, the hourly observed meteorology at Redding Airport is adjusted to Shasta Dam for the W2 model and daily observed meteorology at Redding Airport is retained for application in the statistical model to produce the weather scenarios

c) For each simulated date, the observed daily inflows, outflow, and water temperature data are applied in the W2 model and may also be applied directly in the statistical model (i.e., generate hydrologic scenarios)

d) Instead of using the observed temperature release data on individual days, we use the W2 model to predict the in-reservoir thermal conditions based on the weather scenarios and hydrologic scenarios and replace the original release temperature variable in the statistical model

e) Finally, the adjusted hydrology is input to the statistical model to predict thermal conditions downstream at the compliance point at Balls Ferry

5.4 Results

5.4.1 Weather Generation Performance

The primary variables of interest in the statistical models include daily maximum and minimum air temperature and release flow and temperature from Shasta Dam. Since the weather generator is conditioned on particular years, the expectation is that the observed values from any individual year will fall within the bounds of the simulated variables. Indeed, the weather generator is capable of reproducing the atmospheric and hydrologic conditions at Shasta Dam (e.g., Figure 5.6). Plots for the month of July (Figure 5.6) are representative of those from all other months (not shown) and represent the ensemble of inputs available for application in both W2 and the water temperature attribute ensembles from the GLM.

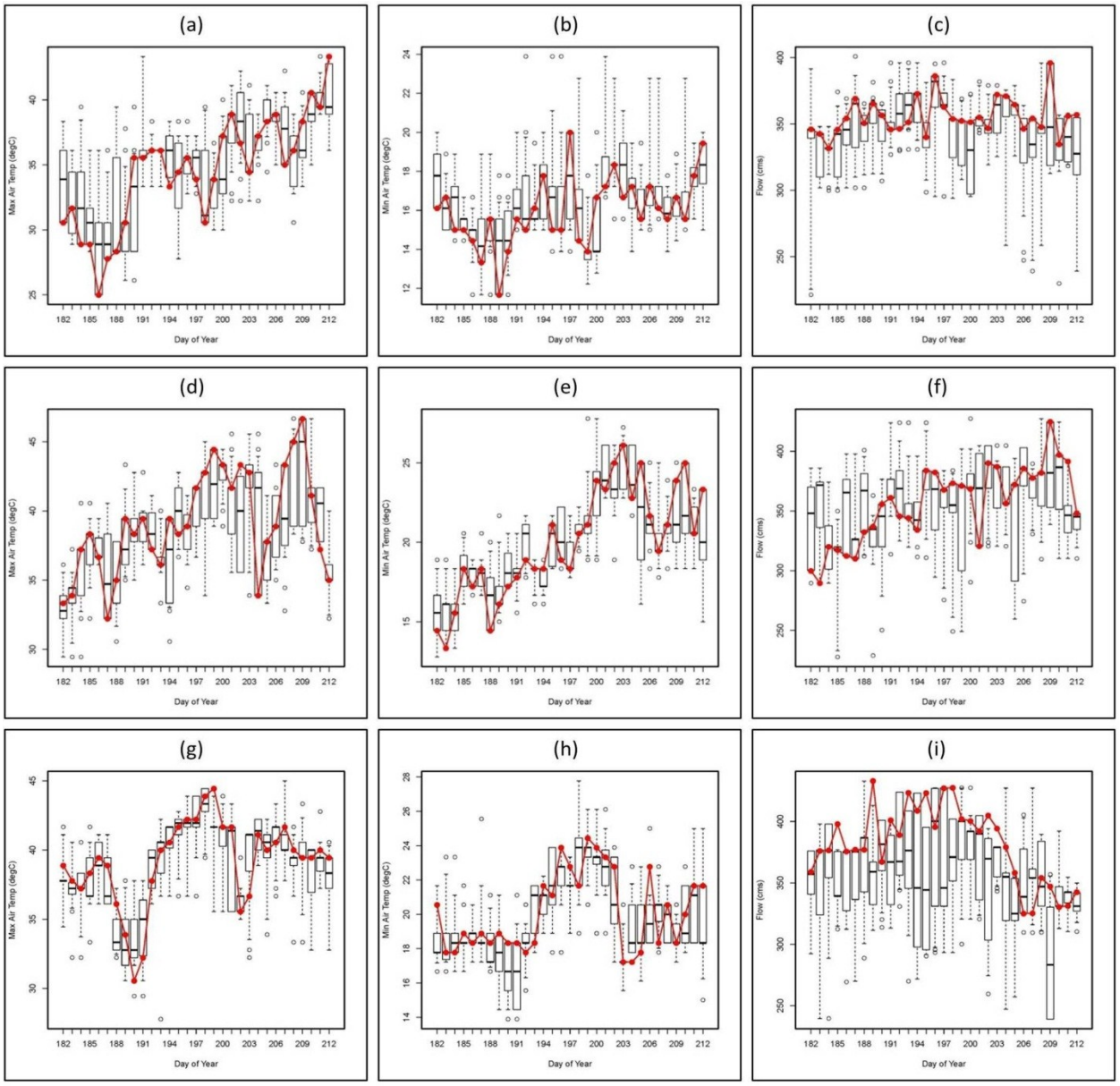

Figure 5.6: Comparison of observed (red lines and points) and simulated (boxplots) values of maximum air temperature (left column), minimum air temperature (center column), and output volume (right column) at Shasta Dam for the different hydroclimate years of 2000 (a, b, c), 2003 (d, e, f), and 2005 (g, h, i) for the month of July.

5.4.2 In-Reservoir Water Temperature Performance

For each of the analog years (i.e., 2000, 2003, and 2005), Reclamation provided in-reservoir thermal profiles approximately 122m upstream of the dam, which corresponds to segment 21 in the W2 model. These data were non-continuous throughout each year and a total

of nine days were available during the summer season (July to October) for the year 2003. The model generally under-estimates the release temperature at the level of TCD release (shown in blue) during the early summer (Julian day ≤ 223) by a mean value of 1.9 °C (Figure 5.7); however, during the latter half of the summer (223 < Julian day < 282), the estimate of release temperature is well-captured by the ensembles with mean error of 0.20 °C. In addition, the W2 model in simulation mode shows similar skill to the calibration run; the mean error at all levels within the thermal profile for all days during the summer season is -0.31 °C with a range of -1.33 to +1.26 °C, which is approximately the same magnitude of the +0.95 °C mean error during the calibration year of 1995.

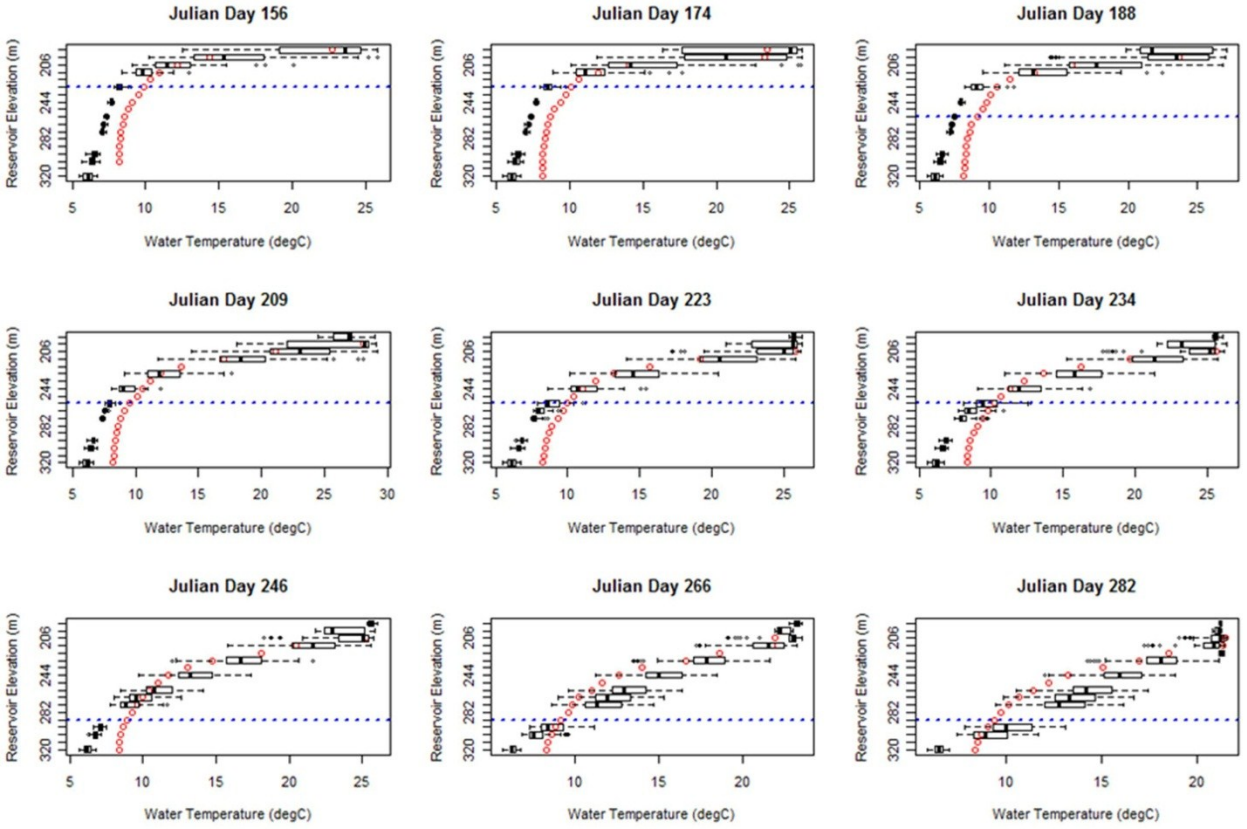

Figure 5.7: Boxplots of the simulated thermal profiles in segment 21 of the W2 model on the Julian day noted during the year 2003 with observed values within that segment from Reclamation (red).

5.4.3 Downstream Water Temperature Performance

After implementing the ensemble of weather and hydrology scenarios within the W2 model, the TCD shutter elevation schedule for operations and the dam outflow temperature prediction from W2 is used to replace the original water temperature release variable from the weather generator. The new water temperature release variable is then applied in the GLM to generate new predicted values of each water temperature attribute at Balls Ferry.

While the models of number of hours exceeding the threshold temperature of 13.3 °C (NHE) and the probability of exceeding that threshold (POE) for each of the hydroclimate conditions (i.e., the years of 2000, 2003, and 2005) generally capture the seasonal variability, there is an under-estimation of NHE, and hence POE, particularly during the summer months of August and September (Figure 5.8 through Figure 5.10). In July, the predictions of POE are highly variable and are roughly normally distributed between the values of 0 and 1. Models of DTR, DTX, DTN, and DTM, however, generally capture the observed values well, with deviations occurring primarily during the cool season and spring runoff season. Mean errors of DTR, DTX, DTN, and DTM are relatively small (Figure 5.11). Largest mean errors exist in September and December for DTN and DTM; however, both are still +/- 2 °C. A preference for under- or over-estimation by the coupled W2-GLM models for the other variables is not evident for other months or hydroclimate type.

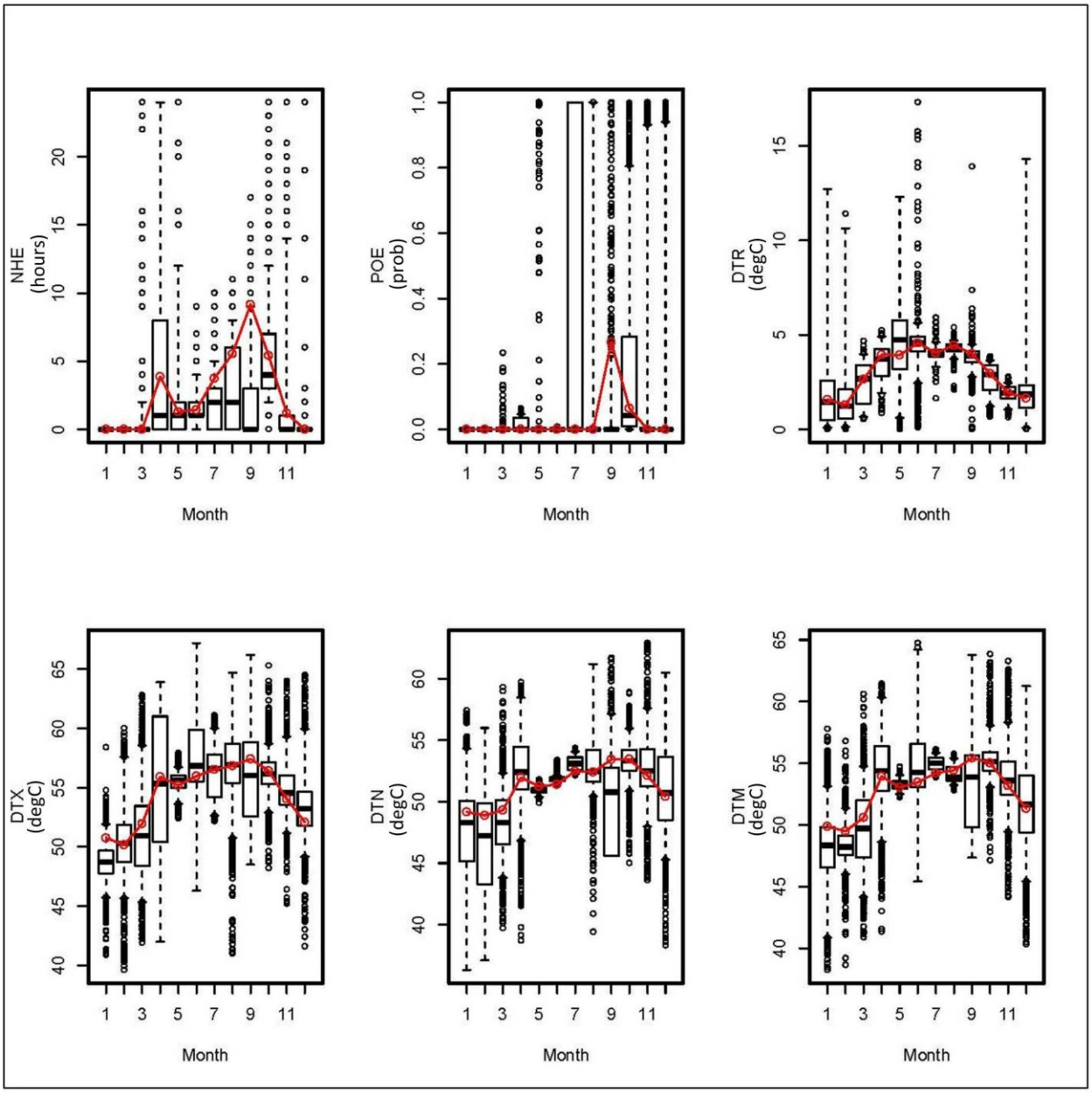

Figure 5.8: Comparison of observed (red lines and points) and simulated (boxplots) values of each water temperature attribute at the Balls Ferry gauge, including number of hours of exceedance (NHE), probability of exceedance (POE), daily water temperature range in °C (DTR), daily maximum water temperature in °C (DTX), daily minimum water temperature in °C (DTN), and daily mean water temperature in °C (DTM) for the cool, wet year of 2000.

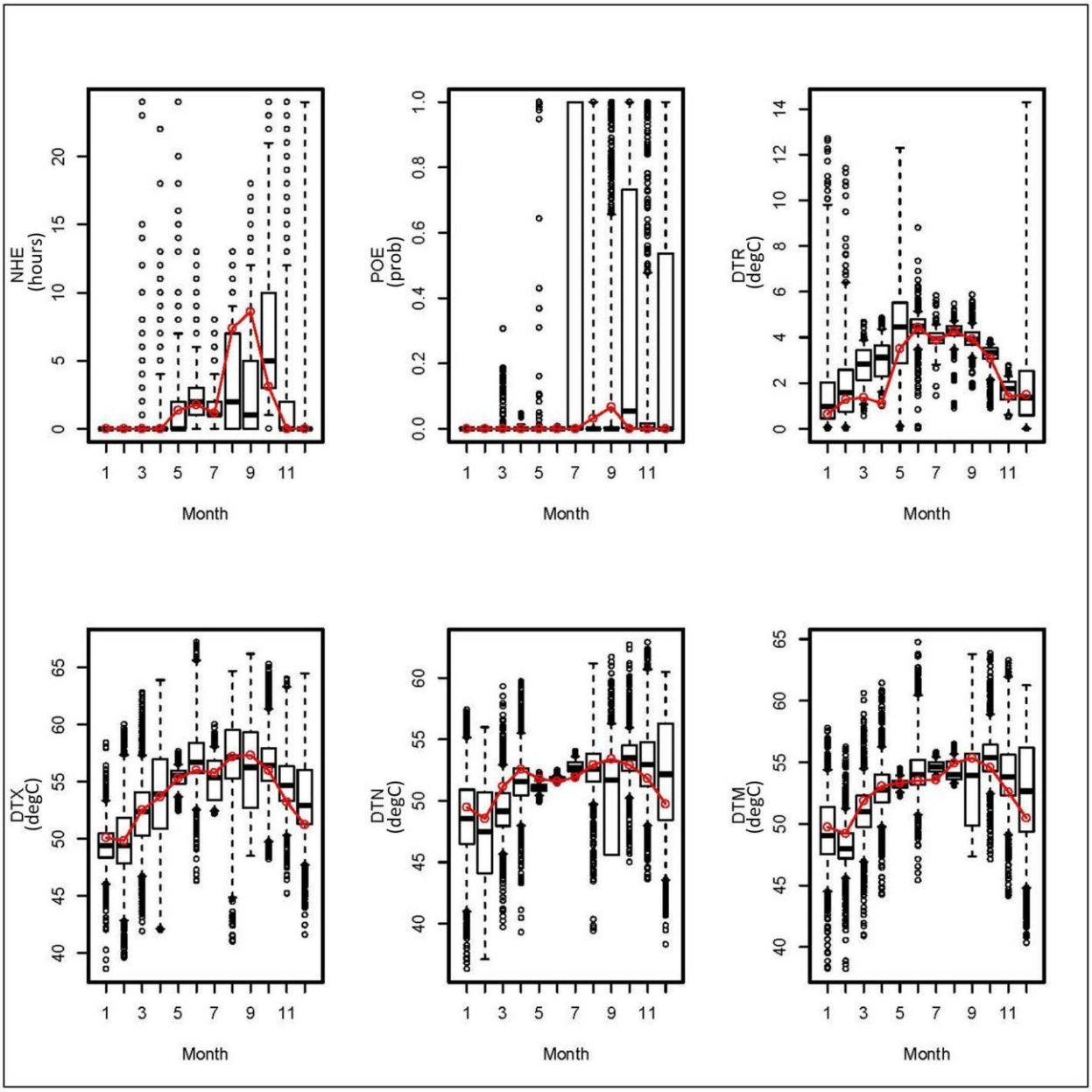

Figure 5.9: Same as Figure 5.8 for the hot year of 2003.

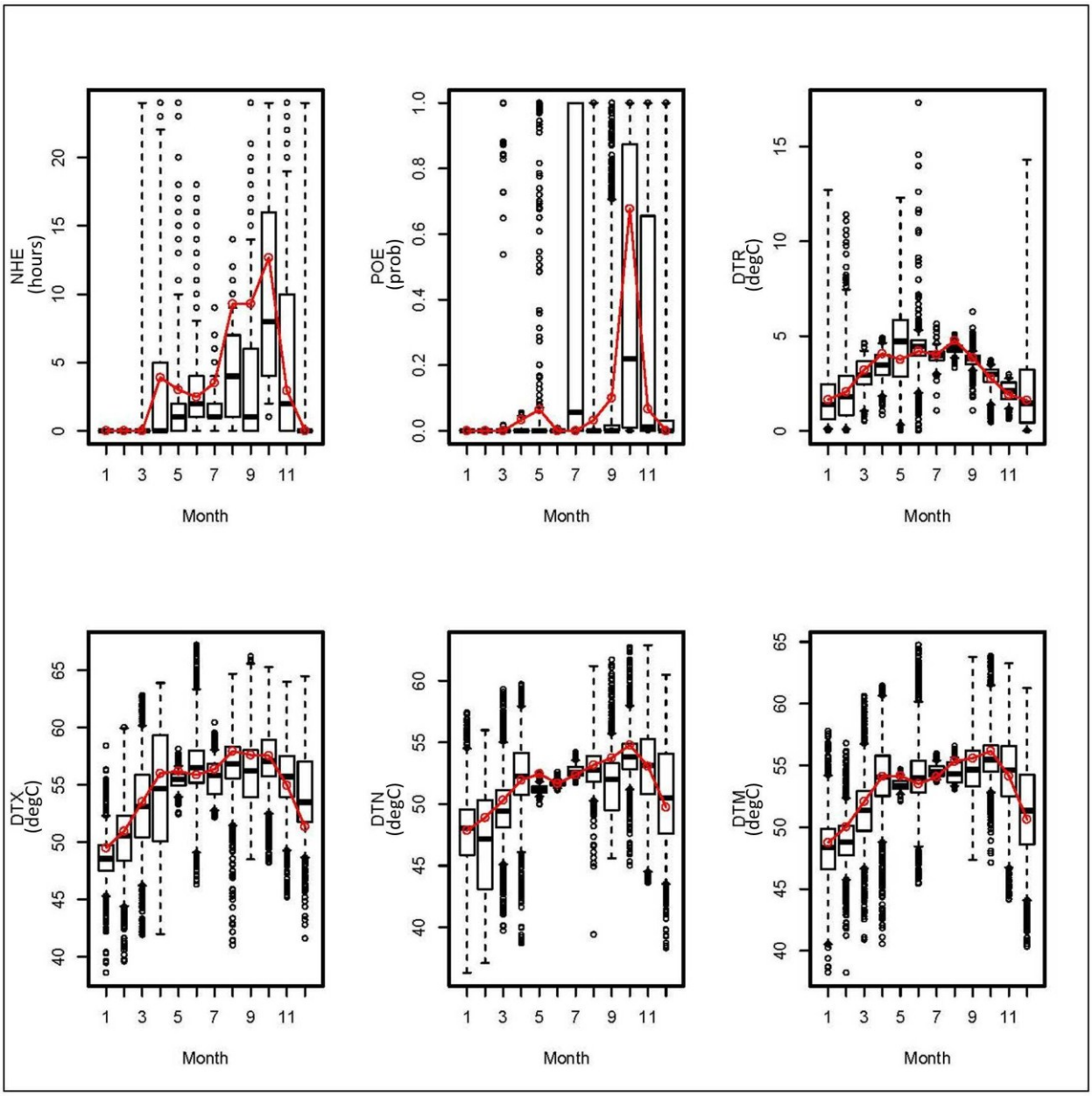

Figure 5.10: Same as Figure 5.8 for the dry year of 2005.

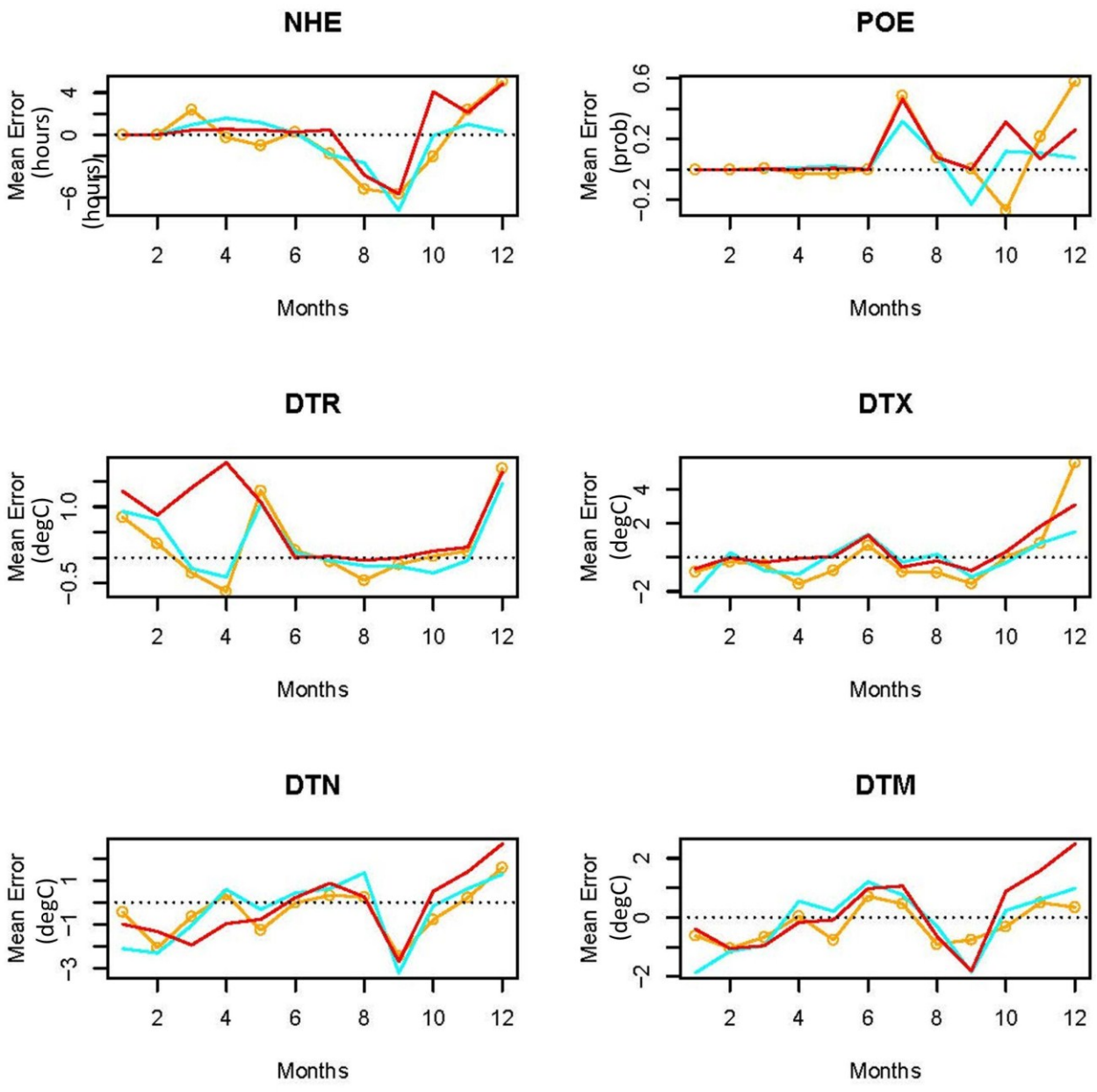

Figure 5.11: Mean error between the observed and simulated values of each water temperature attribute for the cool, wet scenario (cyan), hot scenario (red), or dry scenario (orange).Units are hours (NHE), probability (POE), and °C (DTR, DTX, DTN, and DTM).

5.4.4 Potential Seasonal Planning Application

The potential exists to apply seasonal forecast information in the W2 framework to assess the risk of depleting the in-reservoir cold pool. To elucidate this, we evaluate the reservoir

elevation of the 13.3 °C isotherm at the time when carryover storage and water debt is calculated on November 1st [BOR, 2004] to define the upper boundary of the cold pool (i.e., an estimate of cold water volume at the end of the summer season). We also investigate the reservoir release temperature from Shasta Dam for the hot calendar year 2003. The highest elevation of the 13.3 °C isotherm is compared to the elevation of the TCD withdrawal outlets. The probability density functions of the ensemble from 2003, the unconditional simulations, and the conditional simulations are compared in Figure 5.12. The conditional simulations produce a constant result of a cold pool water surface elevation of 208.6 m, which is well below the lowest TCD gate elevation of 219.5 m. This indicates that the cold pool volume has already been depleted in the conditional simulations by November 1st. The unconditional simulations have a mean cold pool elevation of 233.7 m, and the 2003 ensembles have a mean of 228.43 m. By computing the area under the curve to the left of the lowest TCD elevation in Figure 5.12, we can estimate the probability of running out of cold water pool during the upcoming season. In our case, the seasonal climate forecast was issued on June 1st for the upcoming July to September time frame, providing over 90 days of lead time. In this case, the approximate observed risk is defined by the 2003 ensemble (33 percent). The unconditional run would drastically under-estimate the risk (3.7%), while the conditional run over-estimates the risk with a probability of 100%. Although the skewed climate forecast is an over-estimate, modifications to the default operational scenario to mitigate the anticipated short-fall in cold water pool could provide operators with multiple planning scenarios to address the high potential for cold pool exhaustion and the translated effects on violations at the downstream compliance point at Balls Ferry.

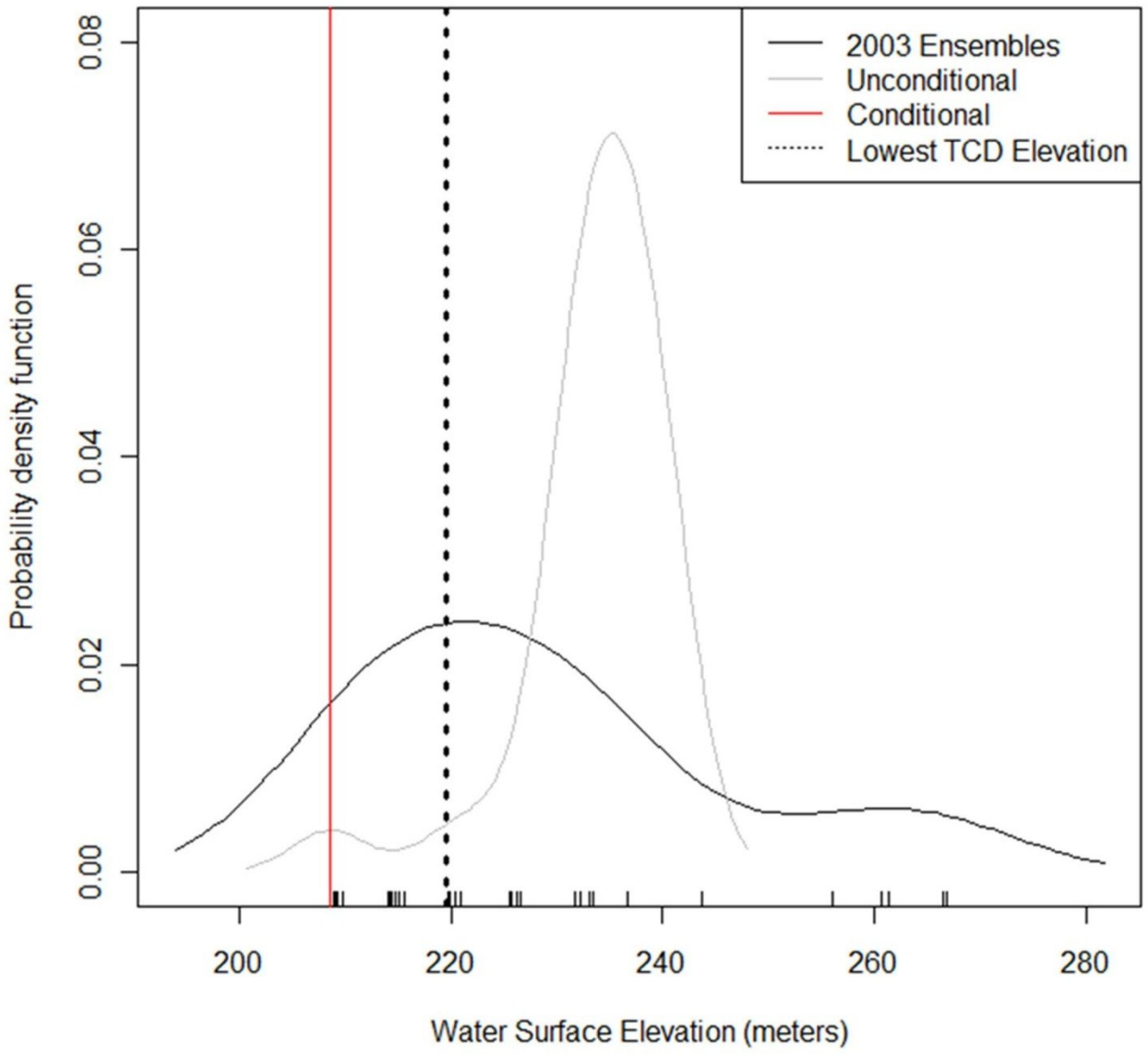

Figure 5.12: Probability density functions for the end of season cold pool elevation defined as the level of the 13.3 °C isotherm for the 2003 ensembles, unconditional simulations, and conditional simulations. The lowest TCD withdrawal elevation of 219.5 meters is shown.

5.5 Summary and Conclusion

In this study, we couple a weather generator, hydrodynamic model, and statistical water temperature model to generate predictions of water temperature attributes at the downstream compliance point at Balls Ferry using a variety of hydroclimate conditions from analog years of 2000, 2003, and 2005. In addition, unconditional and conditional weather generator scenarios are

used as input to the coupled modeling framework to show potential application to seasonal risk assessment of in-reservoir thermal objectives, in particular the upper elevation of the cold pool and reservoir release temperature criteria. An investigation of the effects of reservoir operations on in-reservoir and downstream thermal objectives is currently underway [Caldwell, 2013d].

The coupling of a weather generator, hydrodynamic model, and statistical water temperature model is successful in reproducing the observed meteorological (maximum and minimum air temperatures) and hydrologic (release volume and temperature) predictors included in the GLM model for translation of upstream boundary conditions downstream (Figure 5.6 and Figure 5.7). In addition, the GLM model is successful at generating daily time series of water temperature attributes at the downstream compliance point at Balls Ferry (Figure 5.8 through Figure 5.10). While individual water temperature attributes show a lack of skill during the summer months (e.g., NHE and POE), other variables are adequate for water management applications under the three different hydroclimate regimes with little deviation from observations. The improvement in variability of potential future conditions, while providing deviation from the observed, offers the opportunity to plan for multiple scenarios for the summer season, primarily during the period of July to September. Integration with the GLM statistical model allows the translation of reservoir operations effectively to the downstream compliance location. While the TCD operations schedule in Figure 5.4 establishes release temperature objectives to meet downstream thermal requirements, an important result of the current research is that the number of days of exceedance at the reservoir (125 days) is far higher than the predicted mean of 2 days at the downstream compliance point (not shown); therefore, the coupling of the multiple models is required to estimate the potential impact to fisheries below the dam. Future work should focus on the adjustment of the TCD operations at the dam and the

sensitivity of the downstream temperatures to these adjustments. It is possible that minor changes to the standard operations through manipulation of the rule curves shown in Figure 5.4 could yield great benefits to water supply, particularly under different hydroclimate scenarios.

The methods developed in this study improve on previous work by directly predicting the downstream thermal impacts within the river at a compliance point of interest. The ensemble (i.e., stochastic approach) provides both risk and uncertainty information that was previously unavailable from applications of the W2 model at Shasta Lake. Limitations of this method include the use of a default set of TCD operations and defined daily release volumes from the days selected in the weather generator. Improvements in the quality and consistency of meteorological and hydrological inputs would likely improve the skill of the coupled models. It is anticipated that these improvements, along with continued investigation of climate impacts on fisheries in the Sacramento River, will be completed as part of ongoing research.

This chapter of the dissertation was submitted in July 2013 to Environmental Modeling and Software as an article tentatively entitled: 'Implementation of a Coupled Statistical-Hydrodynamic Modeling System to Predict Water Temperature Attributes under Variable Hydroclimate Conditions'.

6 COUPLING OF WEATHER GENERATOR, CE-QUAL-W2, AND RAFT MODEL

6.1 Background

Although daily operations of the releases from SHD are designed to mitigate potential impacts downstream to protected fishes, seasonal planning requirements for managing the reservoir levels for supply to municipal and agricultural users is also an important consideration. An improved forecast of above or below normal probabilities of risk to fish in the SRB would allow adaptation of current planning methodologies to ensure adequate water for both supply and fisheries protection. Danner et al. [2012] proposed a coupled modeling framework (Figure 6.1) that links mesoscale weather and ecological models to generate inputs for a physically-based water temperature model for monitoring and forecasting water temperature at fine spatiotemporal scales.

The integrated framework also provides the capability to develop long-range (e.g., seasonal) outlooks of risk through coupling with statistical methods. These long-range projections are an important and complementary decision support tool (DST) for reservoir managers interested in meeting the multiple criteria of many competing demands for water supply. By integrating state-of-the-art modeling systems with statistical analysis and prediction methods, a comprehensive set of DSTs can be developed that will best guide water resource management decisions in the SRB.

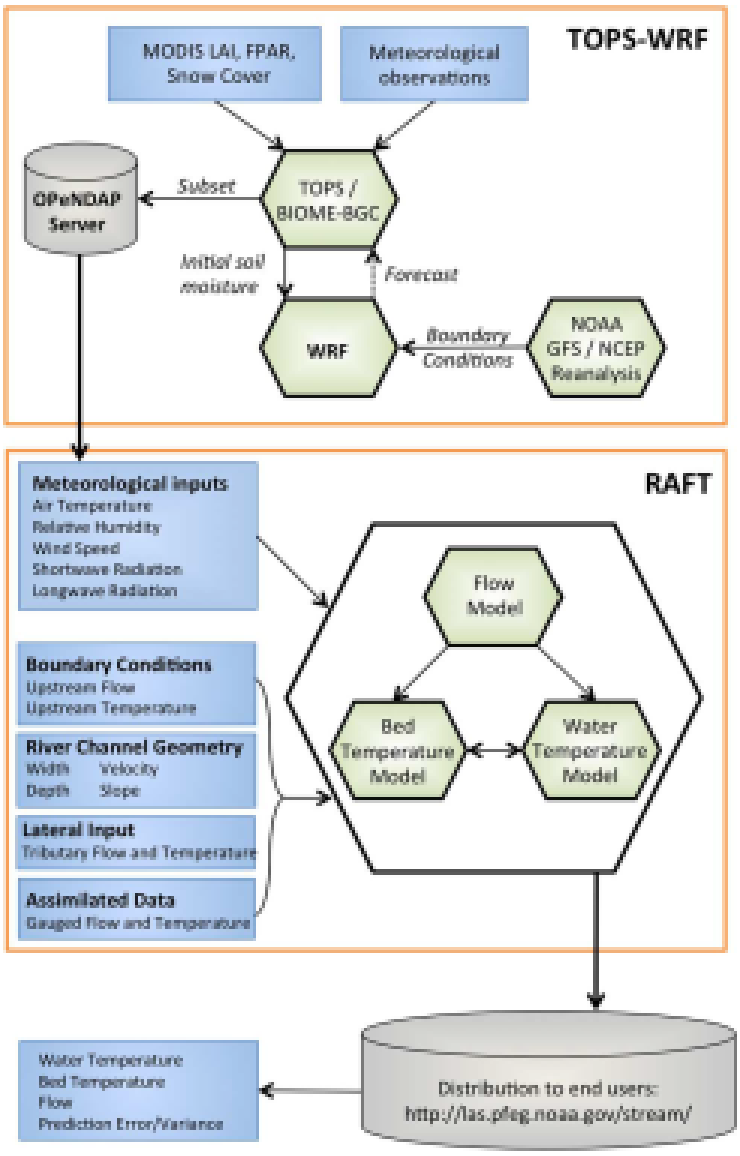

Figure 6.1: The coupled modeling framework of Danner et al. [2012]. A mesoscale weather model, the Weather Research and Forecasting (WRF) model, Biome-BGC, an ecological component model of the Terrestrial Observation and Prediction System (TOPS) are linked to form TOPS-WRF. This provides necessary inputs to the River Assessment for Forecasting Temperatures (RAFT) model. The outputs from RAFT are distributed to the end users through web services and an interactive web site. (Extracted from Danner et al. [2012]).

Pike et al. [2013] develop state-space models (SSMs) to generate spatiotemporally explicit river temperature estimates. State-space time series methods [Bravo et al., 1993; Harvey, 1989] are an attractive approach to modeling river temperature over large areas at relatively fine scales. The model, designated as the River Assessment and Forecasting Temperatures (RAFT)

model, from Pike et al. [2013] closely follows the methodology of Bravo et al. [1993], with the state vector consisting of temperatures and temperature gradients at various points along the river, and forcing terms, including flow, temperature of water released from reservoirs, and climatological variables such as air temperature, insolation, vapor pressure deficit, and wind speed, entering through the system matrices of a Kalman filter. The approach represents a substantial improvement over the existing DSTs because it provides temperature estimates at the appropriate spatiotemporal scales for evaluating the thermal impacts on fish (sub-hourly for every kilometer of river reach), allows for hindcasting and forecasting, and provides a statistically valid measure of uncertainty. Furthermore, once the model has been fit to observational data, it can be used to simulate the system. For example, the performance of various water release strategies in meeting river temperature criteria can be evaluated under historical or hypothetical climate scenarios. The state-space model can also be driven by the output from a weather generator, coupled with corresponding flow information for the selected days. The days simulated by the weather generator are used to extract hourly time series from a particular reference meteorological gauge. The upstream inflow values at the upstream boundary in the RAFT model for the given day are used to force the model at hourly time steps. However, the selection of release flow and temperature relative to a particular day simulated by the weather generator may not be consistent with the weather. Therefore, coupling with a reservoir model would improve the representativeness of the upstream boundary conditions.

Using a coupled approach, sub-hourly high-resolution temperature projections may be generated across an entire season. By doing so, we can estimate the risk of exceeding temperature thresholds at various locations along the river. Due to the complexity of the RAFT, this method is somewhat restrictive due to the computational resources required to generate

multiple scenarios provided by the weather generator. However, the output can be used to identify the associated risk of thermal violations at multiple downstream points along the river. In addition, the RAFT model has the capability to examine the impact of different operations scenarios at the upstream boundary by changing the release temperature and volume at the upstream boundary condition through coupling a hydraulic model of Shasta Lake.

To assess the effects of TCD operations on river thermal conditions at a compliance point downstream under variable hydroclimatological conditions, a modeling effort has been undertaken (Figure 6.2) that links a reservoir water quality model forced with output from stochastic weather generation software to the state-space hydrodynamic model of water temperature from Pike et al. [2013]. This chapter presents simulation results for the single year of 2003, which is representative of hot conditions within the watershed during the summer season.

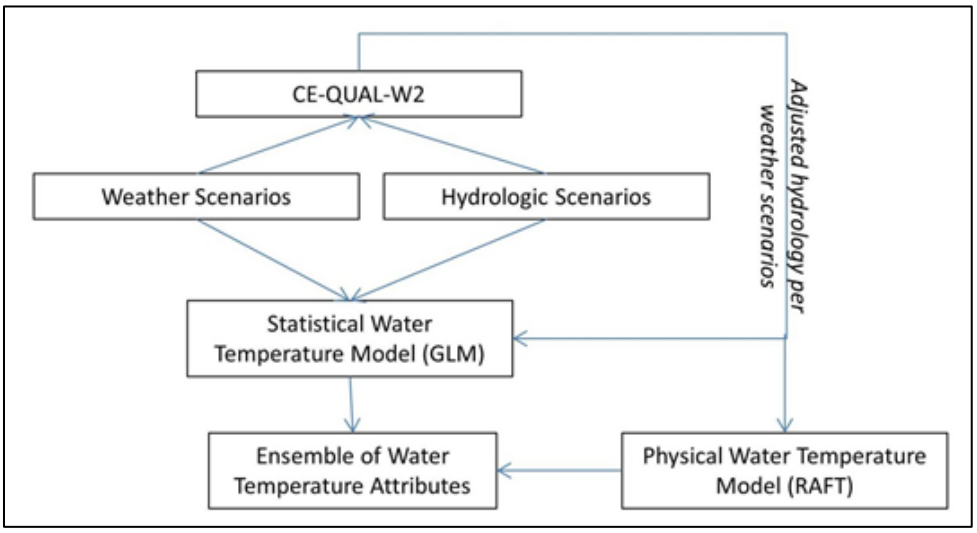

Figure 6.2: Flow chart of the coupled modeling system, including the weather and hydrologic scenarios from the stochastic weather generator, which are used to force either the two dimensional hydraulic model (CE-QUAL-W2) or the statistical model (GLM). Adjusted time series of hydrology and weather are then used in the hydrodynamic model (RAFT) as inputs. Ensembles of hourly and daily water temperatures and attributes can be calculated through either the RAFT model or GLM.

6.2 Data Sources and Methods

6.2.1 Study Area

The current chapter will again focus in the upper Sacramento River Basin (see earlier chapters and Figure 1.1). As discussed previously, Shasta Dam was retrofitted with temperature control devices, which allow selective withdrawals from different depths (and, therefore, different temperatures) in the reservoir based on water temperature requirements downstream. One of three important temperature compliance points at Balls Ferry (BSF). We focus only on BSF as it is highly likely that if temperature objectives are not met at this location that the other compliance points farther downstream will have even poorer compliance statistics. We will use the flow and water temperature data available at several key sites along the river, including: SHD (flow and water temperature) and BSF (water temperature). The flow at BSF is not included as the releases upstream drive this variable. A single meteorological site with hourly observations is available in the valley at Redding, CA, which is approximately half-way between KWD and BSF. The site provides a variety of meteorological variables (except solar radiation); however, we use primarily the maximum and minimum air temperature and precipitation from the site.

The flow, water temperature, and meteorological variables serve as input to the various components of the decision support system. The historical hydrologic information is primarily available for the period 1994 to present. The meteorological variables of air temperature and precipitation are used as input to the stochastic weather generator software. The flow, water temperature, air temperature, and precipitation were used as potential predictors in the statistical models, along with prior day values for each. Additional parameters, such as barometric pressure and wind, are incorporated into the physical water temperature models. No solar radiation data

were available for the physical modeling system and, therefore, were estimated using equations which relate latitude, time of year, and cloud cover to solar radiation.

6.2.2 Year Selection

Again, high quality and primarily continuous measurements of hourly water temperature at the Balls Ferry gauge are available for the period 1994 to present from the California Data Exchange Center (CDEC) of the California Department of Water Resources. Overlapping hourly discharge and water temperature release data at Shasta Dam are also available from CDEC with hourly meteorological data from the National Weather Service automated site at Redding Airport. Since the TCD was installed in early 1997, we restrict our selection of years to the period since 1997. During that period, an evaluation of meteorological data identified three years that represent dry (1995), hot (2003), and cool, wet (2000) conditions (see Chapter 5). The data from a single hot year (2003) will be used to generate multiple scenarios within the weather generator software while constraining the weather scenarios to best match flow conditions in the river system during the observed year. Here, we use only a single year to demonstrate the applicability of the integrated system, though additional years are expected to have similar results.

6.2.3 RAFT Model

The River Algorithm for Forecasting Temperatures (RAFT) model was developed by Pike et al. [2013] and a full description of the model can be found in their publication or a more general description in Danner et al. [2012]. Additionally, a brief description of the model is included in Section 2.5.1. The hydrodynamic model consists of an advection-dispersion equation describing the downstream movement of heat, coupled to a one-dimensional hydrologic routing

model to describe the movement of water downstream. Figure 6.3 provides a schematic of the exchange of heat within a single control volume. Pike et al. [2013] assume the lateral and vertical temperature gradients in the channel are negligible and apply a one-dimensional equation with unsteady, non-uniform dynamics.

The hydrologic routing is accomplished through a one-dimensional Muskingum-Cunge formulation due to its prior application in unsteady, non-uniform flow by Boyd and Kasper [2003] and in state-space applications [e.g., Georgakakos et al, 1990]. The RAFT model involves converting these governing equations into linearized state-space form and assimilating observations via use of a Kalman filter and closes the energy budget equation through time and space using a robust semi-Langrangian numerical scheme. Additional details of these procedures can be found in Pike et al. [2013].

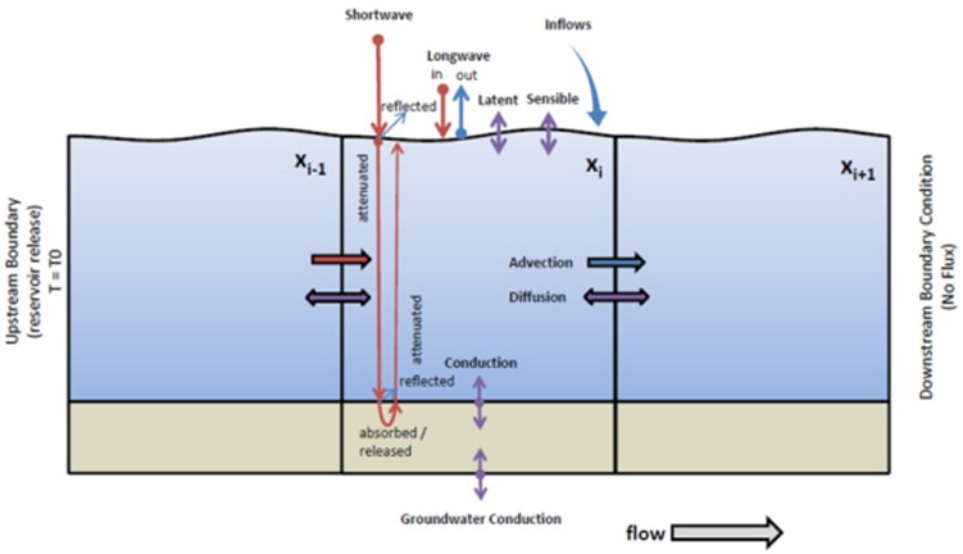

Figure 6.3: Heat pathways into and out of a control volume. Advection and diffusion are the only processes which exchange heat between grid cells. [Extracted from Pike et al. [2013]]

The model utilizes gridded and point input data including: (a) meteorological time series of solar radiation, long-wave radiation, air temperature, dew point temperature, and wind speed with optional entries for cloud cover and atmospheric pressure; (b) channel geometry; and, (c) flow and tributary time-series at the upstream boundary and along tributaries (Table 6.1).

Table 6.1: Input requirements into RAFT (required and supplemental) [Extracted from Pike et al. [2013]]

Input Type	Requirement	Quality-Related	Impacts Model Results
Upstream	Required	No	Necessary boundary condition
Bathymetry	Required	Yes	Channel geometry affects flow routing and rates of heat exchange
Meteorology	Required	Yes	The spatial and forecast quality affects accuracy
Tributary	Required/Supplemental	No	Tributary inputs impact water temperature and flow
Downstream	Supplemental	No	Downstream observation improve prediction via data assimilation

The meteorological data is derived from the combined Weather Research and Forecasting (WRF) and Terrestrial Observation and Prediction System (TOPS) model (Figure 6.1). The WRF-TOPS framework integrates operational satellite data, ground-based monitoring data, microclimate mapping, and physical and ecosystem models, with an industry-standard numerical weather prediction model to generate estimates of each atmospheric variable and can be run in hindcast or predictive mode. The bathymetric data were developed using HEC-RAS model calibration procedures. The flow and water temperature requirements were derived from point observations from at sites along the river at reservoir release sites. Additional details on model validation and performance can be found in Pike et al. [2013].

For the application in the dissertation, the RAFT model incorporates point data uniformly across the gridded domain for meteorology, which is based on the hourly observation site at Redding, California, with adjustment to a location representative of Shasta Dam. The boundary condition inputs include the simulated flow and water temperature releases using the CE-QUAL-W2 model after forcing by the output from the stochastic weather generator. A description of the W2 model and brief introduction to the stochastic weather generator are provided in the following sections.

6.2.4 Hydrologic Model

Hanna et al. [1999] introduced a two-dimensional hydrodynamic model of the reservoir to ascertain the in-reservoir impacts on water temperatures. Shasta Lake is a large, deep, and dendritic system with water quality characteristics that vary spatially and temporally. As such, Hanna et al. [1999] developed and calibrated a CE-QUAL-W2 (W2) model [USACE 1995] for Shasta Lake to simulate TCD operations and predict in-reservoir water temperatures. Reservoir geometry in the W2 model is simplified using lateral averaging and therefore is partitioned into model segments along the length (Figure 2.3). Model output consists of simulated vertical profiles of water quality parameters, including water temperature for each of those segments. TCD operations for the model were established using a set of decision points throughout the year based upon the release temperature target, where release temperatures are as warm as possible from November through April with coolest releases during the period May through August. This requires a step-wise reduction in release elevation throughout the year (see Chapter 5). The output from the W2 model will serve as upstream boundary conditions to the RAFT model.

6.2.5 Weather Generation

Weather generators are typically used to produce multiple, synthetic time series of weather from finite station records of hydrometeorological variables. These time series are expected to reasonably simulate the key climate properties derived from the historical record, such as mean, variance, and skew. The output from weather generators can then be integrated into response models (e.g., W2 and RAFT) to characterize the impact of weather and climate on the system [Wilks 1999; Wilks and Wilby 1999]. Appipatanavis et al. [2007] developed a semi-parametric weather generator (SWG) that uses the *K*-nn resampling technique to generate the weather time series, but also an initial parametric step which applies a Markov chain to model the precipitation occurrence to better capture the wet/dry spell statistics of the historical record. The *K*-nn resampling is then conditioned on the precipitation state, which improves the simulation of the distributional and lag-dependence statistics of the meteorological variables. The method can be easily integrated with seasonal climate forecasts or utilize an analog year, as is done here for 2003, to generate time series of daily weather conditioned on expected future conditions. These ensembles can then be implemented in decision tools to quantify risk for planning beyond the skillful range (i.e., hours to several days) of deterministic models.

In this chapter, conditional weather ensembles were generated using the SWG and the single analog year of 2003 described in Section 6.2.2. The SWG software of Appipatanavis et al. [2007] was adapted such that the observed meteorology, precipitation state, and precipitation transition type for the analog year were applied in the *K*-nn neighbor resampling. Using this method, the antecedent atmospheric conditions may be coupled with the observed flow and water temperature conditions in that year to create an ensemble of hydroclimatologically-similar time

series of atmospheric and hydrologic forcings for both the W2 and RAFT models. Additional, more detailed information on the weather generator can be found in prior chapters.

6.2.6 Statistical Models of Water Temperature

For comparison with the output from the coupled W2-RAFT modeling system, we generate predictions of six water temperature attributes using a generalized linear modeling (GLM) approach, as described in Section 2.5.3. The GLM provides a complementary set of seasonal predictions for the watershed that may be utilized individually or coupled with the physical model output through Bayesian combination methodologies to produce a more skillful forecast. A large number of predictors are considered based on prior research and knowledge of the system – they include the water and air temperatures, precipitation, and hydrologic characteristics of the previous and current day, which are expected to best represent the key physical, dynamical processes ongoing in the basin, including: heat exchange with the atmosphere, advection, dispersion, and turbulent mixing, while neglecting the heat exchange along the bed-water interface.

A separate model is fitted for each water temperature attribute (i.e., NHE, POE, DTR, DTX, DTN, and DTM) for each month to capture the seasonal variability in forcing mechanisms. The GLM is used to translate the release temperature and flow from Shasta Dam to the downstream compliance point at Balls Ferry, allowing the W2 model forced with the ensemble of weather scenarios to determine the vertical temperature profile within the reservoir, and hence, the release water temperature from the dam rather than specifying the actual observed values which may not be consistent with the weather scenario.

6.3 Results

6.3.1 RAFT Model Performance

A total of 50 simulations for the year 2003 were used as forcing for the W2 model, which provided release flow and release temperature as the upstream boundary condition to the RAFT model. The RAFT model provides spatially explicit estimates of water temperature for a total of 48 grid cells of 2-km resolution for each hour of the year. For example, Figure 6.4 shows the statistical properties from the 50 ensembles. Violations are indicated by mean values in the red to maroon shading, which begin to occur downstream around early September (hour=6000) and migrate upstream between Shasta Dam and the Balls Ferry gauge (at distance=21) by mid-October (hour=7000). High values of standard deviation in excess of 1 °C near the dam during the mid-October time frame indicate large uncertainty in the predictions during the fall. Skewed predictions are evident in the summer season and correspond closely with the time just prior to the adjustment of the TCD within the W2 model as the release water and downstream river water warms in response to increasing air temperatures. There is no clear signal in the kurtosis.

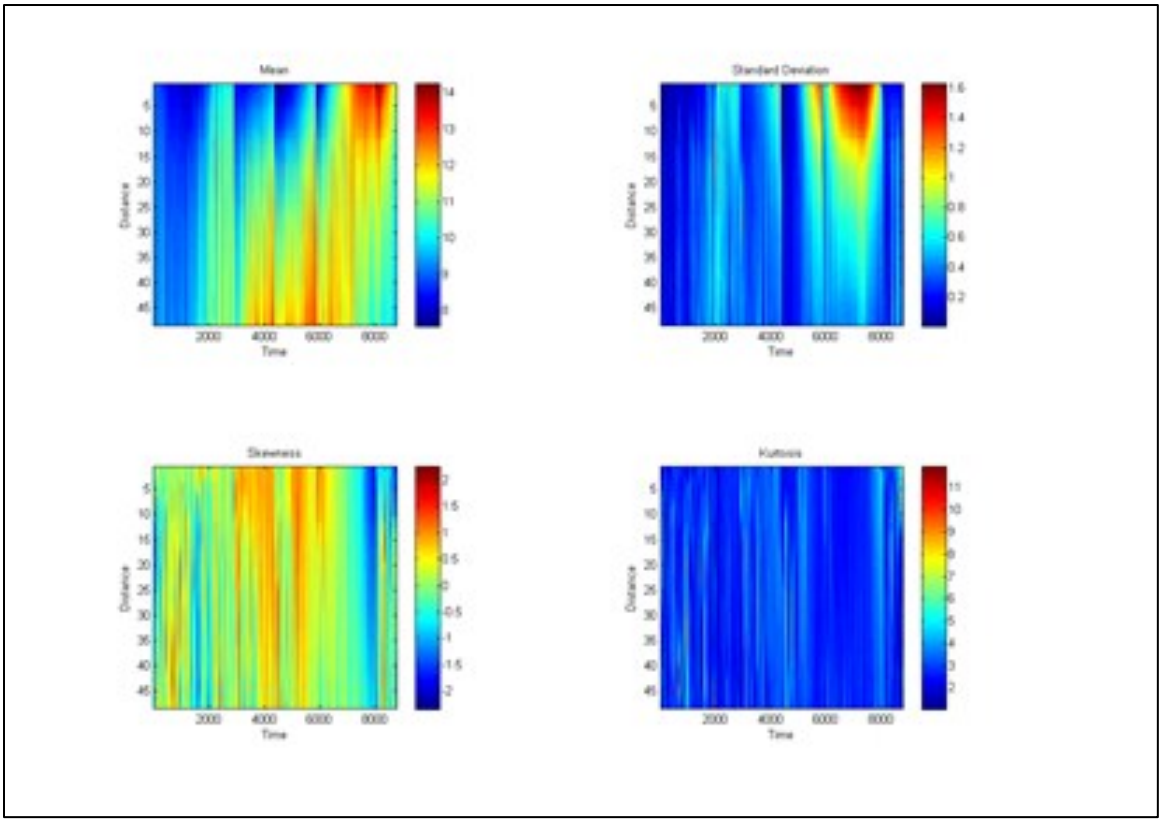

Figure 6.4: Statistical values of the model predicted hourly water temperature from the 50 simulations using W2 as upstream boundary conditions. Distance is given in grid cell lengths of 2 km. For reference, Balls Ferry is approximately 42km downstream of Shasta Dam at Distance =21.

While the spatial variability is important for noting specific recovery regions for the fish during high water temperatures in other sections of the river, the primary objective of water managers is to meet compliance temperatures at one of the three sites downstream of Shasta Dam. Here, we focus on extracting the hourly time series from the grid cell collocated with the gauge at Balls Ferry, again at grid distance=21. For each hour from the 50 simulations, the maximum, minimum and mean water temperature value are extracted and plotted for comparison with the observed (Figure 6.5). While the range from the model ensemble appears to capture the observed data during the cool season (November (hour~7500) through April (hour ~3000)), the observed values during 2003 are nearly equal to or exceed the maximum water temperature predictions from the RAFT model. Using the mean RAFT predicted water temperatures as a

reference, the model generally under-estimates the water temperature at the Balls Ferry gauge, particularly during the summer months (e.g., Figure 6.6).

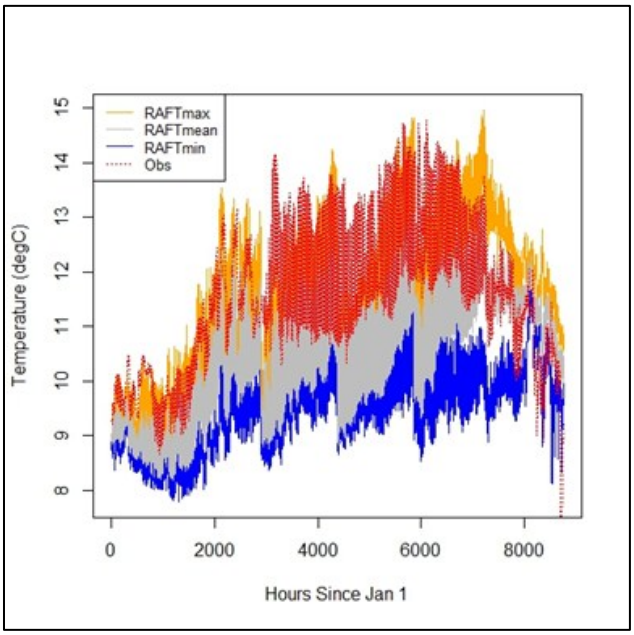

Figure 6.5: Hourly maximum (orange), minimum (blue), and mean (grey) predictions of hourly water temperatures at Balls Ferry from RAFT for the year 2003 with observed data in red.

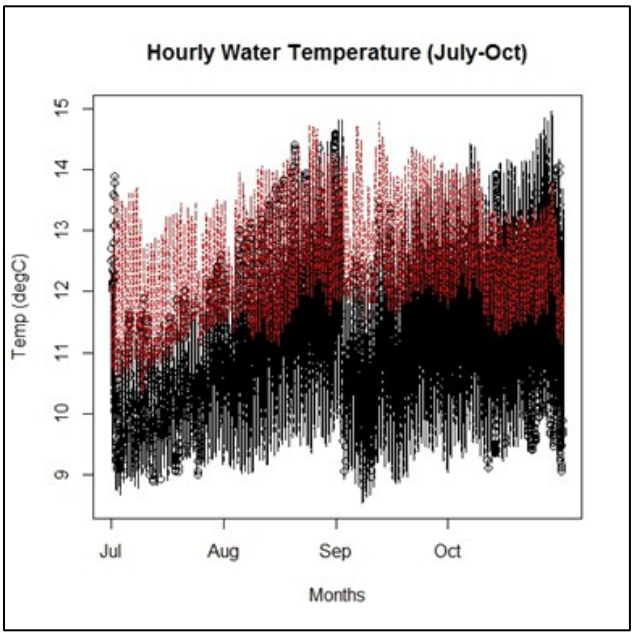

Figure 6.6: Boxplots of hourly water temperature predictions from RAFT during the period July to October 2003 with observed values in red.

To assess the performance of the coupled W2-RAFT model, the hourly water temperature from the 50 simulations were compared to observed hourly values at the Balls Ferry site using the following statistics: Nash-Sutcliffe coefficient [NS; Nash and Sutcliffe, 1970]; ratio of the root mean square error to the standard deviation of the observed data (RSR); percent bias (PBIAS), the ratio of the sum of residual errors between the simulated and observed data and the sum of the observed data; the mean error (ME); the root mean square error (RMSE); and, the adjusted R^2 or the squared correlation between the observed and predicted values adjusted for sample size and degrees of freedom (Figure 6.7). Guidelines established by Moriasi et al. [2007] and applied in Ficklin et al. [2012] where NS > 0.50, RSR < 0.70, and PBIAS between +/- 25 percent are used to qualify the validation results as satisfactory.

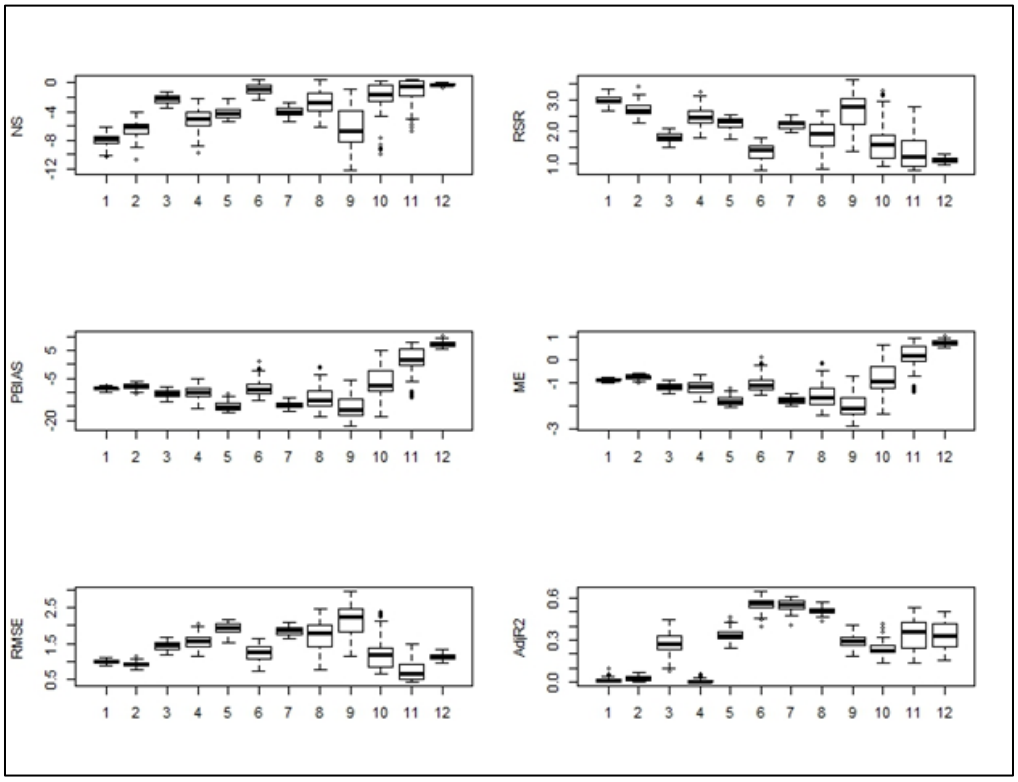

Figure 6.7: RAFT performance skill scores, including the Nash-Sutliffe coefficient (NS), ratio of the root mean square error to the standard deviation of the data (RSR), percent bias (PBIAS), mean error (ME), root mean square error (RMSE), and adjusted R^2 (AdjR2).

From Figure 6.7, the NS scores are almost entirely negative for each month of the year, indicating poor skill and that the observed mean is a better predictor than the current model, such that the residual variance is larger than the data variance. This is not alarming given the purpose of the ensemble is to generate a wide array of potential future scenarios that are representative of a year like 2003. However, we do expect better performance from the coupled model. The RSR values are above 0.7 throughout the year, indicating normalized RMSE values of 1 to 3 C. The smallest residual variations are evidenced by smaller values of RSR in the snow runoff season (May – June) and December. The PBIAS statistic fall within the satisfactory range from Moriasi et al [2007]; however, a general negative (under-estimate) bias is shown through much of the year, with the exception of the November to December time frame, which correlates well with the positive values for mean errors. Mean errors are generally in the +/- 2 C range, which suggests reasonable model performance. In addition, the adjusted R^2 values are above 0.40 from April to December, suggesting that a bias correction alone may improve the model performance.

6.3.2 Comparison with GLM

The coupling of the physical models (W2-RAFT) provides enhanced spatial and temporal resolution of the stream temperatures downstream of Shasta Dam; however, since the GLM is also coupled to the W2 model (W2-GLM), we evaluate the performance of each of the coupled systems using daily water temperature attributes at the Balls Ferry gauge. Comparison of the GLM to the water temperature attributes for three individual years was presented in Chapter 4. For completeness, a different analysis is provided in Figure 6.8, which indicates the observed data are encompassed within the bounds of the W2-GLM daily ensemble boxplots and approximately follow the daily ensemble mean.

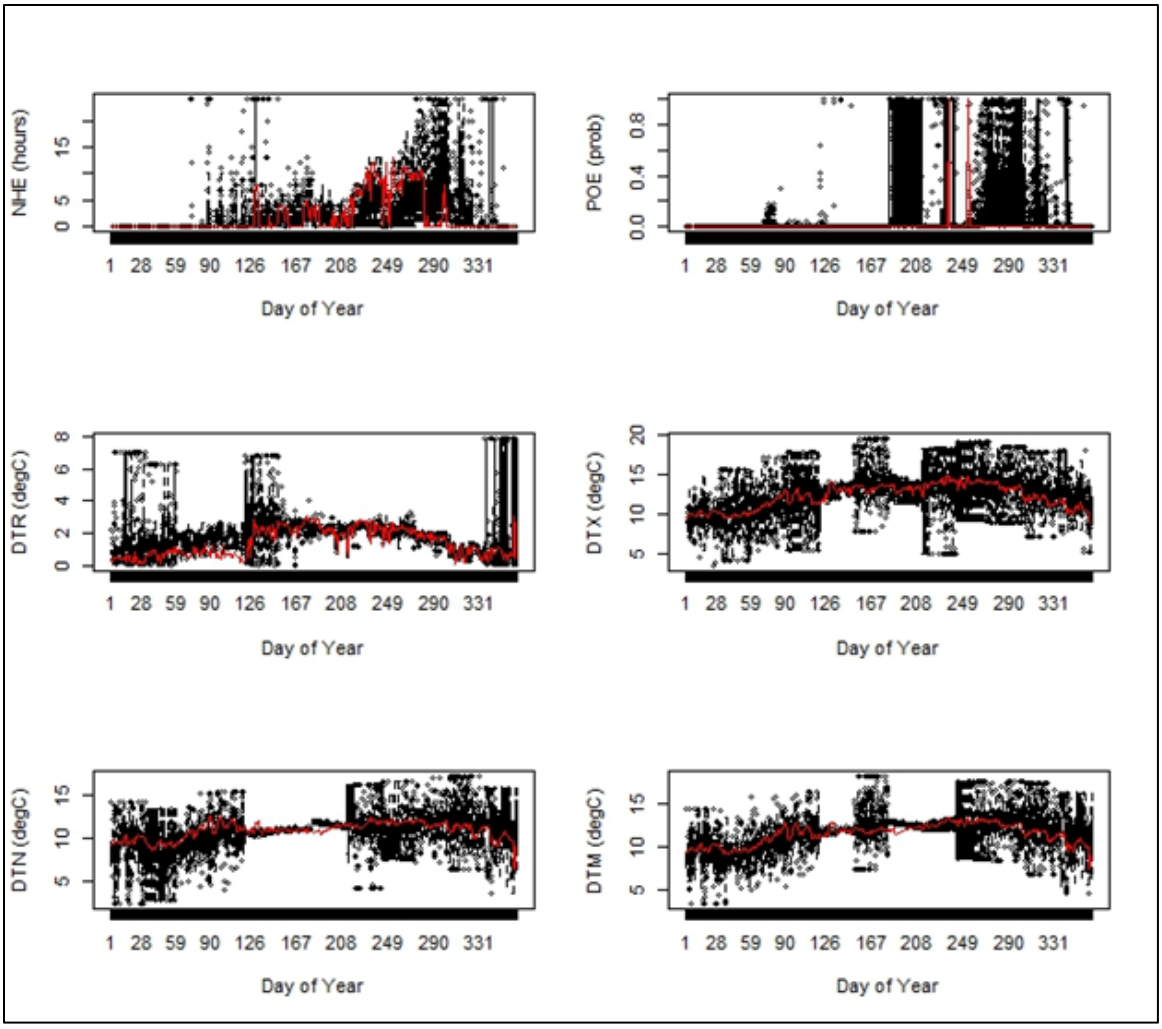

Figure 6.8: Boxplots of the daily water temperature attributes of number of hours exceedance (NHE), probability of exceedance (POE), daily water temperature range (DTR), maximum daily water temperature (DTX), minimum daily water temperature (DTN), and daily mean water temperature (DTM) from the W2-GLM relative to the observed (red).

The low bias in the W2-RAFT model output is again evident in the daily water temperature attributes lumped by month (Figure 6.9), particularly during the summer months. In Figure 6.9, the W2-GLM with Redding meteorology (GLMR) matches the observations much more closely for all months and all variables when compared to the W2-RAFT model results.

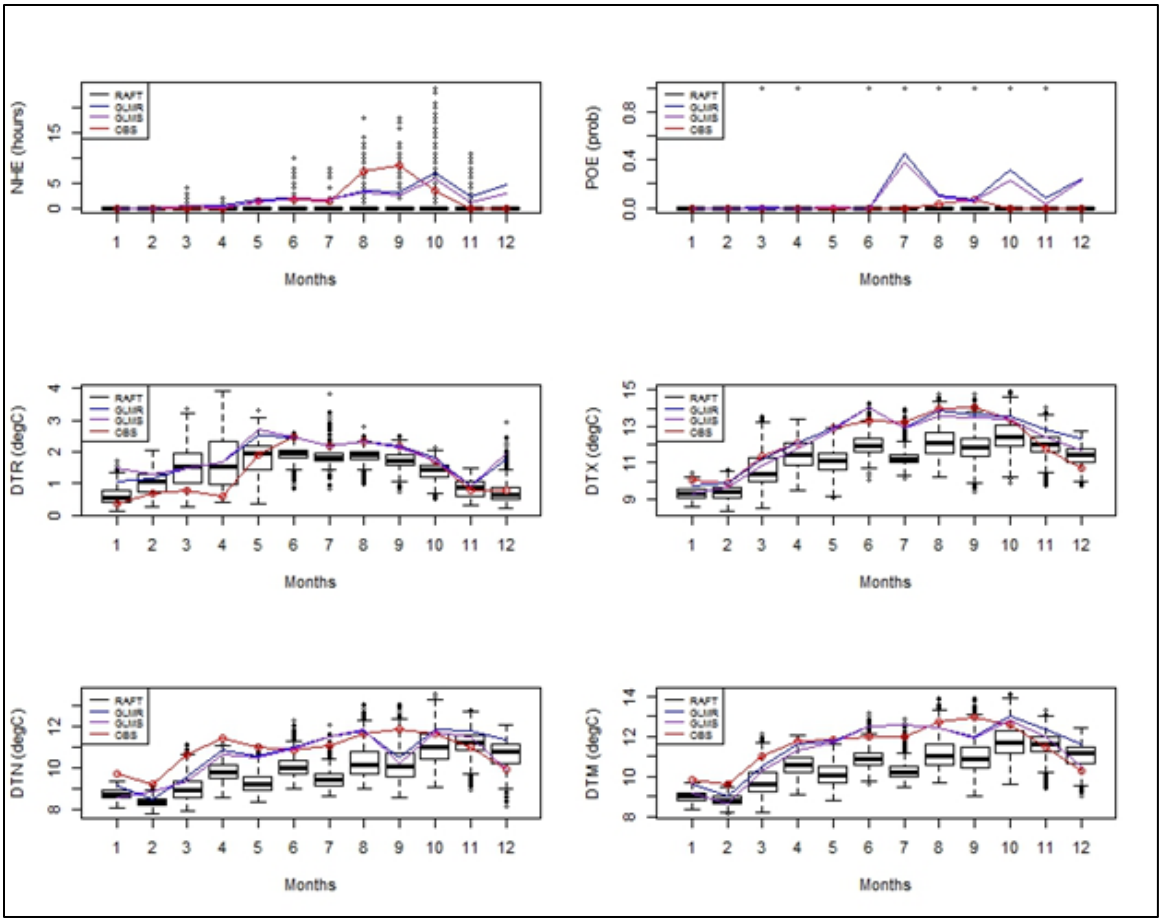

Figure 6.9: Comparison of the RAFT (black boxplots), GLM with Redding meteorology (GLMR, blue line), GLM with Shasta meteorology (GLMS, purple line), and observed (red line) water temperature attributes (same as in Figure 6.8).

6.4 Conclusion

This research investigates the potential for coupling statistical methods in the form of a stochastic weather generator with a 2-dimensional hydraulic model of a reservoir (W2) to provide upstream boundary conditions to a complex hydrodynamic model of water temperature and flow for a section of the Sacramento River (RAFT) (Figure 6.2). The RAFT model has the potential to provide skilled hourly estimates at high spatial and temporal resolution on the Sacramento River from Shasta Dam downstream for approximately 96 km below the last compliance point at Red Bluff Diversion Dam. For example, in Figure 6.4, although there are

violations adjacent to the dam near the end of the mitigation season (i.e., October) in the approximate first 20 grid cells, there is also cool water availability downstream at that time, where the warmer water releases from Shasta Dam are being influenced by the time accumulated impacts of atmospheric cooling during the late fall and early winter. This potential refuge for salmon would not be evident in a single point regression-based model, such as the GLM.

Initial model results indicate that the coupled W2-RAFT system generally under-estimates water temperatures at the Balls Ferry gauge. A potential source of that error is the input meteorology into the RAFT model matches that of the W2 model. In other words, air temperatures that are on average 1.71 C cooler at Shasta Dam than at the Redding location, half-way between the dam and Balls Ferry, are applied over the entire stretch of river. We attempt to gain insight into whether this is the result of the performance differences between the GLM and RAFT by substituting the Shasta Dam meteorology time series into the coupled W2-GLM model (see GLMS in Figure 6.9). While some lowering of the daily values is evident, the slight change in air temperatures within a fitted model has minimal impact on the W2-GLM model output. It is likely that the improvement of the spatial and temporal resolution of meteorology data offered in the TOPS-WRF framework is the key to improved modeling results from the RAFT model (Figure 6.12) and discussed in Pike et al [2013] and Danner et al. [2012]. Due to the obvious limitations of the current W2-RAFT coupling, future efforts should focus on the implementation of the TOPS-WRF output and reanalysis data into both the W2 and RAFT as meteorological inputs instead of using a single point estimate over the entire gridded RAFT domain. That said, a research effort is currently underway to provide the RAFT model with Redding meteorological inputs and the respective W2-generated boundary conditions, which we anticipate will somewhat correct the under-estimation bias presently in the coupled W2-RAFT modeling system.

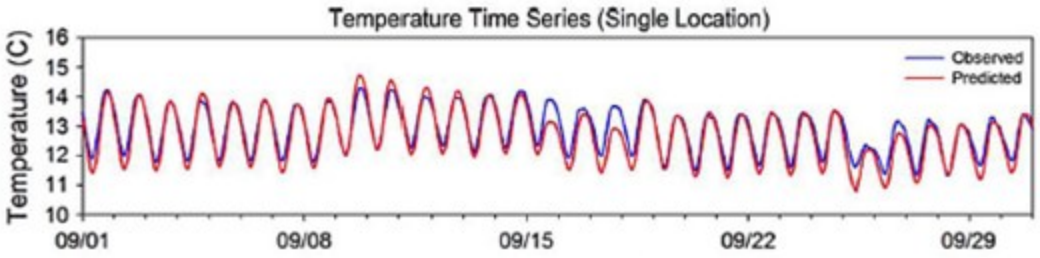

Figure 6.10: Example of the RAFT output temperature time series with model predictions (red) and observations (black) for the month of September 2011. [Extracted from Danner et al. [2012]].

While additional work is necessary to improve upon the W2-RAFT model coupling, this is the first attempt to provide upstream boundary conditions to the RAFT model that are not prescribed, but rather offer an ensemble approach to seasonal planning exercises. Uncertainty, even in a spatial capacity can be gleaned from the coupled models (e.g., Figure 6.4). The current effort focused on the application of an ensemble of future weather conditions representative of the hydroclimate of the year 2003 and, therefore, any uncertainty is related to the variability of the future weather scenario based on a single (i.e., analog-type) year. Additional uncertainty can be incorporated through the weather generator by generating unconditional (climatology) and conditional (climatology shifted per climate forecast or intuitive information) weather scenarios for input to the W2-RAFT model. For example, there may be a management goal to plan for multiple outcomes (e.g., conditional simulations of a 50% warmer than normal summer or a 90% drier than normal winter) and relate them to a climatological (unconditional) set of years.

In conclusion, while the initial results indicate a need for improved representation of the atmospheric inputs, the coupling of the W2-RAFT model was successful in generating estimates of water temperature at 2-km resolution at the hourly time step. The comparison of the GLMR versus GLMS should justify that additional efforts in integrating improved atmospheric forcings

to the coupled system will substantiate its application for seasonal, ensemble-based predictions of water temperature attributes in water management on the Sacramento River.

This chapter of the dissertation will tentatively be submitted in summer 2013 to a peer-reviewed journal as an article tentatively entitled: ‘Linking Statistical and Hydrodynamic Models for Assessment of Climate Impacts on Fisheries’.

7 DECISION SUPPORT SYSTEM

Increasing demands on the limited and variable water supply across the West can result in insufficient streamflow to sustain healthy fish habitat. In addition, construction of dams and diversions along rivers for the purpose of storing and distributing the limited supply of water can further deteriorate natural flow regimes and, often, obstruct important migratory pathways for cold water fish reproduction and development. In regulated systems, such as the Sacramento River system, these impacts are an interaction of volume and temperature of water release from the reservoir and the subsequent exchange with the environment downstream.

We develop an integrated decision support system (DSS) for modeling and mitigating stream temperature impacts and demonstrate it on the Sacramento River system in California. The DSS has four broad components that are coupled to produce the decision tool for stream temperature mitigation: (i) a suite of statistical models for modeling stream temperature attributes using hydrology and climate variables of critical importance to fish habitat; (ii) a reservoir thermal model for modeling the thermal structure and, consequently, the water release temperature, (iii) a stochastic weather generator to simulate weather sequences consistent with seasonal outlooks; and, (iv) a set of decision rules (i.e., 'rubric') for reservoir water releases in response to outputs from the above components. The DSS incorporates forecast uncertainties and reservoir operating options to help mitigate stream temperature impacts for fish habitat, while efficiently using the reservoir water supply and cold pool storage. The use of these coupled tools in simulating impacts of future climate on stream temperature variability is also demonstrated. The results indicate that the DSS could substantially reduce the number of violations of thermal criteria, while ensuring maintenance of the cold pool storage throughout the summer.

7.1 Background

Water allocations in the western United States require consideration of the competing short- and long-term needs of many socioeconomic factors, including, but not limited to: agriculture, urban use (municipal and industrial), flood mitigation, hydropower generation, and environmental regulation. Increasing demands on the limited and variable water supply across the West has resulted in insufficient streamflow to sustain healthy fish habitat and populations. In the late summer and early fall, high air temperature and low flow conditions can cause rapid increases in water temperature, creating critical conditions, particularly for cold water fish such as salmon. In addition, construction of dams and diversions along rivers for the purpose of storing and distributing the limited supply of water can further deteriorate natural flow regimes and, often, obstruct important migratory pathways for fish reproduction and development.

In the Sacramento River Basin (SRB) of California (Figure 1.1), the long-term decline in salmon populations has made management of the remaining freshwater habitat critical. This is magnified by the increasing demands on water resources and an extended drought that has enveloped the western United States in recent years. The construction of Shasta (SHD) and Keswick Dams in the SRB headwaters during the mid-20th century provided additional storage facilities to meet regional water needs; however, hundreds of kilometers of spawning habitat above the dams were lost. The declines of the winter run and the late fall runs of Chinook salmon in the SRB have been listed on the endangered and threatened species lists, respectively, by the Environmental Protection Agency. In 2008 and 2009, the Pacific Fishery Management Council closed the river to commercial and recreational fishing, resulting in economic losses in excess of $500M and over 2000 jobs.

The management of freshwater resources is one of the greatest challenges currently facing society. With increasing demand, alteration of water systems, and a changing climate, the thermal regimes of freshwater habitats are being substantially impacted. The thermal impacts on the ecology of river ecosystems have been well documented [Poole and Berman, 2001; Cassie, 2006; McCullough et al., 2009], yet there is no comprehensive modeling framework in place for accurately modeling climate-related impacts. In regulated systems, these impacts are a complex function of the interaction of release volume and temperature and the subsequent exchange with the environment downstream.

The effective use of water to protect fish requires water managers to modify operational strategies by incorporating water quality objectives into daily operations and long-term (i.e., seasonal) planning; this typically involves management of flow releases to control water quality parameters, such as temperature. Shasta Dam, however, was retrofitted with a temperature control device (TCD) in the mid-1990s, which allows selective withdrawals from different depths (and, therefore, different temperatures) in the reservoir based on water temperature requirements downstream; therefore, water managers may modify either the release volume and/or release temperature to meet objectives downstream. Although Keswick Reservoir lies between Shasta Lake and the downstream compliance locations, it serves as a "pass-through" structure with minimal attenuation in temperature and flow released from Shasta. The three important temperature compliance points exist at Balls Ferry (BSF), Jellys Ferry, and Bend Bridge. As BSF is closest to SHD and, hence, the most influenced by any mitigation efforts from the dams, this point is selected as the focus of the current study. It is highly likely that if temperature objectives are not met at this location that the points downstream will have even poorer compliance statistics. The SRB is a complex hydrologic system with multiple reservoirs

along tributaries to the main stem Sacramento River, which enables operators to perform water exchanges between basins through diversions or collaborated releases at other dams. Therefore, the focus of this study considers only the required adaptations at SHD, with the assumption that changes in operations there may be accounted for through exchanges with other water reserves in the region to meet the multiple demands downstream.

Water quantity and quality require joint management in multi-purpose basins like the SRB. Coupling of multiple modeling techniques have been successfully employed to meet planning objectives related to water quality and quantity [de Azevado et al., 2000]. Neumann et al. [2006] integrated a statistical model with an operational rubric to meet thermal objectives on the Truckee River in Nevada by determining the net flow release required to meet a target temperature with a defined level of risk. Since release volume was the single variable used to mitigate stream temperature violations, the impact to in-reservoir thermal profiles were neglected. The total discharge volume served as a limiting factor [Neumann et al., 2006]. Hanna et al. [1999], Saito et al. [2001], and Bartholow et al. [2001] investigated the effects of TCD operations at SHD on in-reservoir thermal properties and the feedback on biota through application of the two-dimensional, laterally averaged hydrodynamic model, CE-QUAL-W2 [W2; Cole and Wells, 2011]. Operation of the TCD altered both the in-reservoir [Hanna et al., 1999; Bartholow et al., 2001; Saito et al., 2001] and downstream thermal, chemical, and, hence, biological dynamics of the system [Lieberman et al., 2000]. Lieberman et al. [2001] evaluated the effects of the TCD on nutrients, particulate organic matter, and plankton in the SHD tailwaters. In addition, Deas et al. [1997] developed models of river temperature for the Sacramento River downstream of SHD. Caldwell et al. [2013b] developed a statistical prediction

model multiple stream temperature attributes at the compliance point at BSF, using a local polynomial-based, generalized linear model (GLM).

A model-based, DSS that is effective in predicting temperature must also be capable of incorporating stream temperature objectives into daily operating procedures. Paraphrased from Neumann et al. [2006], a practical DSS for daily application has these basic functional requirements:

(i) A set of typical basin operating procedures

(ii) A simplistic and spatially and temporally consistent stream temperature prediction model

(iii) A method to quantify confidence/uncertainty with the temperature prediction

(iv) A set of operating rules that benefit river biota, which incorporate stream temperature prediction and the confidence level

(v) A seasonal strategy to mitigate daily violations, while meeting seasonal demands

This chapter describes the development of a predictive model-based DSS for stream temperature management. The DSS couples a stream temperature forecast model with a stochastic weather generator to a decision rubric. The DSS incorporates forecast uncertainties and reservoir operating options to help mitigate stream temperature impacts for fish habitat, while efficiently using the reservoir water supply and cold pool storage. The use of these coupled tools in simulating impacts of future climate on stream temperature variability is also demonstrated. The remainder of the chapter includes: a general overview of the components of the DSS; the constraints applied in the DSS; the rules developed to manage release volume and release temperature to meet downstream temperature targets, including the seasonal criteria; and,

comparison of the performance of these rules in the SRB under multiple hydroclimate conditions during the period since the TCD installation in 1997..

7.2 Decision Support System

A model-based DSS that meets the functional requirements of a DSS is developed, the schematic of which is shown in Figure 7.1. The DSS includes the daily time-step W2 reservoir model [Cole and Wells, 2012; Cole and Buchak, 1995], a local polynomial-based GLM model [Caldwell et al., 2013b] as the predictive stream temperature model, and the operating procedures to determine reservoir releases each day.. The main objective of the DSS is to provide the water managers with information on the daily water release temperature and volume in response to stream temperature forecast based on weather, while incorporating uncertainty. Furthermore, the goal is to preserve the cold pool (i.e. cold water at the bottom of reservoir) while reducing violations (i.e. stream temperatures exceeding biological targets described later) for fish habitat.

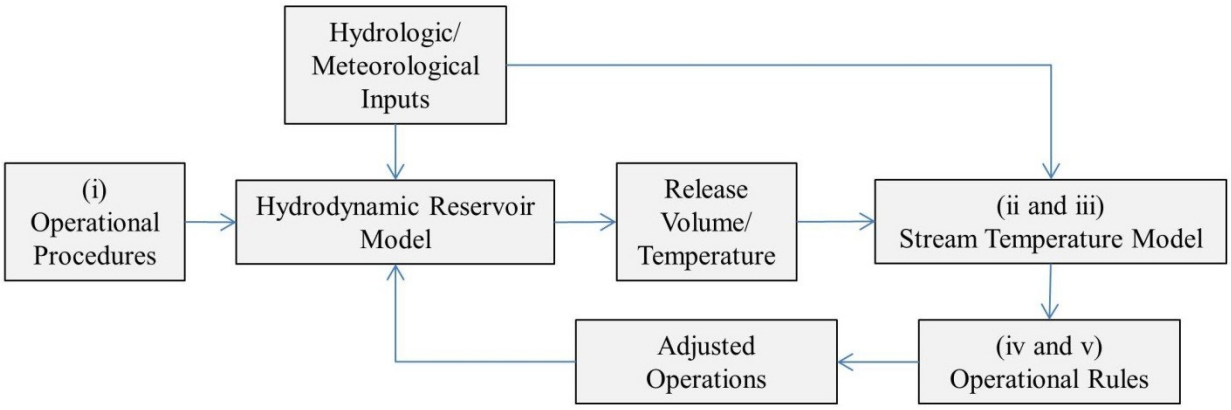

Figure 7.1: Schematic of the DSS with the five functional criteria steps denoted.

For each day of the simulation, the normal operating policy sets the reservoir releases and operations. The release elevation is defined, while the release temperature is extracted from the

prescribed elevation using the thermal profile from the W2 model on that day. Then, the DSS predicts the mean daily stream temperature at BSF. A rule checks whether the predicted temperature is above the threshold. Then, the DSS calculates a corresponding target temperature with the prescribed level of acceptable risk/confidence. A decision is then made on how to operate the releases to meet the target temperature. If adjustments are made during a given week, the W2 model is updated at the end of that week to account for any adjustments in the in-reservoir thermal profile due to changes in operations to meet thermal objectives; this provides updated estimates of release temperature to the predictive stream temperature model and updated end-of-season cold pool elevation for management of the cold water pool. In addition, the DSS must include a source for meteorological and hydrological forcing data for both the reservoir model and predictive stream temperature model. We use both observed data and simulated data from a stochastic weather generator described later in this section. The remainder of Section 7.2 is arranged according to the functional criteria in Section 7.1 and, describes the individual components of the DSS.

7.2.1 Operational Procedures

Functional criterion (i) for a DSS requires the determination of a standard operating policy for the river system. The existing hydrodynamic reservoir model [Hanna et al., 1999] established a set of optimized operating procedures related to TCD operations and reservoir release temperature criteria (Figure 5.4). As temperatures within the reservoir are typically warmer at the surface with decreasing temperatures with depth, water is released from the highest TCD gates during the winter with a drop down schedule throughout the calendar year with lowest level water released during the peak season (July through October, i.e., summer) when stream temperature violations downstream are of major concern. In addition, there are

restrictions to the daily fluctuation of flows (Table 7.1), as well as, a minimum flow requirement of 3250 cfs (~92 cms) and maximum flood control outflow of 75,000 cfs (~2124 cms) [BOR, 2008a].

Table 7.1: Allowed changes in flow releases from Shasta Dam. Nightly values given in BOR [2008a] multiplied by two to estimate daily restrictions.

Flow (cms)	Allowed Daily Variation
≥ 170	+-30%
≥ 113 and < 170	+/- 11.3 cms
< 113	+/- 5.7 cms

Inflows to Shasta Lake come from a combination of rain and snowmelt runoff as large precipitation systems impinge on the mountainous terrain, primarily during the winter season. Hence, storage in Shasta Lake is essential to providing water releases later in the summer to meet the multiple demands in the system, but particularly to provide cold water releases to fish during the hot, dry summer [van Vleck et al., 1988; SFEP, 1992; Yates et al., 2008].

Discharge water from Shasta Lake takes approximately one to two days to reach the nearest downstream compliance point at BSF. During low flow conditions in the summer, the water rapidly warms due to interaction with the environment, leading to water temperatures of detriment to the survivability of cold water fish, such as salmon. Reclamation established the thermal objectives for the river based on multiple studies on anadromous fish and impacts to growth, mortality, and disease [BOR, 1991a, 1991b]. The thermal objective allows a maximum of two consecutive days with daily mean stream temperature in excess of 0.5 °F (0.3 ºC) above the temperature threshold of 56 °F (13.3 ºC). These targets are specific to the compliance points below SHD and should be adjusted for a given river.

Due to the focus on meeting stream temperature objectives and the ability to modify operations at other structures within the SRB, the seasonal criterion (v) is established to both save water and to maximize mitigation of violations throughout the year. The level of the cold water pool can be defined as the level of the 13.3 °C isotherm at the end of the mitigation season. We use Julian day 305 (i.e., November 1st (standard year) or October 31st (leap year)) to extract the elevation of the 13.3 ºC at the dam as a proxy for available cold water storage.

7.2.2 Water Temperature Prediction – Statistical and Hydrodynamical Models

According to functional criteria (ii) and (iii) of a practical DSS, predictions of stream temperatures must include skillful estimates of future stream temperatures, along with the ability to quantify uncertainty. The statistical model of Caldwell et al. [2013a, 2013b], along with the standard error in predictions, are coupled with the methods for computing target temperature from Neumann et al. [2003] to meet these requirements. Caldwell et al. [2013b] developed a regression-based model using a local polynomial, GLM approach to predict stream temperature attributes. The modeled attributes included variables from multiple distributions, including: probability of exceedance (binomial); daily maximum, minimum, and mean stream temperature (Gamma); daily number of hours of exceeding a threshold (Poisson), and daily stream temperature range (Gaussian). The GLM model predicted the downstream values at BSF as a locally fit, linear function of current and prior day values of air temperature, precipitation, and release volume and release temperature at SHD to account for lag time in translation of operational decisions to the downstream compliance location. The simplicity of the model is consistent with the DSS requirements and provides a measurement of standard error with each prediction that can be used in the method of Neumann et al. [2003, 2006] to specify a target temperature. Assuming normally distributed errors about the predicted stream temperature value,

the normal probability distribution function can be shifted such that the area above the thermal criteria is equivalent to the acceptable level of risk/confidence. The target temperature is then calculated as the difference between the predicted stream temperature and the magnitude of the shift. The GLM model can then be used to adjust the input release temperature and release volume to meet the thermal objective. Adjustments can be made by utilizing the W2 model of Shasta Lake.

Hanna et al. [1999] and Saito [1999] developed and calibrated a W2 model for Shasta Lake to simulate TCD operations and predict in-reservoir water temperatures. W2 is a two-dimensional hydrodynamic and water quality model that can simulate reservoir operations [Cole and Buchak, 1995]. This study uses the most recent version 3.7 of W2 from Cole and Wells [2011]. Reservoir water quality is assumed in the model to be well-mixed laterally across the reservoir. Water quality varies with depth and longitudinally in the reservoir; therefore, two-dimensional representation of the reservoir with lateral averaging is assumed. Model output for Shasta Lake consists of simulated vertical profiles of water quality parameters, including water temperature, for each of 63 model segments. We focus on the use of the segment nearest the dam for extraction of water temperature release data at the appropriate TCD elevation based on the operations schedule outlined in Hanna et al. [1999]. Additional details on the updated W2 model may be found in Caldwell et al. [2013c].

Both the statistical model and hydrodynamic models require hydrological and meteorological inputs. Historical data may be used to provide a single trace of predicted stream temperatures for comparison with observations; however, to provide a measure of uncertainty for short-term and seasonal planning, a variety of daily weather input scenarios is required. Stochastic Weather generators are typically used to produce multiple, synthetic time series of

weather from finite station records of hydrometeorological variables. These time series are designed to simulate the statistical properties of the historical data such as probability density function, mean, variance, and skew. The output from weather generators can then be integrated into process response models (e.g., the GLM, W2 model, crop model, hydrologic models, etc.) to characterize the impact of weather and climate on the decision systems [Wilks 1999; Wilks and Wilby 1999, Podesta et al., 2010; Apipattanavis, 2010a, 2010b]. Appipatanavis et al. [2007] developed a semi-parametric weather generator (SWG) that can be easily integrated with seasonal climate forecasts or utilize an analog (i.e., climatologically or hydrologically similar) year to generate time series of daily weather conditioned on expected future climate conditions – such as seasonal climate forecasts – which will be of immense use in seasonal planning efforts. We refer the readers to Apipattanavis et al. [2007] for details on SWG and its application and, to references therein for an overview of stochastic weather generators. The SWG software of Appipatanavis et al. [2007] was adapted such that the observed meteorology, precipitation state, and precipitation transition type for any given analog year could be applied in the resampling. Using this method, the antecedent atmospheric conditions may be coupled with the observed flow and water temperature conditions in that year to create an ensemble of hydroclimatologically-consistent time series of atmospheric and hydrologic forcings. In addition, unconditional (33.3 percent probability in each tercile) and conditional weather ensembles (using a seasonal climate forecast of 40 percent above normal, 35 percent near normal, and 25 percent below normal air temperatures) were generated to indicate the potential application to seasonal planning during the year of 2008.

7.2.3 Operational Rules - Rubric

In order to accomplish the fourth and fifth functional criteria a set of operational rules also called 'rubric' is necessary. The operational rules developed recommend releases that vary in magnitude and release level from the TCD at SHD to meet the thermal objectives at the compliance point at BSF. Multiple release scenarios to improve the stream temperature through operations of the TCD are evaluated. Feedback from water managers provided insightful, yet non-specific, guidelines for operations of the TCD structure at SHD. Essentially, there exist three independent options for TCD operations:

Option 1: Release from the current elevation, as in the default configuration above

Option 2: Release sufficiently cool water from the one of the next two lower elevations

Option 3: Release a mix of water from the current and one of the next two lower elevations

The final option is that none of the three options are required and, therefore, no change is made to operations.

7.2.3.1 Option 1 – Current Level Release

The first release rule can be considered the default and may only be active if the current elevation temperature is below the target temperature. A check is made to evaluate if the current day's predicted temperature and the prior two days' temperatures are above the threshold of 13.6 °C. If this is the third day of violation, the DSS determines the additional flow required to alleviate the violation on the current day with the level of acceptable risk/confidence. If this is not the third day of violation and the prior day is not a violation, a check is performed to ensure

the level of the 13.3 ºC isotherm on Julian day 305 is above the elevation of the lowest TCD gate at 219.5 m. If ample cold water pool is anticipated, a violation is allowed to conserve the cold water pool. The appropriate release volume to meet the thermal objective is determined by iterating through the GLM with the current release temperature and multiple flow releases at 100 cfs increments between the minimum and maximum values calculated using Table 7.1. If these values fall outside the flood control and minimum flow requirements, the respective maximum or minimum value would be used, respectively. If allowing a violation, the flow magnitude typically corresponds to the minimum flow calculated from Table 7.1.

7.2.3.2 Option 2 – Lower Level Release

Like Option 1, the second option uses the same criteria for deciding whether to modify releases to meet a target temperature or to allow a violation; however, this rule is active when the current elevation water temperature release is above the target temperature. First, the water temperatures at the next two lower TCD elevations are extracted from the in-reservoir thermal profile at the dam. The uppermost TCD elevation with sufficiently cold water (i.e., less than the target temperature), is defined as the new release elevation and temperature. The appropriate release volume to meet the thermal objective is determined by iterating through the GLM with the new release temperature and multiple flow releases at 100 cfs increments between the minimum and maximum values calculated using Table 7.1. As in Option 1, the new flow must fall within the flow constraints and, for violations, typically corresponds to the minimum flow calculated from Table 7.1.

7.2.3.3 Option 3 – Mixed Release

Like Options 1 and 2, the third option uses the same criteria for deciding whether to modify releases to meet a target temperature or to allow a violation; however, this rule attempts to conserve cold water through mixing different temperature water from multiple levels within the reservoir. This option is active when the current elevation water temperature release is above the target temperature. First, the water temperatures at the next two lower TCD elevations are extracted from the in-reservoir thermal profile at the dam. A mixed water temperature release temperature is calculated using a combination of the current and one of the next two lower elevations' water temperatures with the total release volume equal to the current release volume. The total release volume is the cumulative flow from the two selected levels. Multiple potential flow releases are generated at 100 cfs increments for the uppermost elevation between 0 cfs and the total release volume. The difference between the iterated flow and the total release volume is applied at the lower level. The final mixed temperature (T_f) is then calculated using an equilibrium temperature formula in Equation 7.1,

$$T_f = \frac{V_1 T_1 + V_2 T_2}{V_1 + V_2} \quad , \qquad (7.1)$$

where T and V are the temperature and volume of releases, respectively, at the two selected levels (i.e., *1* and *2*). The appropriate release volume at each level to meet the thermal objective is determined by iterating through the GLM with the mixed release temperature and total flow release to determine the mixture with the least release volume at the lower level that also meets the target temperature requirement.

7.3 Test Scenarios

The DSS was applied to the Sacramento River to improve stream temperature predictions at the BSF gauge. We assess the effects of TCD operations on river thermal conditions under variable hydroclimatological conditions and two risk levels (α=0.05 and α=0.50).The release volume and temperature from SHD and meteorological variables from Redding Airport (Figure 1.1) are used to generate inputs to the various components of the DSS. High quality and primarily continuous measurements of hourly stream temperature at the BSF gauge are available for the period 1994 to present from the California Data Exchange Center (CDEC) of the California Department of Water Resources. Overlapping hourly discharge and water temperature release data at SHD are also available from CDEC with hourly meteorological data from the National Weather Service automated site at Redding Airport. Since the TCD was installed in early 1997, we restrict our selection of years to the period after 1997.

During that period, an evaluation of meteorological data identified three years that represent dry (2005), hot (2003), and cool, wet (2000) conditions. The observed daily weather is used in the DSS described earlier, resulting in decisions of water release temperature and amount. Stream temperature attributes and violations are compared with baseline or 'observed'. Actual operations are a result of several subjective factors in addition to the rules described in the DSS. Hence a fair comparison is to compare each simulation with the DSS (i.e., With DSS) to a 'baseline' run using observed meteorology and flow releases based on the water temperature releases from the W2 model (i.e., No DSS). This 'baseline' output is mentioned as 'observed', henceforth. This is a standard approach in all such DSS evaluations (see e.g., Regonda et al., 2011; Grantz, 2006). The metrics of concern to water resources include: total annual release volume (acre-feet); total annual energy (Joules); and, end-of-season level of 13.3 °C isotherm

(meters). For biological impacts, the metrics considered include: annual total daily violations (count); total number of hours exceeding 13.3 ºC (count); total days of daily maximum temperature above 13.3 ºC (count); mean seasonal (June through October) probability of exceedance (percent); and, mean magnitude of stream temperatures above 13.3 °C.

To demonstrate the utility of the DSS in short term (few days ahead) and long term (seasonal) planning with uncertainty - we use the SWG approach to generate daily weather ensembles based on just the previous day's weather (i.e., ' unconditional') and based on seasonal climate forecast as well (i.e., ' conditional'). For seasonal application, we focus on the year 2008, which was a dry and hot year and had a strong forecast climate signal from seasonal climate projection of above normal temperatures. The combination of SWG and GLM stream temperature model with the W2 model for thermal structure and release temperature from Shasta Lake is demonstrated in Caldwell et al. [2013c].

7.4 Results

7.4.1 Short-term Forecast Application

This capability of the DSS is examined through the use of observed data within the W2 model for a select set of years: 2000 (cool, wet); 2003 (hot); and, 2005 (dry). While we used different levels of risk (α=0.05 and α=0.50) and alternated between Options 2 and 3, the DSS failed to offer any difference in the operations of the TCD. For that reason, we apply only Option 1 with a risk level of α=0.05 in the forthcoming comparisons. In general, the W2 model is capable of reproducing the observed flows in the individual years (e.g., Figure 7.2); however, due to the prescribed release schedule in the model, the release temperatures vary significantly (e.g., Figure 7.3). The examples shown for the year 2003 are representative of the other two

years, where the release flow is captured but the release temperature predictions are poor (not shown).

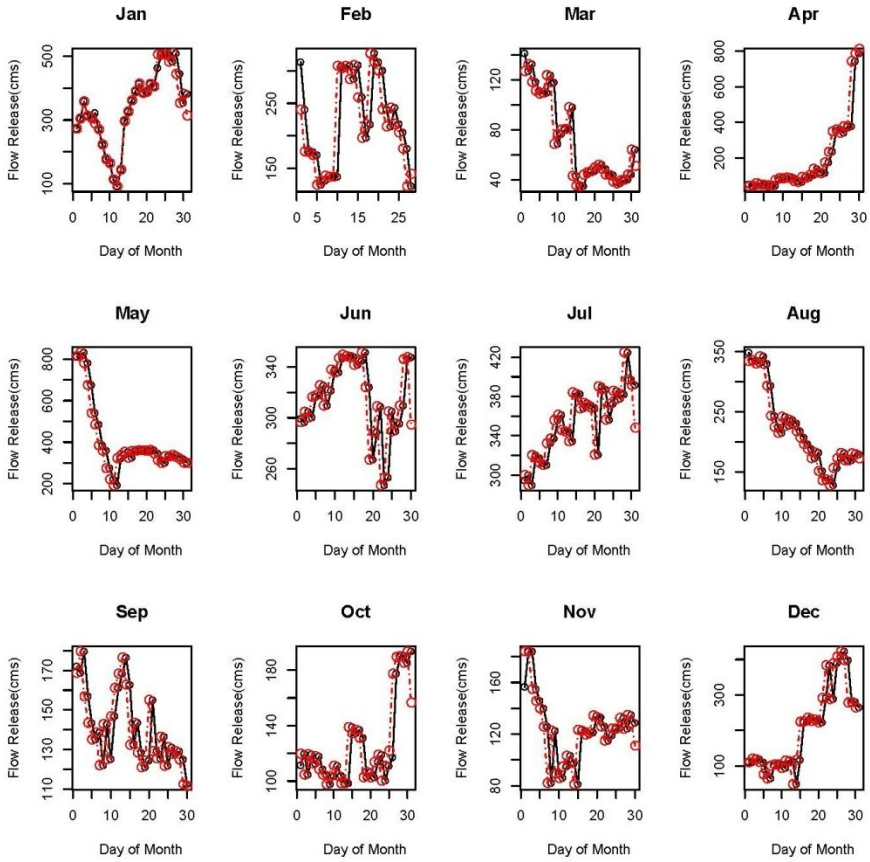

Figure 7.2: Comparison of observed (red) and simulated (black) daily flow releases from Shasta Dam in 2003.

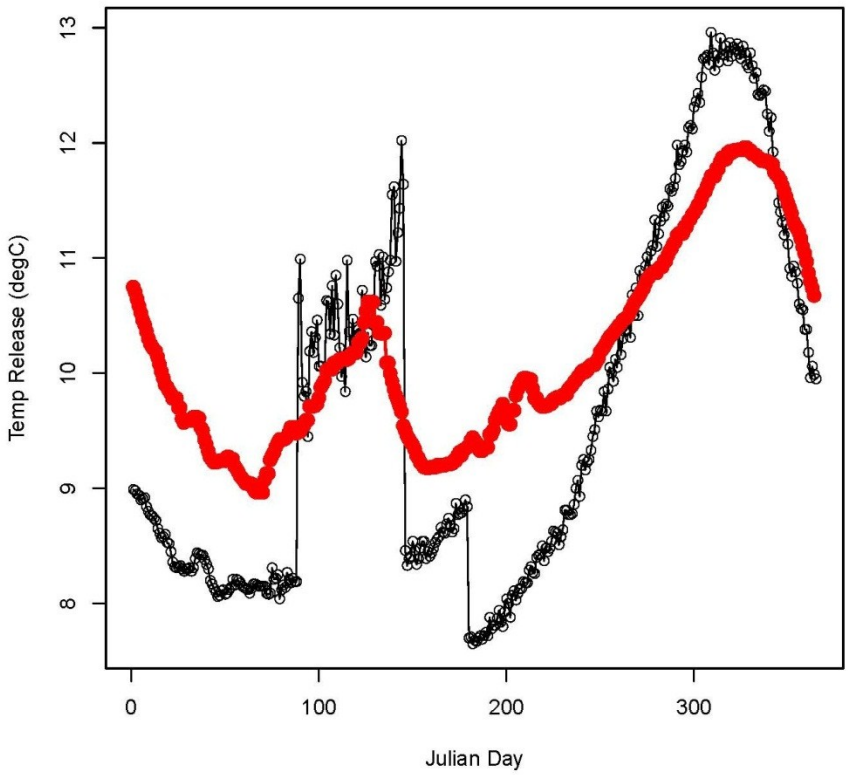

Figure 7.3: Comparison of observed (red) and simulated (black) daily temperature releases from Shasta Dam in 2003.

Examination of the DSS indicates that net savings in the volume of releases prior to July negate the requirement for manipulations of the flow regime during the summer and fall for all three years (Figure 7.4). There is also a cumulative reduction in the number of daily violations in each of the three hydroclimate conditions by the end of the year (Figure 7.5). In fact, the greatest benefit comes during the hot year of 2003 when allowance of violations early in the year result in less than 3 non-consecutive violations during the summer season (not shown).

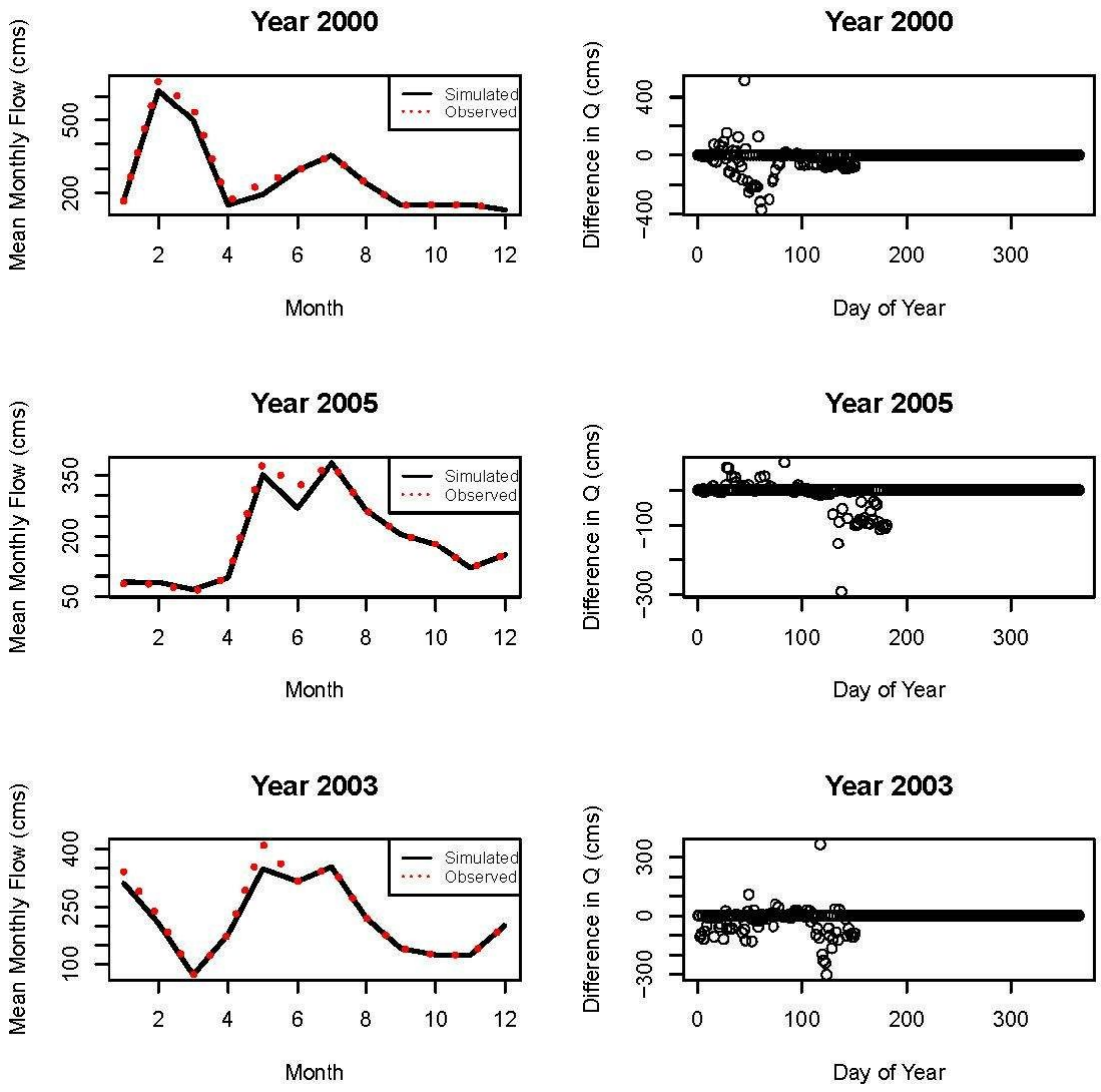

Figure 7.4: Comparison of observed (red, dashed) and simulated (black) mean monthly flow (left) and change in daily flow release (right) from Shasta Dam in the years 2000, 2003, and 2005.

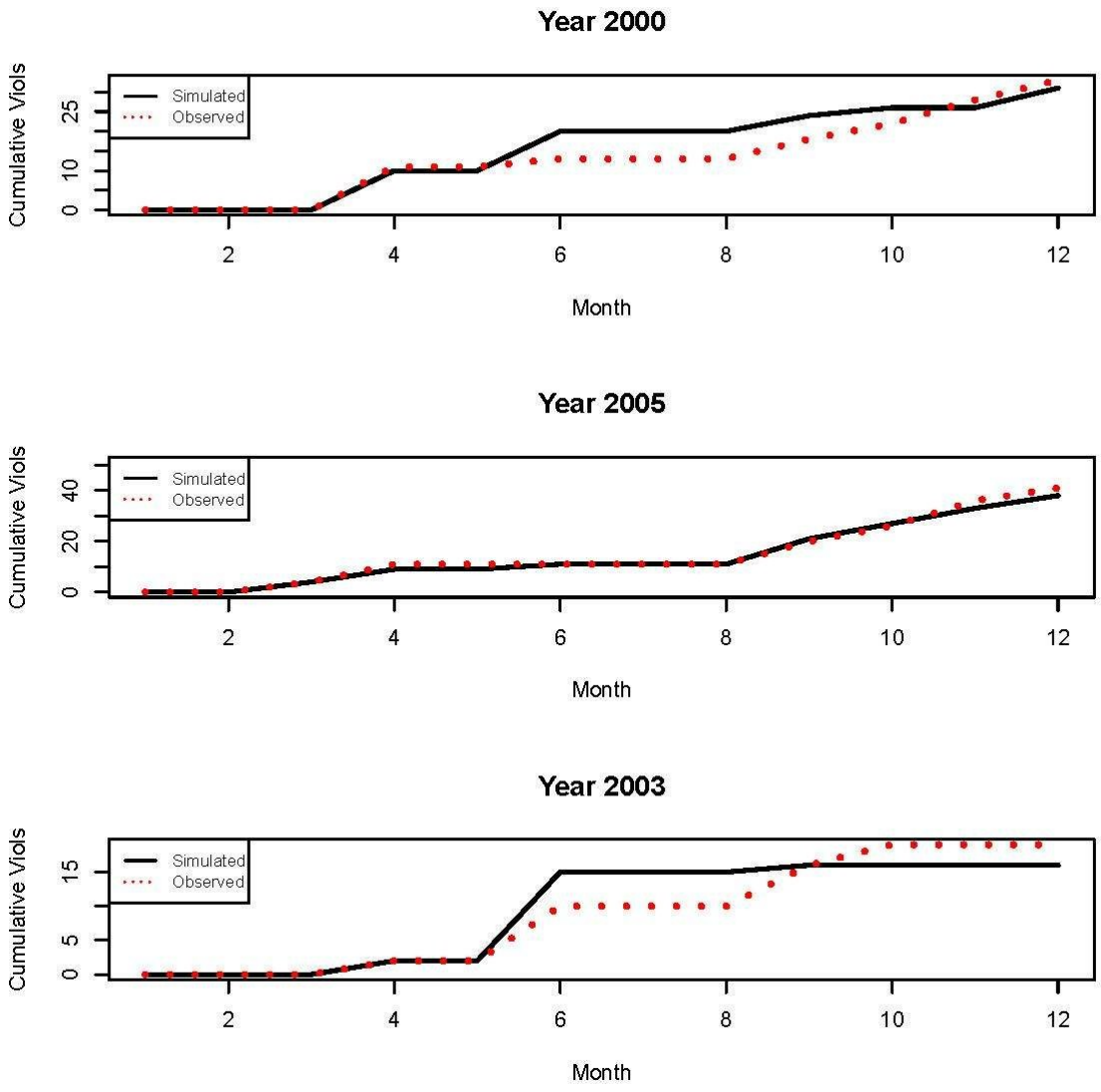

Figure 7.5: Comparison of observed (red, dashed) and simulated (black) cumulative daily violations during the years 2000, 2003, and 2005.

Comparison of each of the years with and without the DSS identifies a general increase in the end of year cold pool volume as elevations of the 13.3 °C isotherm increase, except for in the dry case, where we expect limited water supply to have an effect (Table 7.2). Table 7.2 also shows that the total volume of water released while using the DSS is less in all three cases, as is the cumulative energy released throughout the year. A reduction in the number of violations is evident in all three cases, although minor because instead of having consecutive days of

violations late in the year, we instead see multiple instances of one- or two-day violations in the spring, when the violations are less critical to salmon (not shown). Significant reductions in the number of hours over the critical threshold are seen in the total number of hours above the threshold; so despite the additional daily violations, they are shorter lived. In addition, the number of days that the maximum is above the threshold temperature is reduced, suggesting that the hottest days are not as hot. The probability of exceedance during the summer is also reduced in all three cases, though the cool, wet season shows the greatest dividends. The final comparison in Table 7.2 is the mean difference between the daily mean water temperature and the threshold value, which indicates that the daily means are as cool or cooler overall with the DSS rather than without the DSS in place.

Table 7.2: Hydrological and biological metrics used to assess the DSS for the years of 2000, 2003, and 2003.

Metric	2000 (Cool, Wet)		2005 (Dry)		2003 (Hot)	
	No DSS	With DSS	No DSS	With DSS	No DSS	With DSS
End of Year Cold Water Pool Elevation (m)	214.6	232.6	214.6	214.6	255.2	261.1
Annual Volume Released (af in millions)	71	68	51	50	60	57
Annual Energy Released (J)	3.8E+18	3.5E+18	2.9E+18	2.8E+18	3.3E+18	3.1E+18
Annual Total Daily Violations (count)	33	31	41	38	19	16
Annual Total Number of Hours > 13.3 °C (count)	1081	748	1144	1041	649	491
Annual Number of Days > 13.3 °C (count)	108	90	112	100	99	83
Average Seasonal (Jun 1 - Oct 31) POE (percent)	13	7	29	26	19	15
Mean Magnitude of Difference from 13.3 °C	-1.9	-2.4	-1.8	-1.8	-1.6	-1.9

For each of the three years above, we also ran the stochastic weather generator in an 'unconditional' mode to generate ensembles of weather scenarios for each day and consequently from a suite of stream temperature predictions at the downstream compliance point at BSF to indicate the ability of the weather generator to capture the observed variability. Despite the issues at the upstream boundary in the simulated release temperature (Figure 7.3), the translation of the releases downstream through the GLM model yield excellent results. For example, in

2000, the coupled weather generator, W2, and GLM captures the observed seasonality in each variable (Figure 7.6). Similar results were found for the hot and dry years, as well (not shown).

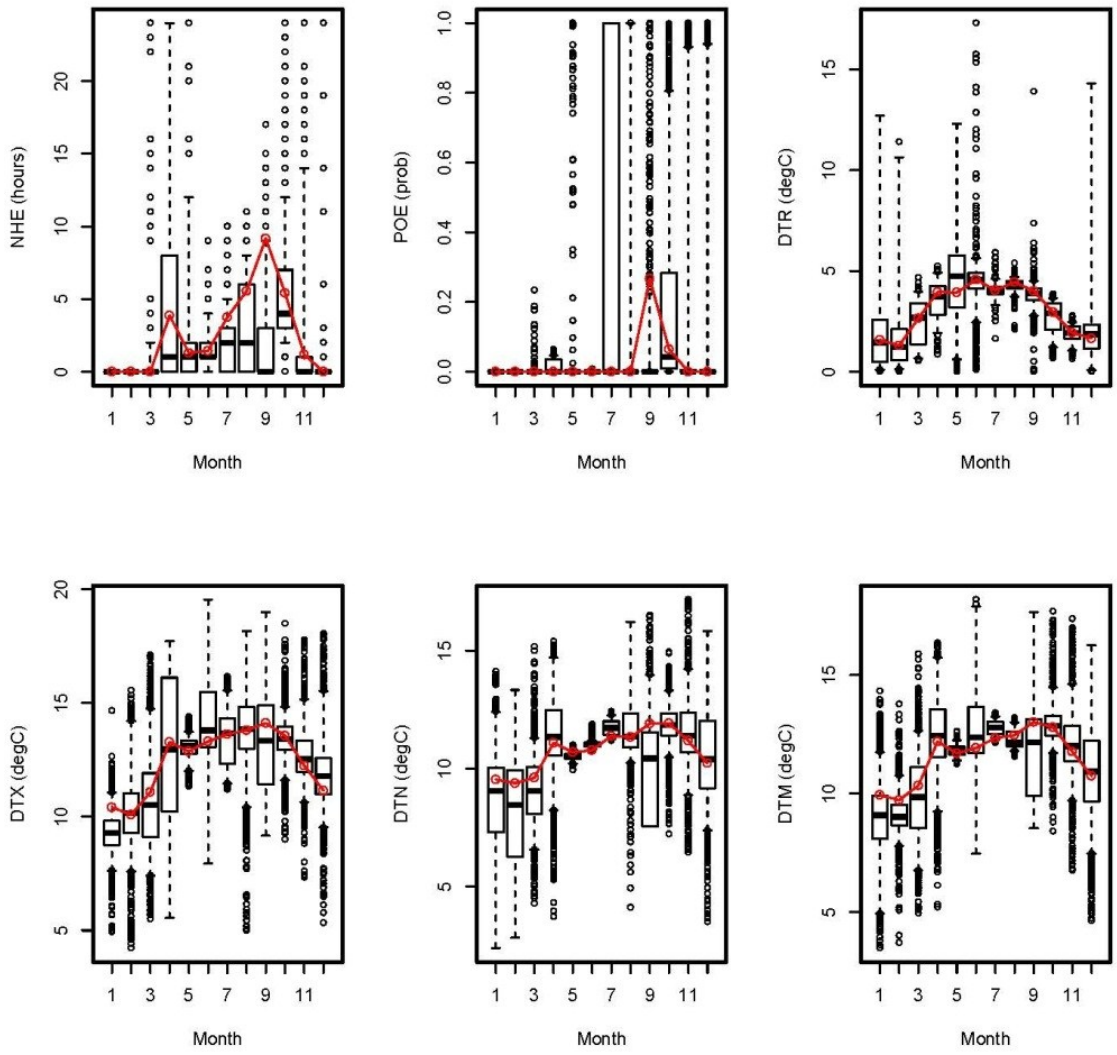

Figure 7.6: Comparison of observed (red line) and simulated (black boxplots) water temperature attributes for the year 2000, including number of hours of exceedance (NHE), probability of exceedance (POE), daily water temperature range (DTR), daily maximum water temperature (DTX), daily minimum water temperature (DTN), and daily mean water temperature (DTM).

7.4.2 Seasonal Forecast Application

This application is of interest for seasonal water resources management planning. At the start of a season (typically July 1st the start of dry season), we need to anticipate stream temperature risk throughout the season and how the DSS might assist in mitigating that risk. From the prior section, we found that the results were independent of the level of acceptable risk and the type of operational change applied (i.e., mixing or not). Therefore, for the seasonal application too, the non-mixing Option 1 with a risk of α=0.05 is used for the analysis. We also chose the year 2008, which was a hot and relatively dry year [Caldwell, 2013c]. In addition, a seasonal climate forecast for 40% chance of above normal temperatures the International Research Institute for Climate and Society at Columbia University (http://iri.columbia.edu/climate/forecast/net_asmt/) for the period July through August enabled conditional weather generation for comparison. We apply the DSS for the Jul-Oct season of 2008 using the conditional weather ensembles and we also compare with unconditional weather ensembles – this enables to see the effect of using seasonal climate forecasts. The comparisons of the metrics are on the 'observed' metrics from 2008 based on the observed hydroclimate described earlier. The observed water temperature release from SHD matches more closely with that from the conditional scenarios as opposed to the unconditional scenarios (Figure 7.7). The improvement is also evident in the translation of that water temperature release downstream to the compliance point at BSF. For example, in the month of September, the simulated values of each of the six water temperature attributes are more in line with the conditional simulations than that of the unconditional (Figure 7.7). The unconditional runs can be viewed as standard operations scenarios, which lend credibility to application of seasonal forecast information in planning scenarios.

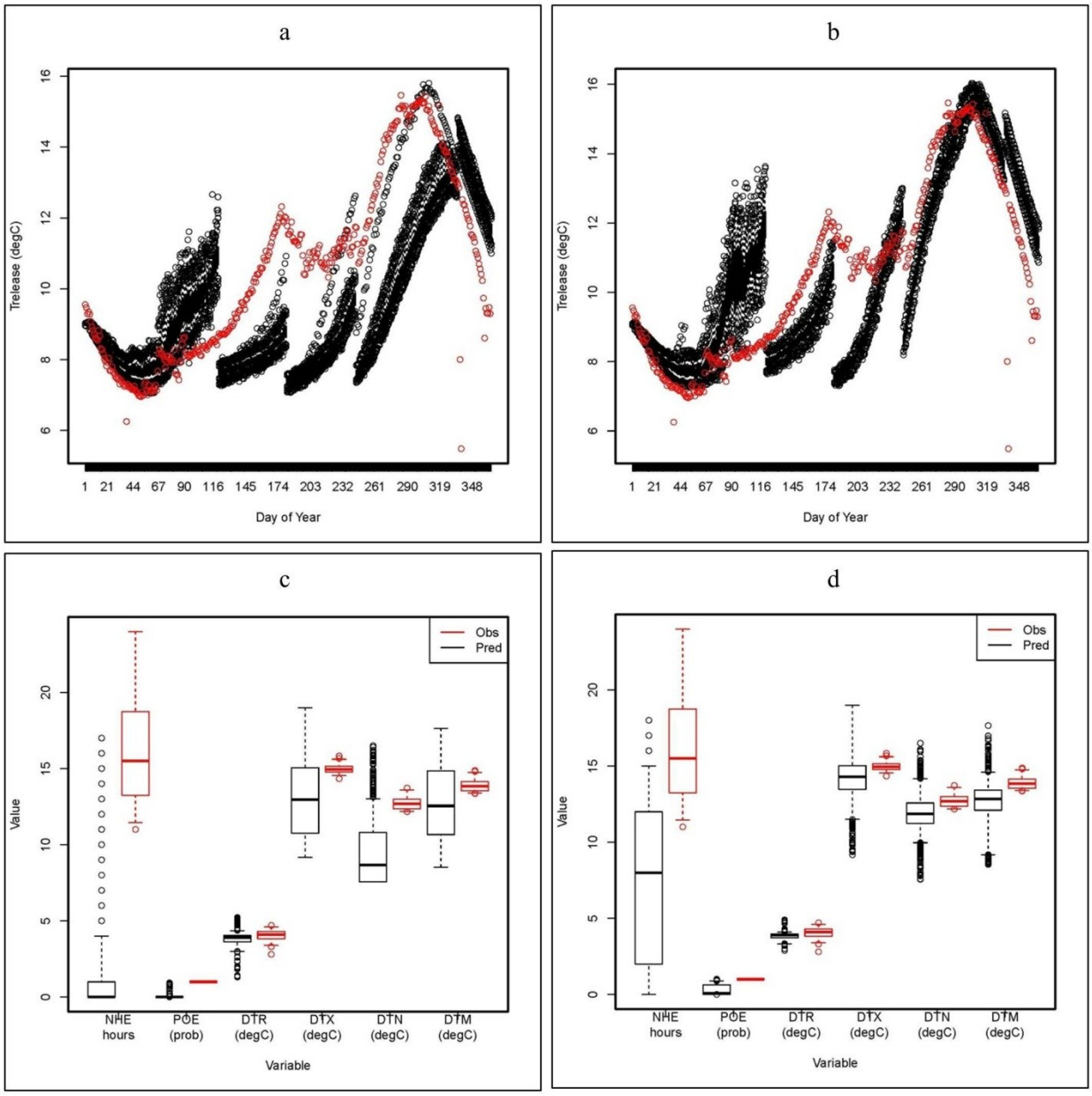

Figure 7.7: Comparison of observed (red) and predicted (black) daily water temperature release from Shasta Dam (a and b, respectively) and September water temperature attributes for the (c) unconditional and (d) conditional simulations in 2008.

Evaluation of the metrics shows that the conditional runs best capture the mean observed statistics in 2008 (Table 7.3). From a hydrological perspective, using the 'No DSS' case as the baseline, the conditional forecast provides an extra 1.8 m of cold water pool elevation on November 1st, with over 4 million acre-feet of cumulative volume savings over the year. At the

same time, a small reduction in the daily violations is seen, which corresponds to an increase in spring season violations and reduction of summer violations, as seen in the single year case. The average probability of exceedance is reduced by 10 percent, with nearly 300 fewer hours of exceedance, a great benefit to the fisheries. The unconditional simulations show the lack of skill that can accompany using climatological averages as a means for prediction (not shown). There is a prediction for much more end of year cold water than expected and under-estimation of critical thermal criteria. The actual observations again are somewhat different than those from the DSS, but indicate that an alternative schedule as prescribed in the W2 model may better serve the health of fish populations.

Table 7.3: Hydrological and biological metrics used to assess the DSS for the seasonal application in 2008.

Metric	No DSS	With DSS	Observed
End of Year Cold Water Pool Elevation (m)	210.3	212.1	NA
Annual Volume Released (af in millions)	59	55	44
Annual Energy Released (J)	3.3E+18	2.4E+18	2.7E+18
Annual Total Daily Violations (count)	47	47	82
Annual Total Number of Hours > 13.3 °C (count)	1564	1292	2592
Annual Number of Days > 13.3 °C (count)	131	131	176
Average Seasonal (Jun 1 - Oct 31) POE (percent)	37	27	48
Mean Magnitude of Difference from 13.3 °C	3.2	2.9	3.2

Finally, the application at the seasonal scale using the weather generator provides an opportunity to examine the probability distribution functions of water temperature attributes and metrics (Figure 7.8). The same relationships can be seen as described in Table 7.3; however, it is possible to compute the reduction in risk relative to using the 'No DSS' option as the difference between the areas under the curves above some threshold value. We focus here on the DTM variable, since it is of greatest interest. While the risk of DTM exceeding 13.6 °C is reduced by only 1.8 percent, there is an opportunity to save the cold water pool, while reducing the NHE, POE, and DTX during the summer season.

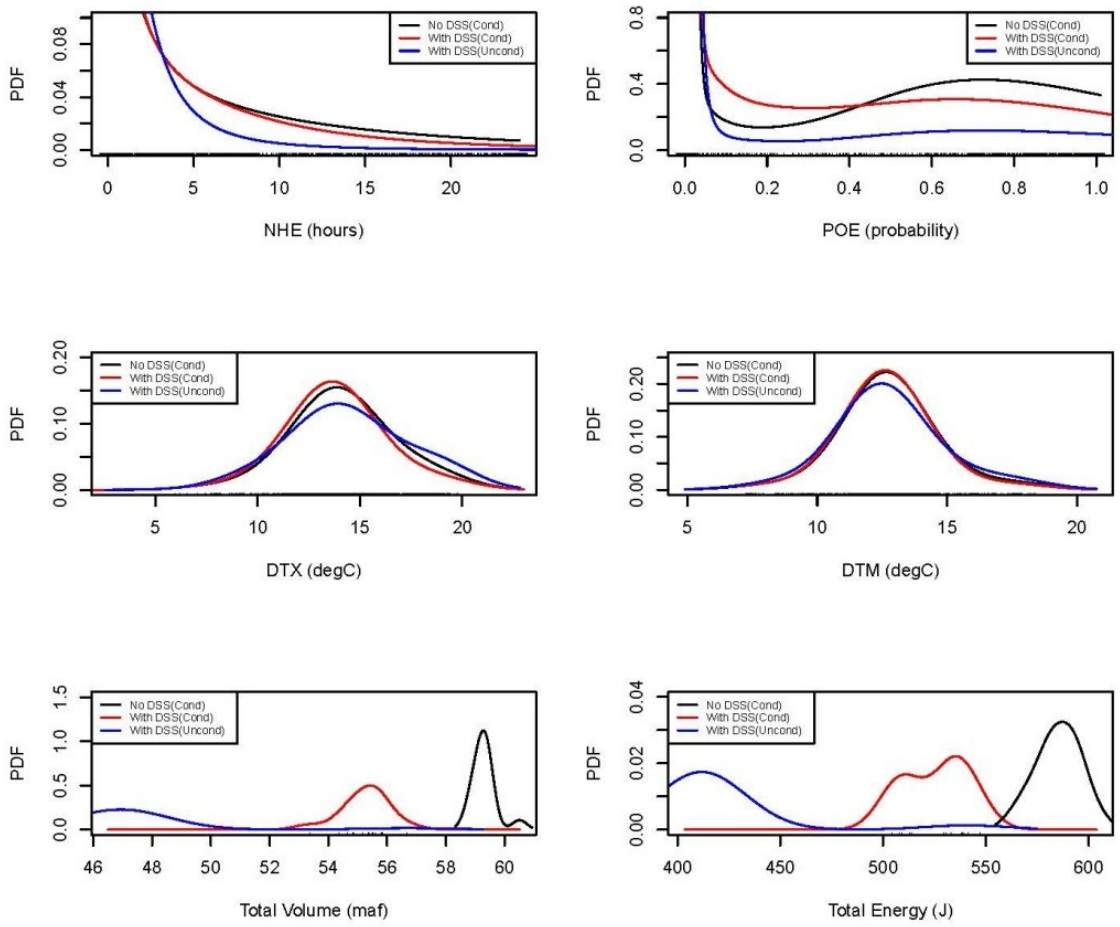

Figure 7.8: Probability density functions for the number of hours of exceedance (NHE, in hours), probability of exceedance (POE, as probability), daily maximum water temperature (DTX, in °C), daily mean water temperature (DTM, in °C), total release volume (in maf), and total energy used (in J) for the 'No DSS', unconditional 'With DSS', and conditional 'With DSS' simulations in 2008.

7.5 Summary

Water management in the Sacramento River is a complex task with a diverse set of demands ranging from municipal supply to mitigation of fisheries impacts due to high water temperatures. Current operations utilize the TCD structure at Shasta Dam to mitigate these high water temperatures downstream at designated compliance points. The TCD structure at Shasta Dam offers a rather unique opportunity to mitigate water temperature violations through adjustments to both release volume and temperature. In this study, we develop and evaluate a

model-based DSS that links weather generator software, a predictive stream temperature model, and a hydrodynamic reservoir model and compared results to standard operating procedures. The weather generator enables the application of analog year and ensemble-based approaches that provide estimates of variability in predicted conditions at the short-term and seasonal time scales. The predictive stream temperature model translates the reservoir operations to the downstream compliance point, while providing the ability to include risk estimates using the methods of Neumann et al. [2003, 2006]. In addition, the GLM is capable of predicting other important water temperature attributes of interest to fisheries management, including the number of hours exceeding a threshold temperature and probability of exceedance of that threshold, among others. The hydrodynamic model includes the reservoir operations (i.e., volume and temperature of releases), enabling modifications based on the operating rules in Section 7.2.3. Following modifications via the DSS, regular updating to the in-reservoir thermal profile prior to prediction using the GLM is also accomplished via the W2 model.

Multiple options for modifying releases at Shasta Dam were considered in the DSS, including mixing water from multiple elevations through the TCD and using different acceptable levels of risk. Despite anticipated water savings from utilization of a multi-elevation release schedule, the DSS failed to activate Option 3. In addition, the DSS was insensitive to the risk level; therefore, a high level of confidence and Option 2 were applied for all evaluations. During the three years tested in the short-term application, activation of the DSS late in the year was non-existent with all modifications to reservoir releases occurring before the month of July. This suggests that summer season mitigation can be managed with ample lead time if there is some knowledge of the upcoming season's hydroclimate. In fact, if operators allow consecutive violations of less than three days in the first half of the year while ensuring adequate end-of-

season cold water volume, violations after July are non-existent under multiple hydroclimate states. An additional benefit is a savings of one to four million acre-feet of water volume over the course of the year, which may be applied to other demands. The reduction in total volume released also manifests as an additional 1 to 18 meters of cold water pool by November 1st, providing a buffer in the situation where the seasonal hydroclimate deviates substantially from the climate forecast or the analog year selected for planning.

The DSS developed here utilizes a rubric-based mechanism for adjusting release volume and temperatures; however, a full, multi-objective optimization problem could be solved, as in the manner of Carron and Rajaram [2001]. We utilized the rubric-based approach due to the complex interactions of humans and operations and the respective impact on thermal regime and habitat. This approach allows the consideration of other options for mitigation and system-specific operational rules. For example, we used a simplified operational procedure for the TCD as defined in Hanna et al. [1999]; but, the flexibility of the DSS could incorporate any given default procedure. The DSS is general in nature in that the user can replace any of the modules with their preferred methods and it is easy to transfer to any other site. For example, forecasts from short term weather forecasting models (e.g., WRF) [Danner et al., 2012] can be used for real-time operations and management; the rubric could be replaced with a multi-objective optimization approach [e.g., Carron and Rajaram, 2001]; a dynamical stream temperature model can be used instead of the statistical GLM approach [Pike et al., 2013]. This flexibility will be of immense help for water managers to adapt the developed DSS to their systems.

This chapter of the dissertation was submitted in July 2013 to Environmental Modeling and Software as an article entitled ‘Managing Water Temperatures in the Sacramento River, California’; see the Caldwell et al. [2013d] reference.

8 CONCLUSION AND FUTURE WORK

In 2004, the National Oceanic and Atmospheric Administration's (NOAA's) National Marine Fisheries Service (NMFS) issued a Biological Opinion (BiOp) to outline the decisions support system for water allocations in the Sacramento River Basin (SRB), particularly the Central Valley Project, with respect to impacts on threatened and endangered species in the SRB [NMFS, 2004]. Peer-review of the BiOp identified fundamental flaws in two critical components, the stream temperature and fish mortality models, due to limitations of the proposed methods in both temporal and spatial resolution [Lichatowich et al., 2005; Maguire, 2006; McMahon, 2006]. According to the peer-review, the BiOp also failed to adequately address uncertainty and risk. For example, there was no effort made within the BiOp to include the impacts of climate change over the course of the licensing timeframe, which could be up to 50 years. As a result of the limitations of the existing DSS, fisheries and water managers are in a position of making water allocation decisions based on inadequate information about stream temperatures and thermal impacts on salmon and steelhead. To address these issues, an integrated framework was proposed that would result in the development of a suite of decision support tools (DSTs) for resource managers [Danner et al., 2007].

The framework of Danner et al. [2007] envisioned satellite-derived inputs in ecological and numerical weather prediction models to provide environmental inputs to the stream temperature models at increased temporal (~15 minutes) and spatial (~3 km) resolutions. The higher-resolution stream temperature forecasts can then be implemented in fish mortality models. In this research we developed several complementary components culminating in their coupling into a Decision Support System (DSS) for managing the water releases from Shasta Dam to mitigate stream temperature impacts. The individual components and their integration to a DSS

are a novel and original contribution of this research. The contributions of this dissertation are summarized followed by potential benefits of this research to SRB water resources system, concluding with extensions for future research.

8.1 Summary

The individual components of the integrated framework are described in five central chapters (Chapters 3, 4, 5, 6 and 7) and are summarized below. Chapter 1 provides an overview of the water resources system in SRB, the stream temperature issues and the problem description in general. Chapter 2 is a detailed survey of stream temperature modeling approaches – covering physically based approaches that model the thermodynamic and hydraulics in great detail to statistical models.

In Chapter 3 we developed a complementary statistical modeling tool using local polynomial based Generalized Linear Model (GLMs) that provides monthly to seasonal forecasts of key water temperature attributes and probabilistic estimates of risk of meeting or exceeding predetermined thresholds of each attribute. The GLM framework can model a variety of variables such as discrete, binary, and continuous, among others. For example, we fitted models to predict a variety of water temperature attributes such as number of hours of exceedance (discrete), probability of temperature exceeding a threshold (binary), and daily maximum water temperature and daily water temperature range (both continuous). We fitted models for each month and for each variable separately using a large pool of predictor variables based on atmospheric variables (e.g., temperature, precipitation from current and previous day) and water variables (e.g., flow, temperature from previous day). Based on cross validated skill scores, the models performed well, especially during the summer months of interest.

We applied the stochastic weather generator (SWG) to generate ensembles of daily weather sequences in an unconditional manner (i.e., assuming all of the historical years are equally likely) and conditional manner (based on probabilistic seasonal climate forecast). Consequently, we also generated ensembles of water temperature attributes using the local polynomial GLMs. We found that these ensembles were consistent with the seasonal forecast, demonstrating the ability of the proposed methodology to provide projections of water temperature attributes before the start of the season. The ensembles of water temperatures provide the estimates of risk of exceeding various compliance thresholds. These risk estimates can be of immense help to water managers in making plans for additional water or changes in operations before the start of the season to help mitigate water temperature risk in a sustainable manner.

Chapter 4 provides an application of the GLM in the Pacific Northwest, which incorporates output from a coupled hydrology model (VIC) and global climate models. The objective of Chapter 4 is to identify the expected change in water temperatures in the Methow River Basin, Washington, under future climates. Compared to the results from Chapter 3, the GLM model performs well in the unregulated Methow Basin with excellent skill scores observed at the daily time scale. The GLM model developed in the Methow Basin, however, is designed for later application in an hourly time-step, two-dimensional hydraulic model. In order to downscale the coarse resolution of the data to hourly, the methodology of Nowak et al. [2010] was employed for spatial and temporal disaggregation. A variety of metrics indicated excellent skill in the hourly water temperature predictions, as well. The results from the climate change assessment show a mean increase in water temperatures near the confluence of the Methow and Chewuch Rivers by the year 2080; however, care must be taken in that these results do not

include potential changes in riparian vegetation and do not fully incorporate changes in snowmelt hydrology.

In Chapter 5, we coupled the SWG, the two dimensional hydrodynamic model, W2, for Lake Shasta, and the local polynomial GLM stream temperature model from Chapter 3 to generate predictions of water temperature attributes at the downstream compliance point at Balls Ferry using a variety of hydroclimate conditions. We demonstrated this for three years of 2000, 2003, and 2005. In addition, unconditional and conditional weather generator scenarios are used as input to the coupled modeling framework to show potential application to seasonal risk assessment of in-reservoir thermal objectives, in particular the upper elevation of the cold pool and reservoir release temperature criteria. Furthermore, the W2 model in conjunction with the stream temperature model provides appropriate amount of water release from the lake (dam), the release temperature and the level to release from the temperature control device (TCD) installed in the reservoir. This successful coupling of the three models provides an attractive option for use in decision support.

The coupling of the SWG and W2 is a flexible tool and allows integration with other types of water temperature models, including physically-based, dynamic models that require upstream boundary conditions at Shasta Lake. As an example, preliminary results from application in the River Assessment and Forecasting Tool (RAFT) model of Pike et al. [2013] is provided in Chapter 6. The advantage of the RAFT model is the ability to produce spatially-explicit, high temporal resolution (i.e., hourly) estimates of water temperature throughout the upper SRB, including Balls Ferry and other compliance points. The results from this are comparable to those from the statistical stream temperature model described in Chapter 5.Culmination of all the models described earlier into a robust DSS occurs in Chapter 7. In this,

we developed an integrated decision support system (DSS) for modeling and mitigating water temperature impacts and demonstrate it on the SRB. The DSS has four broad components that are coupled to produce the decision tool for stream temperature mitigation: (i) a suite of statistical models for modeling stream temperature attributes using hydrology and climate variables of critical importance to fish habitat; (ii) a reservoir thermal model for modeling the thermal structure and, consequently, the water release temperature, (iii) a stochastic weather generator to simulate weather sequences consistent with seasonal outlooks; and, (iv) a set of decision rules (i.e., 'rubric') for reservoir water releases in response to outputs from the above components. The DSS incorporates forecast uncertainties and reservoir operating options to help mitigate stream temperature impacts for fish habitat, while efficiently using the reservoir water supply and cold pool storage. The use of these coupled tools in simulating impacts of future climate on stream temperature variability is also demonstrated.

The results of the DSS indicate that allowing non-consecutive violations during the first half of the calendar year, within the constraints of reservoir operations, enables significant savings in volume released throughout the year. In addition, evaluation of key metrics of both hydrologic and biological significance suggests these adjustments to operations yield improvements to the overall water quality at the downstream compliance point of Balls Ferry. The results indicate that the DSS could substantially reduce the number of violations of thermal criteria, while ensuring maintenance of the cold pool storage throughout the summer.

8.2 Potential Benefits

The developed DSS represents a substantial improvement over existing decision methods which are not well integrated and, thus, will translate into considerable long and short-term direct and indirect socio-economic benefits by efficient management of water resources. These benefits

would come as a result of the extensive improvements in the DSTs, including: (i) model outputs that are at spatiotemporal scales that are orders of magnitude finer than the current outputs (i.e., RAFT); (ii) provision of risk and uncertainty estimates through coupling with weather generation software; and, (iii) the ability to test alternative operations scenarios while monitoring the potential impacts on hydrology and fisheries. The socioeconomic impacts of the DSS will likely be wide-ranging. By providing fisheries managers with future projections of water temperature and fish-related metrics, agencies will be better equipped to protect California salmon stocks. However, the economic impacts of the proposed DSS improvements will likely be substantially greater to the hydropower industry and to the electric utility rate payers in California. In order to meet temperature compliance regulations, water managers at generating stations direct cold water through low- level river outlets instead of passing water through the hydro turbines, which results in the loss of potential power generation. The savings of water indicated in Chapter 7 would allow additional water to be passed through the hydropower generators. The same efficiency principles apply to the Environmental Water Account (EWA) which is a system jointly administered by fisheries and water management agencies for purchasing water for the purpose of protecting endangered species. Between 2001 and 2004 state and federal contributions to the EWA exceeded $414 million. Better management of water resources through improved modeling could significantly reduce these values, reducing the cost burden on the state and federal agencies.

8.3 Future Work

There are several extensions to the integrated framework developed in this dissertation listed below some of which are already underway.

(i) The meteorology over the lake is not simulated well; currently it is simulated based on the weather data at lower elevation. A multi-site weather generator that can provide consistent and correlated weather ensembles on lake and the river reach downstream is important for better modeling of lake thermal structure and release temperatures.

(ii) Inflows to the lake at the upstream are not incorporated. This needs to be modeled separately and coupled with the lake model to provide realistic thermal structure.

(iii) The stream temperature and flow projections from the DSS need to be driven through fish mortality model to evaluate the performance of this integrated DSS in mitigating fish mortality. We evaluated the performance on temperature threshold which are a surrogate for fish mortality but not its direct indicator.

(iv) The advantage of the RAFT model, however, is its capability to model at high spatial and temporal resolution (i.e., hourly and 1 km). The work presented in the dissertation does not fully capitalize on this benefit. At the simplest level, additional verification of the coupled RAFT model should be performed to determine the spatial limit of effectively modeling the water temperature downstream. Also, investigation of the spatial distribution of temperatures throughout the river relative to the timing of different life stages of particular fish species would provide additional insight into the movement of fish throughout the season and, therefore, feedback to water managers on when and where to relocate the compliance point for meeting thermal objectives. Using the ensemble approach, probabilistic estimates of water temperature may be provided at the 1-km scale.

(v) The DSS developed herein excludes the consideration of operations at other structures within the SRB (e.g., Whiskeytown and Trinity Dams). A more robust water management tool would provide the ability to incorporate the many decisions on allocations within the SRB (e.g., RiverWare; http://cadswes.colorado.edu/creative-works/riverware). The current DSS offers the potential to save a significant amount of water through investigation of other operations considerations, including trade-offs with other adjacent and contributing basins. A full evaluation of the set of decisions in the entire SRB that maximize benefits to the multiple sectors of water use in the region would assist in the substantiation of any modification to existing operating rules.

BIBLIOGRAPHY

Apipattanavis, S., G. Podesta, B. Rajagopalan, and R.W. Katz (2007), A semi-parametric multivariate and multisite weather generator, Water Resources Research, 43, W11401.

Apipattanavis, S., F. Bert, G. Podesta, and B. Rajagopalan (2010a), Linking weather generators and crop models for assessment of climate forecast outcomes, Agricultural and Forest Meteorology, 150, 166-174.

Apipattanavis, S., K. Sabol, K.R. Molenaar, B. Rajagopalan, Y. Xi, B. Blackard, and S. Patil (2010b), Integrated framework for quantifying and predicting weather-related highway construction delays, Journal of Construction Engineering and Management, 136(11), 1160-1168.

Apipattanavis, S., B. Rajagopalan, and U. Lall (2010c), Local polynomial-based flood frequency estimator for mixed population, Journal of Hydrologic Engineering, 15, 680.

Bannayan, M., and G. Hoogenboom (2008), Predicting realizations of daily weather data for climate forecasts using the non-parametric nearest-neighbor resampling technique, International Journal of Climatology, 28(10), 1357-1368.

Bartholow, J., R.B. Hanna, L. Saito, and M.J. Horn (2001): Simulated limnological effects of the Shasta Lake temperature control device. Environmental Management, 27(4), 609-626.

Bartholow, J.M. (2003), Modeling Chinook Salmon with SALMOD on the Sacramento River, California, paper presented at International IFIM Users' Workshop, 1-5 June 2003, Fort Collins, CO.

Benson, N.G. (1953), The importance of ground water to trout populations in the Pigeon River, Michigan, Transactions of the Eighteenth North American Wildlife Conference, Washington, D.C., 9-11 March 1953, Wildlife Management Institute, Wire Building, Washington, D.C., 269-281.

Benyahya, L., D. Caissie, A. St-Hilaire, T.B.M.J. Ouarda, and B. Bobee (2007), A review of statistical water temperature models, Canadian Water Resources Journal, 32(3), 179-192.

Bettelheim, M. (2001), Temperature and flow regulation in the Sacramento River and its effect on the Sacramento Pikeminnow: a literature review, Department of Fish and Game, State of California, 9 pp.

Bjorn, T.C., and D.W. Reiser (1991), Habitat requirements of salmonids in streams, American Fisheries Society Special Publication, 19, 83-81.

Bogan, T., J. Othmer, O. Mohseni, and H. Stefan (2006), Estimating extreme stream temperatures by the standard deviate method, Journal of Hydrology, 317, 173-189.

Boyd, M., and B. Kasper (2003), Analytical methods for dynamic open channel heat and mass transfer: methodology for heat source model Version 7.0.

Bracken, C., B. Rajagopalan, and J. Prairie (2010), A multisite seasonal ensemble streamflow forecasting technique, Water Resources Research, 46, W03532.

Bravo, H.R., W.F. Krajewski, and F.M. Holly (1993), State-space model for river temperature prediction, Water Resources Research, 29, 1457-1466.

Brock, J.T., and C.L Caupp (1996), Application of a DSSAMt water quality model - Truckee River, Nevada for Truckee River Operating Agreement (TROA) DEIS/DEIR: simulated river temperatures for TROA, Technical Report No. RCR96-7.0, Rapid Creek Research, Inc., Boise, Idaho.

Brown, L.R. (2000), Fish communities and their associations with environmental variables, lower San Joaquin drainage, California, Environmental Biology of Fishes, 57, 251-269.

Brown, L.R., and S. Greene (1992), Biological Assessment: Effects of Central Valley Project and State Water Project Delta Operations on Winter-Run Chinook Salmon, California Department of Water Resources, October 1992, 135 pp.

Brown, L.R., and P.B. Moyle (1993), Distribution, ecology, and status of fishes of the San Joaquin drainage, California, California Fish and Game, 79, 96-114.

Buishand, T.A., and T. Brandsma (2001), Multisite simulation of daily precipitation and temperature in the Rhine basin by nearest neighbor resampling, Water Resources Research, 37(11), 2761-2776.

Bureau of Reclamation (BOR) (1991a), Appendixes to Shasta Outflow Temperature Control: Planning Report/Environmental Statement - Appendix A: Modeling, U.S. Department of Interior, Bureau of Reclamation, Mid-Pacific Region, May 1991, 176 pp.

Bureau of Reclamation (BOR) (1991b), Appendixes to Shasta Outflow Temperature Control: Planning Report/Environmental Statement - Appendix B: Environmental, U.S. Department of Interior, Bureau of Reclamation, Mid-Pacific Region, May 1991, 128 pp.

Bureau of Reclamation (BOR) (2004), Long-term Central Valley Project Operations Criteria and Plan, U.S. Department of Interior, Bureau of Reclamation, Mid-Pacific Region, Sacramento, California, 30 June 2004, 238 pp.

Bureau of Reclamation (BOR) (2008a), Biological Assessment on the Continued Long-term Operations of the Central Valley Project and the State Water Project, U.S. Department of Interior, Bureau of Reclamation, Mid-Pacific Region, Sacramento, California, 30 August 2008, 1089 pp.

Bureau of Reclamation (BOR) (2008b), Methow Sub-basin Geomorphic Assessment, Okanogan County, Washington, Technical Service Center, Denver, CO, 844 pp.

Caissie, D. (2006), The thermal regime of rivers: a review, Freshwater Biology, 51, 1389-1406.

Caissie, D., N. El-Jabi, and M.G. Satish (2001), Modeling of maximum daily water temperatures in a small stream using air temperatures, Journal of Hydrology, 251, 14-28.

Caldwell, R.J., and B. Rajagopalan (2011): Statistical modeling of daily stream temperature for mitigating fish mortality, Abstract H43A-1188, American Geophysical Union, Fall Meeting, San Francisco, CA.

Caldwell, R.J., S. Gangopadhyay, J. Bountry, Y. Lai, and M. Elsner (2013a), Statistical modeling of daily and sub-daily stream temperatures: application to the Methow River Basin, Washington, Water Resources Research.

Caldwell, R.J., B. Rajagopalan, and E. Danner (2013b), Statistical modeling of daily water temperature attributes on the Sacramento River, submitted to ASCE J. Hydrologic Engineering, in review.

Caldwell, R.J., L. Saito, B. Hanna, and B. Rajagopalan (2013c), Implementation of a coupled statistical-hydrodynamic modeling system to predict stream temperature attributes, submitted to Environmental Modeling and Software, in review.

Caldwell, R.J., E. Zagona, and B. Rajagopalan (2013d), Managing water temperatures in the Sacramento River, California, submitted to Journal of the American Water Resources Association in July 2013.

California Data Exchange Center (CDEC) (2011), Hydrologic data download, California Department of Water Resources, http://cdec.water.ca.gov.

California Department of Fish and Game (CDFG) (2005), Fish Passage Improvement, An Element of CALFED's Ecosystem Restoration Program, http://www.watershedrestoration.water.ca.gov/fishpassage/b250/content.html.

Carron, J., and H. Rajaram (2001), Impact of variable reservoir releases on management of downstream water temperatures, Water Resources Research, 37(6), 1733-1743.

Chandler, R.E. (2005), On the use of generalized linear models for interpreting climate variability, Environmetrics, 16, 699–715.

Chandler, R.E., and H.S. Wheater (2002), Analysis of rainfall variability using generalized linear models: a case study from the west of Ireland, Water Resources Research, 38(10).

Cole, T.M., and E.M. Buchak (1995), CE-QUAL-W2: A two-dimensional, laterally averaged hydrodynamic and water quality model, version 2.0, Instruction Report EL-95-U.S. Army Corps of Engineers, Waterways Experiment Station, Vicksburg, 59 pp.

Cole, T.M., and S.A. Wells (2011), CE-QUAL-W2: A two-dimensional laterally averaged, hydrodynamic and water quality model, version 3.7, User Manual, Portland State University. US Army Corps of Engineers Instruction Report EL-11-1, 759 p.

Danner, E., S. Lindley, R. Nemani, B. Rajagopalan, and F. Melton (2007), Improving stream temperature predictions for river water decision support systems, NASA Earth-Sun Science, Applied Sciences Program, NNH07ZDA001N-DECISION.

Danner, E., F. Melton, A. Pike, H. Hashimoto, A. Michaelis, J. Caldwell, B. Rajagopalan, R. Nemani, L. Dewitt, and S. Lindley, (2012), River temperature forecasting: a coupled-modeling framework for management of river habitat. IEEE Journal of Selected Topics in Applied Earth Observations and Remote Sensing. 5 SI (6), 1752-1760.

de Azevado, L.G.T., T.K. Gates, D.G. Fontane, and J.W. Labadie (2000), Integration of water quantity and quality in strategic river basin planning. Journal of Water Resources Planning and Management, ASCE 126 (2), 85-97.

Deas, M.L., C.B. Cook, C.L. Lowney, G.K. Meyer, and G.T. Orlob (1997), Sacramento River Temperature Modeling Report 96-1, Center for Environmental and Water Resources Engineering, University of California, Davis.

Deas, M.L., and C.L. Lowney (2000), Water Temperature Modeling Review: Central Valley, California Water Modeling Forum, 113 pp.

Dunham, J.B., G. Chandler, B.E. Rieman, and D. Martin (2005), Measuring stream temperature with digital dataloggers: a user's guide, USDA Forest Service, Rocky Mountain Research Station, GTR-RMRS-150, Fort Collins, CO, http://www.treesearch.fs.fed.us/pubs/9476.

Edinger, J.E., D.K. Brady, and J.C. Geyer (1974), Heat exchange and transport in the environment, Publication No. 74-049-00-3, Electric Power Research Inst., Palo Alto, CA.

Ficklin, D.L., Y. Luo, I.T. Stewart, and E.P. Maurer (2012), Development and application of a hydroclimatological stream temperature model within the Soil and Water Assessment Tool, Water Resources Research, 48, W01511.

Fish and Wildlife Service (FWS) (1999), Effect of Temperature on Early-Life Survival of Sacramento River Fall- and Winter-Run Chinook Salmon, U.S. Department of Interior, Fish and Wildlife Service, Final Report, January 1999, 41 pp.

Furrer, E.M., and R.W. Katz (2007), Generalized linear modeling approach to stochastic weather generators, Climate Research, 34, 129-144.

Furrer, E.M., and R.W. Katz (2008), Improving the simulation of extreme precipitation events by stochastic weather generators, Water Resources Research, 44, doi:10.1029/2008WR007316.

Georgakakos, A.P., K.P. Georgakakos, and E.A. Baltas (1990), A state-space model for hydrologic river routing, Water Resources Research, 26(5), 827-838.

Grantz, K. (2003), Using large scale climate information to forecast seasonal streamflow in the Truckee and Carson Basins, M.S. thesis, University of Colorado, Boulder, CO.

Grantz, K., (2006), Interannual variability of North American Monsoon hydroclimate and application to water management in the Pecos River Basin. Ph.D. Dissertation, University of Colorado, Boulder, CO, 171 pp.

Grantz, K., B. Rajagopalan, M. Clark, and E. Zagona (2005), A technique for incorporating large-scale climate information in basin-scale ensemble streamflow forecasts, Water Resources Research, 41, W10410, doi:10410.11029/12004WR003467.

Hallock, R.J., and F.W. Fisher (1985), Status of winter-run Chinook salmon in the Sacramento River, Anadromous Fisheries Branch, California Department of Fish and Game, 25 January 1985.

Hamlet, A.F., P. Carrasco, J. Deems, M.M. Elsner, T. Kamstra, C. Lee, S.Y. Lee, G. Mauger, E.P. Salathe, I. Tohver, and L. Whitely Binder (2010), Final Project Report for the Columbia Basin Climate Change Scenarios Project, http://www.hydro.washington.edu/2860/report.

Hamlet, A.F., M.M. Elsner, G. Mauger, S.Y. Lee, and I. Tohver (2013), An overview of the Columbia Basin Climate Change Scenarios Project: approach, methods, and summary of key results, Atmosphere-Ocean, in press, 42 pp.

Hanna, R.B., L. Saito, J.M. Bartholow, and J. Sandelin (1999), Results of simulated temperature control device operations on in-reservoir and discharge water temperatures using CE-QUAL-W2, Lake and Reservoir Management, 15(2), 87-102.

Harvey, A.C. (1989), Forecasting structural time series models and the Kalman filter, Cambridge University Press.

Hobson, A.N. (2005), Use of a stochastic weather generator in a watershed model for streamflow simulation, M.S. thesis, University of Colorado, Boulder, CO

Isaak, D. J. (2011), Stream temperature monitoring and modeling: recent advances and new tools for managers, Stream Notes, Stream Systems Technology Center, July 2011, 7 pp.

Jobson, H.E. (1980), Thermal modeling of flow in the San Diego Aqueduct, California, and its relation to evaporation, U.S. Geological Survey Professional Paper No. 1122, 24 pp.

Jobson, H.E., and T.N. Keefer (1979), Modeling highly transient flow, mass, and heat transport in the Chattahoochee River near Atlanta, Georgia, U.S. Geological Survey Professional Paper No. 1156, 41 pp.

Lall, U., and A. Sharma (1996), A nearest neighbor bootstrap for time series resampling, Water Resources Research, 32(3), 679-693.

Lall, U., B. Rajagopalan, and D.G. Tarboton (1996), A nonparametric wet/dry spell model for daily precipitation, Water Resources Research, 32(9), 2803-2823.

Lenhart, T., K. Eckhardt, N. Fohrer, and H.-G. Frede (2002), Comparison of two different approaches of sensitivity analysis, Physics and Chemistry of the Earth, 27, 645-654.

Liang, X., D.P. Lettenmeier, E.F. Wood, and S.J. Burges (1994), A simple hydrologically based model of land surface water and energy fluxes for general circulation models, Journal of Geophysical Research, 99(D7), 14415-14428.

Liang, X., E.F. Wood, and D.P. Lettenmeier (1996), Surface soil moisture parameterization of the VIC-2L model: evaluation and modifications, Global Planetary Change, 13, 195-206.

Lichatowich, J., J.J. Anderson, M. Deas, A.E. Giorgi, K.A. Rose, and J.G. Williams (2005), Review of the Biological Opinion of the long-term Central Valley Project and State Water Project operations criteria and plan, California Bay-Delta Authority, Sacramento, CA.

Lieberman D.M., M.J. Horn, and S. Duffy (2001), Effects of a temperature control device on nutrients, POM and plankton in the tailwaters below Shasta Lake, California. Hydrobiologia, 452, 191-202.

Loader, C. (1999), Local Regression and Likelihood, Statistics and Computing, Springer, 290 pp.

Lowney, C.L. (2000), Stream temperature variation in regulated rivers: evidence for a spatial pattern in daily minimum and maximum magnitudes, Water Resources Research, 36(10), 2947-2955.

Maguire, J.J. (2006), Report on the 2004 National Marine Fisheries Service's (NMFS) Biological Opinion (BO) on the long-term Central Valley Project and State Water Project Operations, Criteria and Plan (OCAP). Center for Independent Experts, University of Miami, Miami, FL.

Mantua, N., I. Tohver, and A. Hamlet (2010), Climate change impacts on streamflow extremes and summertime stream temperature and their possible consequences for freshwater salmon habitat in Washington State, Climatic Change, 102, 187-223.

Maurer, E.P., A.W. Wood, J.C. Adam, D.P. Lettenmeier, and B. Nijssen (2002), A long-term hydrologically-based data set of land surface fluxes and states for the conterminous United States, Journal of Climate, 15(22), 3237-3251.

May, J.T., and L.R. Brown (2002), Fish communities of the Sacramento River Basin: implications for conservation of native fishes in the Central Valley, California, Environmental Biology of Fishes, 63, 373-388.

McCullagh, P., and J.A. Nelder (1989), Generalized Linear Models, Chapman and Hall: London.

McCullough, D.A., J.M. Bartholow, H.I. Jager, R.L. Beschta, E.F. Cheslak, M.L. Deas, J.L. Ebersole, J.S. Foott, S.L. Johnson, K.R. Marine, M.G. Mesa, J.H. Petersen, Y. Souchon, K.F. Tiffan, and W.A. Wurtsbaugh (2009), Research in thermal biology: burning questions for coldwater stream fishes, Reviews in Fisheries Science, 17(1), 90-115.

McMahon, T. (2006), CIE review of NOAA-Fisheries Biological Opinion on effects of proposed Central Valley Project changes on listed fish species Center for Independent Experts, University of Miami, Miami, FL.

Mehrotra, R., and A. Sharma (2006), Conditional resampling of hydrologic time series using multiple predictor variables: a k-nearest neighbor approach, Advances in Water Resources, 29, 978-999.

Mohseni, P.B., H.G. Stefan, and T.R. Erickson (1998), A nonlinear regression model for weekly stream temperatures, Water Resources Research, 34, 2685-2692.

Moriasi, D.N., J.G. Arnold, M.W.V. Liew, R.L. Binger, R.D. Harmel, and T.L. Vieth (2007), Model evaluation guidelines for systematic quantification of accuracy in watershed simulations, Transactions of the American Society of Agricultural and Biological Engineers, 50(3), 885-900.

Moyle, P.B. (1976), Fish introductions in California: history and impact of native fishes, Biological Conservation, 9, 101-118.

Moyle, P.B., and P.J. Randall (1998), Evaluating the biotic integrity in the Sierra Nevada, California, Conservation Biology, 12, 1318-1326.

Myrick, C.A., and J.J. Cech (2000), Swimming performances of four California stream fishes: temperature effects, Environmental Biology of Fishes, 58.

Myrick, C.A., and J.J. Cech (2001), Temperature Effects on Chinook Salmon and Steelhead: A Review Focusing on California's Central Valley Populations, Bay Delta Modeling Forum, Technical Publication 01-1, 57 pp.

Myrick, C.A., and J.J. Cech (2002), Growth of American River fall-run Chinook salmon in California's central valley: temperature and ration effects, California Fish and Game, 68, 57-59.

Myrick, C.A., and J.J. Cech (2004), Temperature effects on anadromous salmonids in California's Central Valley: what don't we know?, Reviews in Fish Biology and Fisheries, 14(1), 113-123.

Nash, J. E., and J.V. Sutcliffe (1970), River flow forecasting through conceptual models part I - a discussion of principles Journal of Hydrology, 10(3), 282-290.

National Climatic Data Center (NCDC) (2011), Daily and hourly meteorology download, National Oceanic and Atmospheric Administration, Asheville, NC, http://www.ncdc.noaa.gov.

National Marine Fisheries Service (NMFS) (2004), Biological Opinion on the long-term Central Valley Project and State Water Project operations criteria and plan, http://www.science.calwater.ca.gov.

Neumann, D.W., B. Rajagopalan, and E. Zagona (2003), Regression model for daily maximum stream temperature, Journal of Environmental Engineering, 129(7), 659-666.

Neumann, D.W., E. Zagona, and B. Rajagopalan (2006), A decision support system to manage summer stream temperatures, Journal of the American Water Resources Association, 42(5), 1275-1284.

Nijssen, B., D.P. Lettenmeier, X. Liang, S.W. Wetzel, and E.F. Wood (1997), Streamflow simulation for continental-scale river basins, Water Resources Research, 33, 711-724.

Nowak, K., J. Prairie, B. Rajagopalan, and U. Lall (2010), A nonparametric stochastic approach for multisite disaggregation of annual to daily streamflow, Water Resources Research, 46, W08529.

Null, S. E., J.H. Viers, M.L. Deas, S.K. Tanaka, and J.F. Mount (2012), Stream temperature sensitivity to climate warming in California's Sierra Nevada: impacts to coldwater habitat, Climatic Change, doi:10.1007/s10584-012-0459-8.

Pike, A., E. Danner, D. Boughton, F. Melton, R. Nemani, B. Rajagopalan, and S. Lindley (2013), River temperature prediction: an updated stochastic dynamics approach, in prep.

Podesta, G., F. Bert, B. Rajagopalan, S. Apipattanavis, C. Laciana, E. Weber, W. Easterline, R.W. Katz, D. Letson, and A. Menendez (2010), Decadal climate variability in the Argentine Pampas: regional impacts of plausible climate scenarios on agricultural systems, Climate Research, 40, 199-210.

Poole, G.C., and C.H. Berman (2001), An ecological perspective on in-stream temperature: natural heat dynamics and mechanisms of human-caused thermal degradation, Environmental Management, 27(6), 787-802.

Prairie, J. (2006), Stochastic non-parametric framework for basin-wide streamflow and salinity modeling: application for the Colorado River Basin, Ph.D. thesis, University of Colorado, Boulder, CO.

Rajagopalan, B. (1995), Nonparametric Stochastic Generation of Daily Precipitation and Other Weather Variables, PhD dissertation, Utah State University, Logan, UT, 1995.

Rajagopalan, B., and U. Lall (1999), A k-nearest neighbor simulator for daily precipitation and other weather variables, Water Resources Research, 35(10), 3089-3101.

Rajagopalan, B., J. Salas, and U. Lall (2010), Stochastic methods for modeling precipitation and streamflow, in Advances in Data-based Approaches for Hydrologic Modeling and Forecasting, Ed. by B. Sivakumar and R. Berndtsson, World Scientific, Singapore.

Regonda, S. K., B. Rajagopalan, M. Clark, and J. Pitlick (2005), Seasonal cycle shifts in hydroclimatology over the Western United States, Journal of Climate, 18, 372-384.

Regonda, S. K., B. Rajagopalan, M. Clark, and E. Zagona (2006), A multi-model ensemble forecast framework: application to spring seasonal flows in the Gunnison River Basin, Water Resources Research, 42, W09404.

Reisner, M. (1986), Cadillac Desert, Viking-Penguin, New York, 582 pp.

Saito L. (1999), Interdisciplinary modeling at Shasta Lake, Ph.D. dissertation, Colorado State University, Fort Collins, CO, 341 pp.

Saito, L, B.M. Johnson, J. Bartholow, and R.B. Hanna (2001), Assessing ecosystem effects of reservoir operations using food web-energy transfer and water quality models, Ecosystems, 4, 105-125.

San Francisco Estuary Project (SFEP) (1992), State of the estuary: a report on conditions and problems in the San Francisco Bay/Sacramento-San Joaquin Delta Estuary, SFEP, Oakland, California.

Sinokrot, B.A., and H.G. Stefan (1993), Stream temperature dynamics: measurements and modeling, Water Resources Research, 29(7), 2299-2312.

Smith, K., and M.E. Lavis (1975), Environmental influences on the temperature of a small upland stream, Oikos, 26(2), 228-236.

Taylor, R.L. (1998), Simulation of hourly stream temperature and daily dissolved solids for the Truckee River, California and Nevada, Water Resources Investigations Report, WRI 98-4064, U.S. Geological Survey, Reston, Virginia.

Torgersen, C.E., R.N. Faux, B.A. McIntosh, N.J. Poage, and D.J. Norton (2001), Airborne thermal sensing for water temperature assessment in rivers and streams, Remote Sensing of Environment, 76, 386-398.

Towler, E., B. Rajagopalan, R.S. Summers, and D. Yates (2010a), An approach for probabilistic forecasting of seasonal turbidity threshold exceedance, Water Resources Research, 46, W06511.

Towler, E., B. Rajagopalan, E. Gilleland, R.S. Summers, D. Yates, and R.W. Katz (2010b), Modeling hydrologic and water quality extremes in a changing climate: a statistical approach based on extreme value theory, Water Resources Research, 46, W11504.

van Vleck, G.K., G. Deukmejian, and D.N. Kennedy (1988), Water temperature effects on Chinook salmon with emphasis on the Sacramento River - a literature review, California Department of Water Resources, Northern District.

van Vliet, M. T. H., F. Ludwig, J.J.G. Zwolsman, G.P. Weedon, and P. Kabat (2011), Global river temperatures and sensitivity to atmospheric warming and changes in river flow, Water Resources Research, 47(2), W02544.

Venables, W. N., and B.D. Ripley (2002), Modern applied statistics with S, Springer, New York.

Ward, J. (1963), Annual variation of stream water temperature, ASCE, Journal of the Sanitary Engineering Division, 89, 3710-3732.

Webb, B.W., P.D. Clack, and D.E. Walling (2003), Water-air temperature relationships in a Devon river system and the role of flow, Hydrological Processes, 17(15), 3069-3084.

Webb, B.W., D.M. Hannah, R.D. Moore, L.E. Brown, and F. Nobilis (2008), Recent advances in stream and river temperature research, Hydrological Processes, 22, 902-918.

Weirich, S. R., J. Silverstein, and B. Rajagopalan (2011), Effect of average flow and capacity utilization on effluent water quality from U.S. municipal wastewater treatment facilities, Water Resources Research, 45(14), 4279-4286.

Wells, S.A., and T.M. Cole (2000), Theoretical basis for the CE-QUAL-W2 river basin model, Water Quality Research Program, U.S. Army Corps of Engineers, August 2000.

Wilks, D.S. (1999), Multisite downscaling of daily precipitation with a stochastic weather generator, Climate Research, 11, 125-136.

Wilks, D.S., and R.L. Wilby (1999), The weather generation game: a review of stochastic weather models, Progress in Physical Geography, 23, 329-357.

Wood, A.W., L.R. Leung, V. Sridhar, and D.P. Lettenmeier (2004), Hydrologic implications of dynamical and statistical approaches to downscaling climate model outputs, Climatic Change, 15, 189-216.

Wood, A.W., and D.P. Lettenmeier (2006), A test bed for new seasonal hydrologic forecasting approaches in the Western United States, Bulletin of the American Meteorological Society, 87, 1699-1712.

Yates, D., S. Gangopadhyay, B. Rajagopalan, and K. Strzepek (2003), A technique for generating regional climate scenarios using a nearest neighbor algorithm, Water Resources Research, 39(7), 1199.

Yates, D., H. Galbraith, D. Purkey, A. Huber-Lee, J. Sieber, J. West, S. Herrod-Julius, and B. Joyce (2008), Climate warming, water storage, and Chinook salmon in California's Sacramento Valley, Climatic Change, 91, 335-350.

Yearsley, J.R. (2009), A semi-Langrangian water temperature model for advection-dominated river systems, Water Resources Research, 91(3-4), 335-350.

Zwieniecki, M.A., and M. Newton (1999), Influence of streamside cover and stream features on temperature trends in forested streams of Western Oregon, Western Journal of Applied Forestry, 14, 106-113.